STRUCTURE-FUCTION STUDIES OF NICOTINIC ACETYLCHOLINE RECEPTORS USING UNNATURAL AMINO ACIDS

Thesis by

Joanne (Xinan) Xiu

In Partial Fulfillment of the Requirements
for the degree of
Doctor of Philosophy

California Institute of Technology
Pasadena, California
2007
(Defended 12 December 2007)

To my parents, Ruiling Xiu and Changfan Guo,
my husband, Gang Duan,
and my son, Ryan Duan

ACKNOWLEDGEMENTS

The five and half years at Caltech have been the most memorable time in my 28 years of life so far. I owe many thanks for my experience here. First of all, I have to thank Prof. Dennis Dougherty, who has been a most wonderful advisor to me. The enthusiasm and persistence of Dr. Dougherty regarding science have motivated me and encouraged me from the very beginning, when I joined the lab in the summer of 2003, and I am sure will benefit me for my whole life. His inspiration and encouragements over the past years were always there whenever I needed them. Talking with Dennis has always been enlightening, and I count myself among the luckiest to have benefited from his broad knowledge in various areas of science. Dennis has also been very accessible and patient, which is extremely important for me to learn along the way of research.

It has been great to work with Dr. Henry Lester as well. Collaborations with the Lester group have been very fruitful and enjoyable. Here I would also like to thank my committee, Prof. Dough Rees, Prof. Erin Schuman, and Prof. Carl Parker, for their time and commitment.

The Dougherty group is a greatest place to work and to study and I have enjoyed each andevery day working with the brilliant group of people here. My thanks go to the many people who are now no longer in the lab but helped me tremendously when I first started out. Dr. Sarah May helped me get started from the first day I arrived in the lab. She is a wonderful biologist and chemist and holds genuine enthusiasm for life. I thank Dr. Niki Zacharias for the lots of help that she has offered me both in the lab and at

Neurion, Inc., on experiments that I couldn't have performed without her. Dr. James Pettersson was a good resource to go to whenever I had questions about anything in the lab. Dr. Amanda Cashin helped me with numerous experiments in molecular biology and electrophysiology recordings and her delightful personality made it always a pleasure to be around her. I cannot thank Dr. Tingwei Mu enough for his warm words and valuable suggestions throughout the years, even after he left the lab. Dr. David Dahan was a knowledgeable and warm-hearted scientist and talking with him was always a pleasure. I also want to thank Dr. Steve Spronk and Dr. Lori Lee, who are both postdocs at University of Michigan right now. Steve worked on computational simulation which was a new area to me. Lori helped me with the few proline analog incorporation experiments and I appreciate her input very much.

My daily life at Caltech could not have been such a pleasant experience if it hadn't been for the wonderful people in the Dougherty group. I have truly enjoyed the happy, friendly, active, and warm atmosphere in the lab, which has undoubtedly helped with my academic work as well. I thank Amy Eastwood for helping me with dCA coupling O-Me-Ser and for being a great listener and helper with my problems. I thank Michael Torrice for being a great Opus captain and a great FPLC captain. I thank Erik Rodriguez for being a strict safety officer and for the countless suggestions on various experiments. These are people from my year and I feel lucky to have them go through candidacies, committee meetings, and graduations together with me. People from the next year from us are a fun group as well. Kiowa Bower was a great neighbor in the office and always a fun person to talk with, and I enjoyed working with him as Bi1 TAs and also on the FPLC project. Ariele

Hanek is also a great Opus captain and she also impresses me for never hesitating to go out her way to do her job excellently. Working with her on my first publication on nAChR gating mechanism was a great pleasure. Katie McMenimen has interests in numerous areas in chemistry, biology, and computation, and she never ceases to learn new things. I would also like to thank the newer people in the lab. Jai Shanata has taught me a lot about single-channel recordings and also his interest in philosophy has stimulated my curiosity as well. Kristin Rule is not only a dedicated researcher but also a great dancer, and I will always remember her infectious laughter. Kay Limapichat and I sat together for the last few months and I enjoyed being her neighbor in the office. Angela Blum is a hard worker and she holds interest in various aspects in chemistry and biology. Sean Kedrowski is a very devoted researcher and his love for science is apparent to all.

The last but certainly not the least, I owe my deepest thanks to my family. I thank my parents for always being there for me whenever I needed them. I thank my husband for being supportive of me all the time. I also want to thank my new son, Ryan Duan, for all the new meanings that he has brought to my life.

ABSTRACT

Nicotinic acetylcholine receptors (nAChR) are an important family of ligand gated ion channels found throughout the CNS and the PNS. They have been indicated in a series of physiological functions and pathological states. nAChRs have received extensive study in the past as a prototype of the Cys loop LGIC member. Growing interest in developing subtype specific agents targeting nAChRs to treat neurological diseases require more detailed structural and functional information in the numerous members of the nAChR family.

We performed structure-function studies on the chemical scale of several of the most important members of this family using a powerful combination of conventional mutagenesis and unnatural amino acid incorporations. Chapter 2 describes our research in studying the channel gating mechanism of the prototypic nAChR, the muscle type $(\alpha_1)_2\beta\gamma\delta$. We studied thoroughly the gating interface of the receptor and concluded that the overall charging pattern of the gating interface, and not any specific pairwise electrostatic interactions, controls the gating process in the Cys loop superfamily. Chapter 3 reports our studies in the ligand binding mechanism of the most prevalent neuronal type $\alpha4\beta2$ and $\alpha7$ nAChR. We identified a cation-π interaction and a hydrogen bond employed by nicotine with the $\alpha4\beta2$ receptor. These two key interactions are absent or significantly diminished in both the muscle type receptors and in the $\alpha7$ form of neuronal receptor. In Chapter 4 we studied the ligand binding mechanism of a relatively newly characterized neuronal receptor ,$\alpha4\beta4$.

From these studies, we found that in the Cys loop superfamily, homology in amino acid sequences and structures do not translate into a shared functional mechanism. In fact, different sets of chemical interactions are adopted between ligands and the receptor, and between amino acids within the ion channel proteins, both in ligand binding and channel gating.

Ion channels are membrane bound multi-subunit macromolecules. We are able to carry out such exhaustive detailed structure-function studies by means of the fast-developing methodology of unnatural amino acid incorporation by nonsense suppression. This thesis also describes our effort to improve the efficiency of nonsense suppression. In particular, we designed multiple 21nt small interfering RNA (siRNA) targeting release factor 1 (eRF1) in both HEK cells and *Xenopus* oocytes, and monitored the nonsense suppression efficiency change *in vivo* and *in vitro* by RNA PCR, Western blotting, fluorescence, and electrophysiology (Chapter 5).

TABLE OF CONTENTS

LIST OF FIGURES

LIST OF TABLES

Chapter 1

INTRODUCTION

1.1. Molecular Neurobiology and Chemistry

The brain is the most complex organ of the human body and it is comprised of about 10^{11} neurons [1]. A synapse is the basic unit of signal transmission between the neurons and between one neuron to non-neural cells such as those in muscles or glands. Each neuron usually has multiple dendrites; serving as the postsynaptic component, but only one axon, which forms the presynaptic component. It is estimated that one neuron forms 10^3~10^4 synapses with other neurons. The vast volume of information transmission between these numerous neural cells is largely dependent on small molecules called neurotransmitters, the most studied of which is acetylcholine [2].

At rest, neurotransmitter-containing vesicles are stored in the presynaptic cell either close to the presynaptic membranes in places called active zones, or further away from the active zones by cytoskeleton elements until they are needed. At a synaptic cleft, signal transmission is triggered by the arrival of an electric signal from the cell body of a presynaptic cell, causing the membrane potential to rise from its resting state. An electric signal large enough to open voltage-gated calcium channels on the cell membrane of the presynaptic neuron results in the inflow of calcium ions, causing the docking of the vesicles at the active zones and then the fusion of the vesicle membrane and the presynaptic membrane, and finally causing the release of the neurotransmitters into the cleft from the storage vesicles[1].

The released neurotransmitters diffuse across the thin synaptic cleft where they bind their corresponding receptors embedded in the postsynaptic membrane of the neighboring neuron. This binding causes a conformational change in the receptors, opening an ion pore in the receptor, allowing a selection of ions to flow through. This ion flow changes the membrane potential of the postsynaptic cell, either exciting it or inhibiting it. Thus the electric-chemical-electric transmission of the information is completed from one cell to the next.

In this process, a ligand gated ion channel could play important roles at two locations: the presynaptic part and the postsynaptic part. The presynaptic channels are usually regulatory, the opening of which contributes to raising the membrane potential of the presynaptic cell, thus easing the opening of the voltage gated calcium channels, finally resulting in the transmitter release [3-5]. The postsynaptic channels contribute to the fast electric signal transmission between two cells, converting the chemical signal carried by the small molecule neurotransmitter into an electric signal. Despite the variable locations and functions of different families of ligand ion channels, the ability to bind a small molecule neurotransmitter and to allow ion flow upon opening is essential for a ligand gated ion channel (Figure 1.1).

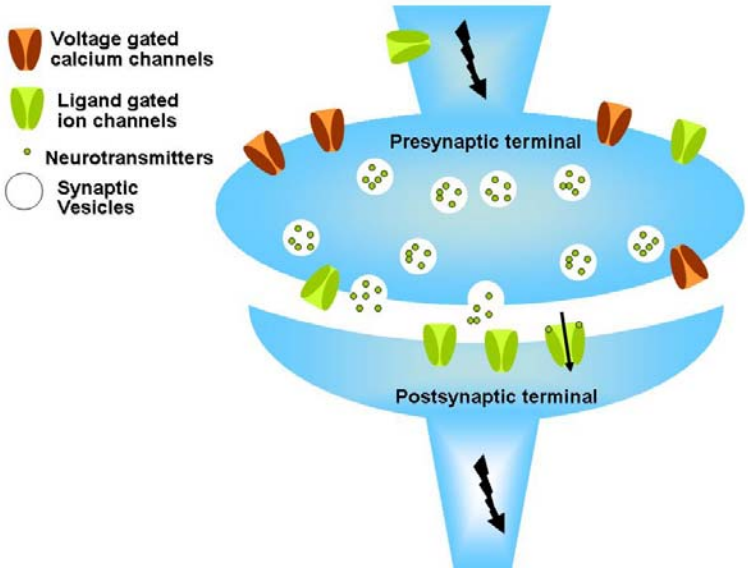

Figure 1.1 A simplified view of a chemical synapse. Both presynaptic and postsynaptic ligand gated ion channels are shown in green and the voltage gated calcium channels are shown in brown. The bolts show the direction of electric signal transmission. The arrow in the ion channel shows the direction of ion flow in the case of an open postsynaptic nAChR.

The structure-function study of these highly specialized ion channels at the molecular level requires chemistry to combine with structural biology, molecular biology, and electrophysiology. In our lab, we take advantage of recent advances in high-resolution structural data, fast-developing protein modification techniques (in particular, incorporation of unnatural amino acids), and the sensitive functional assay of electrophysiology to monitor the functional changes induced by structural modifications.

1.2 Muscle type and neuronal nAChR receptors

The acetylcholine receptor family has two members: the muscarinic acetylcholine receptor (mAChR) which is a G-protein coupled receptor, and the nicotinic acetylcholine receptor (nAChR) which is a ligand gated ion channel. nAChRs purified from the electric organ of *Torpedo* were

resolved into four different subunits designated α, β, γ(ε), and δ. These subunits were later sequenced and cloned, paving the way for the molecular analysis of nicotinic receptors, especially for those at the neuromuscular junction, which show a stoichiometry of $\alpha_2\beta\gamma(\varepsilon)\delta$, γ in the fetal form and ε in the adult form [6].

The muscle type nicotinic receptor turns out to be the best studied and thus the prototypic nAChR so far. This pentameric ion channel carries two inequivalent ligand binding sites at the large extracellular N-terminal domain subunit interfaces. Following the N-terminal domain are four α-helices within the membrane, the third and the fourth of which are separated by a large cytoplasmic loop carrying the phosphorylation sites and the trafficking signals for the receptor transport [7] (Figure 1.2 A). The α subunits differ from the others by the two adjacent cysteines close to the ligand binding site [8].

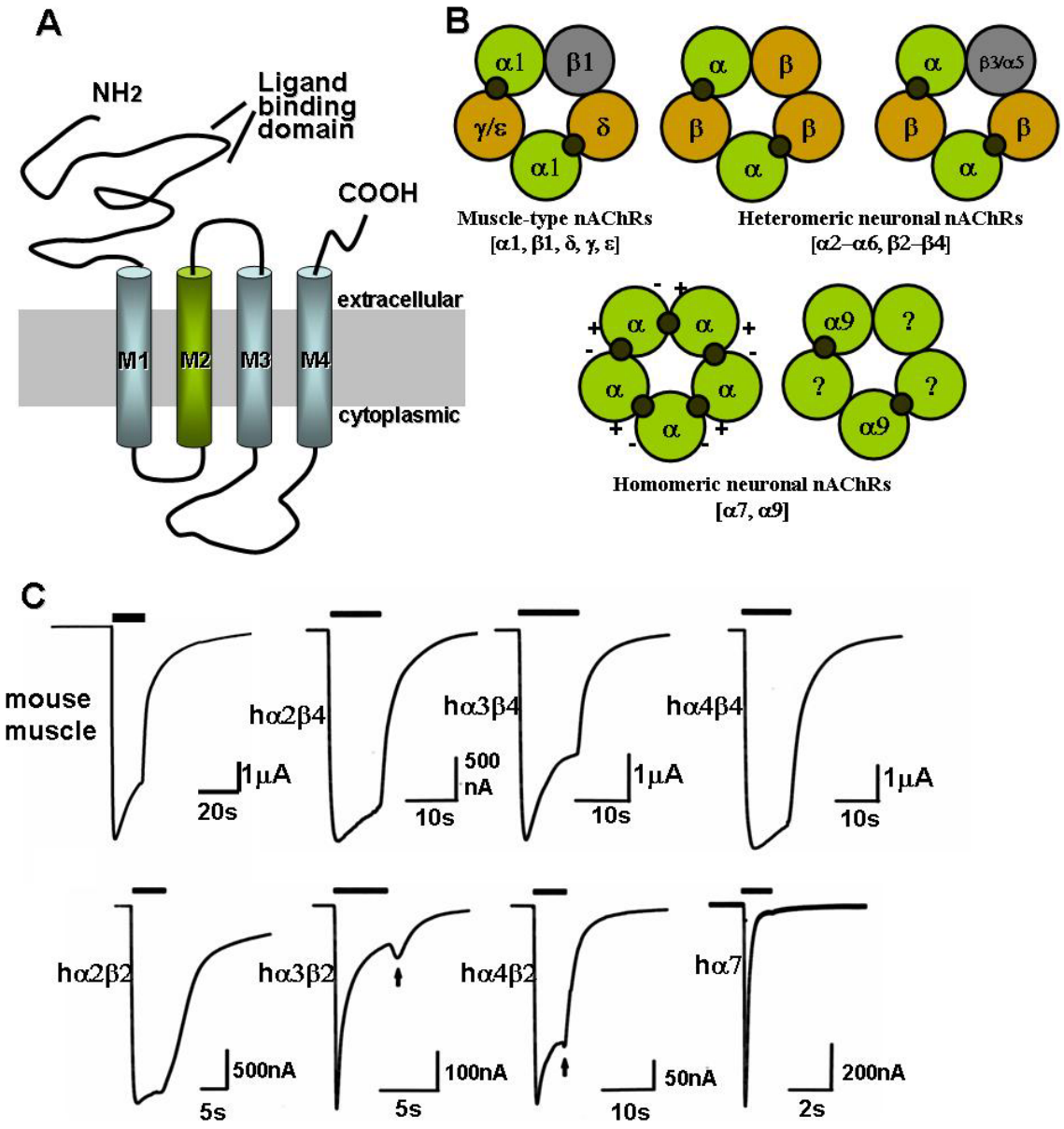

Fig 1.2 Topology and diversity of nAChR subtypes. A: Topology of one subunit of nAChR. The green M2 transmembrane domain lines the ion pore of the channel. B: The subunit arrangements of various heteromeric and homomeric nAChR subtypes. The green and yellow circles represent the subunits that carry the principle and complementary parts of the ligand binding domain, respectively. The gray subunits are mainly structural subunits that don't contribute directly to ligand binding. The dark circles represent the ligand binding sites. C: Saturating dose of acetylcholine induced electric signals recorded in *Xenopus* oocytes expressing various nAChR subtypes. B and C adapted from Fig. 1 in [9], except for the mouse muscle trace which is from our recording.

In the 1980s, almost a decade after the muscle type nAChRs were discovered, nAChRs were characterized in the central nervous system with a much more complex subunit composition. Although subunits from only the α and β families were found, the pentameric combinations of α2-α10 and β2-β4 make possible the existence of a great number of neuronal nicotinic receptors [10, 11] (Figure 1.2 B and C). Adding to this complexity is the variable stoichiometry of many neuronal nAChRs, the most well known example being the existence of at least two subgroups of α4β2 receptors: $(\alpha4)_2(\beta2)_3$ and $(\alpha4)_3(\beta2)_2$ [9, 12].

While distributed throughout the nervous system, neuronal receptors are preferentially located presynaptically, regulating the release of neurotransmitters, in contrast to the mainly postsynaptic location of the muscle type nAChR. A particular kind of neurotransmitter can be regulated by different neuronal nAChR subtypes at different CNS regions. For instance, α4β2-containing receptors are important both at the striatum and the thalamus in regulating the release of the pleasure-inducing dopamine; α6β2β3-containing receptors were found to also play an important role at the striatum [5, 12].

More than 90 percent of the nAChR in the CNS contain the α4 and β2 subunits, and the other major group contains α7. In the PNS, the most abundant subunits are α3 and β4, which colocalize with α5 and/or β4; α7 are also found in the ganglia in the PNS. The α4β2-containing, α7-containing, and α3β4-containing receptors are the best characterized subtypes in terms of ligand selectivity, as they can be purified from animal tissues and studied by radio-labeled ligands. [^{3}H]-cytisine, [^{3}H]-nicotine, or [^{3}H]-epibatidine can label α4β2-containing receptors, and [^{125}I]-Bgtx or [^{3}H]-methyllycaconitine ([^{3}H]-MLA) are used to label α7-containing receptors. However,

complication could be caused by the lack of high selectivity of these ligands. For example, α-Bgtx binds to α7-containing, α8-containing, and α9-containing homomeric and heteromeric receptors, and MLA also recognizes receptors that contain α3 or α6 subunits. Also, epibatidine binds α2–α4 and β2-β4 subunits with high affinity [9, 12].

The addictive properties of nicotine lead to over 5,000,000 smoking-related deaths annually, producing the largest source of preventable mortality in the western world. One of the earliest uses of nicotinic drugs dates back to 1932 when the antinociceptive activity of nicotine was discovered. Later epibatidine was discovered, displaying outstanding analgesic properties and high affinity for the nicotinic receptors [13]. However, lack of selectivity for specific subtypes compromised the wide use of epibatidine, due to the serious side effects. Other physiological functions and pathological effects are also mediated by one or a small selection of neuronal nAChR subtypes. The heterogeneity of the native nAChR populations in the CNS presents major challenges in developing therapeutics targeting these receptors. Targeting one or a few nAChR subtypes without affecting other subtypes avoids the cardiovascular, gastrointestinal, and other side effects, making such targeting a main goal of designing such agents [6]. The main role of nicotinic receptors in the brain seems to be that of enhancing neurotransmitter release of several kinds; therefore, several pathological states could be alleviated by the activation of neuronal nAChRs.

Targeting presynaptic nicotinic receptors to enhance the release of neurotransmitters such as ACh and dopamine may be advantageous for treating neurodegenerative diseases and for improving cognition. In fact, epidemiological evidence has identified several pathological states that might benefit from nicotinic drugs [14]. For instance, a negative correlation between smoking and the incidence of Alzheimer's disease or Parkinson's disease has been supported by *in vitro* and

in vivo studies [15, 16]. There has also been a consistent observation of widespread decline in nicotinic receptors in aging normal human brains or the brains of neurodegenerative disease patients [17]. The nicotinic cholinergic systems have been shown to be involved in several cognitive functions including attention, learning, and memory [18]. Among the many subtypes present in the brain, the α4β2-containing and α7-containing subtypes seem particularly important.

In the post-mortem brains of schizophrenic patients, it was found that nicotinic receptors, in particular the α7-containing receptors, are reduced in number [19]. Association between smoking and major depression and anxiety has also been shown by several studies. Despite the complex effects of nicotine on these pathological psychiatric states, cholinergic agonists and antagonists aiming to treat several psychiatric disorders have been proposed recently [20].

In addition to the therapeutic potentials of targeting nicotinic receptors mentioned above, using nicotinic drugs including nicotinic antagonists such as mecamylamine or partial agonists such as varenicline are the most popular strategies to aid smoking cessation [21]. The possibility of treating epilepsy and Tourette's syndrome has been explored as well [18, 22].

1.3 Gating of the Cys loop ligand gated ion channels

Ligand gated ion channels are membrane-bound macromolecules capable of 1) binding ligands of various sizes and properties, 2) structural changes that produce dramatically different functional states identified as open, closed, or desensitized, and 3) selectively allowing ions to flow through a pore region usually far away from the ligand binding region. Ion channels perform these functions on the time scale of milliseconds, enabling them to fine-tune the fast electric transmission of the complicated nervous network [23].

When we talk about the gating of an ion channel, we generally refer to the channel opening and closing processes (desensitization is usually considered part of the gating, but is not stressed here), which involves multiple structural elements in the protein, including the ligand binding site, the channel gate, and many other structural elements of the protein [24]. There are several critical and important questions to ask when studying the gating mechanisms. Which structural elements are involved in this process? What is the nature of the chemical interactions employed to transmit these interactions from one amino acid to another? In what order or fashion do these changes occur? Are these changes conserved in structurally/functionally related proteins, and so on and so forth.

The Cys loop superfamily of neurotransmitter-gated ion channels includes receptors for acetylcholine (nicotinic ACh receptor, nAChR), serotonin (5-HT_3 receptor), γ-aminobutyric acid (GABA, types A and C receptors), and glycine. These receptors are classified as excitatory (cation-conducting; nAChR and 5-HT_3) or inhibitory (anion-conducting; GABA and glycine) [25]. Tremendous efforts have been put into revealing structures at different states of the receptor or receptor analogs, aiming to find changes that may help in defining different functional stages of the protein. Apart from the difficulty of envisioning dynamic and continuous movements of a complicated macromolecule by generating static "snapshots", there are innate difficulties of getting the crystal structure of this membrane-bound protein.

Despite these difficulties and inaccuracies, there have been suggestive structural data from several labs. AChBP is a secretory protein from glia cells in the CNS of the fresh water snail, *Lymnaea stagnailis,* where it modulates synaptic transmission. Being highly homologous to the extracellular domain of the nAChRs and carrying high pharmacological similarity to nAChRs, α7

in particular, AChBP structures from multiple organisms with various ligands bound have provided great insight into the ligand binding mechanism of the nicotinic receptors for the past few years [26-33]. Agonist and antagonist bound forms of AChBP show dramatic differences in certain structural elements. This protein lacks completely the transmembrane part where the ion pore is located, however it was shown to be a "gate-able" protein when conjugated with the transmembrane part of the serotonin receptor [34]. Unwin and co-workers refined the cryo-EM model of the whole receptor from the electric organ of *Torpedo* to a resolution of 4Å [35]. However, the model still lacks the resolution to draw any conclusion at the mobile loops which are of critical importance when it comes to the channel gating study [35-37]. Furthermore, it has not been determined whether the agonist bound form of AChBP structures is in the active or desensitized state; therefore, conclusions from the structural data alone seem imprudent [38].

By looking at the several AChBP crystal structures with or without different ligands bound, loop C seems to be a structural unit that moves significantly. An "uncapped" conformation of C loop corresponds to a closed or resting state of the receptor, while a "capped" loop C corresponds to an open or desensitized receptor. Other elements indicated to have moved include β1−β2 loop (loop 2), Cys loop (loop 7) and β8−β9 loop (loop 9) [38].

Recently, a 1.94 Å crystal structure of the mutated single monomer of the extracellular domain of mouse muscle α1 nAChR subunit bound with α-bungarotoxin provided interesting new results suggesting important structural features. A water molecule buried in the core of the subunit and a well ordered carbohydrate chain are seen. Functional studies indicate that both features are important in regulating the gating of the channel [39].

In addition to structural biology, chemistry, biochemistry, chemical labeling, and electrophysiology come into play to study the gating of this family of receptors. In earlier days, using SCAM (substituted cystein accessibility mutagenesis), Karlin suggested that during gating the α M2 domain undergoes significant changes in secondary structure, from a nonhelical to an α-helical conformation [40]. Backbone amide-to-ester mutations disrupting backbone hydrogen bonds performed in our lab supported this mechanism, with a few modifications to Karlin's model of the exact locations where the largest conformational changes are seen [41].

From mutational studies, it was proposed by Sine et al. that after ligand binding, a conserved tyrosine residue (Y185, *Lymnaea* AChBP) in the C-loop is drawn closer to a conserved lysine residue (K139) in the β7 strand, breaking an interaction between this lysine and an aspartate residue (D194) in the β10 strand (K145 and D200 in the mouse muscle α subunit) [34, 42].

For the 5-HT_3 receptor, Lummis and co-workers from our lab have proposed that structural changes induced by ligand binding lead to the *cis-trans* isomerization of a conserved proline residue (Pro 8*) on the M2-M3 linker and subsequent channel opening [43]. Thus it has been proposed that upon agonist binding, the C-loop is pulled into to a "capped" position leading to an interaction between K139 and Y185, a disruption of a salt bridge between the β10 strand and the β1−β2 linker, followed by the isomerization of a proline residue on the M2-M3 linker, leading to channel opening [42]. However, although this proline exists for nAChRs, no similar proline exists in either the GABA or glycine members of this superfamily. Instead, electrostatic and hydrophobic interactions might be responsible for gating of these receptors [42, 44-48].

"A stepwise mechanism for channel gating" or what was previously called a "conformational wave" has become more complete as more regions are explored by a combination of point mutation and single channel recording in the Auerbach lab [49-52]. By looking at a "Linear Free Energy Relationship", Auerbach and co-workers applied model-based kinetic analyses to quantify the effects of mutations made on various domains of the mouse α1 subunit of nAChR. It is proposed that nAChR gating occurs as a series of stepwise movements of such domains that link the low-to-high affinity conformational change in the agonist binding site with the low-to-high conductance conformational change in the pore. Specifically, they suggested blocks of coordinated motions starting with the β4-β5 linker, the β7-β8 linker, and loop C, through the Cys loop and the β1-β2 linker to the pore region M2, and finally the gating of the channel. This stepwise motion propagates throughout the nAChR via Brownian motion [49, 53]. This model provides a more complete view of nAChR gating than previous studies.

1.4 Nonsense suppression to incorporate unnatural amino acids

Site-specific incorporation of unnatural amino acids *in vitro* or *in vivo* is a powerful extension of conventional site-directed mutagenesis to study structure-function relations of macromolecules, and also it enables addition of biophysical probes and photo-reactive cross-linking reagents when the mutant proteins are produced in large enough quantities [54, 55]. The chemically synthesized unnatural amino acids are either chemically ligated to a "suppressor tRNA", an engineered orthogonal tRNA that cannot be acylated by an endogenous aminoacyl-tRNA synthetase (aaRS) in the expression system used, or recognized by an engineered twenty-first aaRS [56].

Our lab uses the first methodology, so that a wide variety of amino acids with distinctly different properties can be incorporated in a similar fashion (Figure 1.3). The limitation of this method is that the chemically ligated tRNA is a stoichiometric reagent, so that the quantities of protein produced are limited to the amount of tRNA introduced. Using the high-sensitivity assay of electrophysiology, large electric currents can be seen from *Xenopus* oocytes that are expressing as little as 10 attomol of receptor on their surface. A patch clamp experiment has also made the detection of a single channel possible [57, 58].

Our lab described the first incorporation of an unnatural amino acid into a protein expressed in a living cell [59]. In this method, the unnatural amino acid is introduced after it is chemically acylated to an *in vitro* transcribed tRNA, transferred to the site of interest, which is engineered as a stop codon. Specifically, both mRNA and tRNA can be injected into *Xenopus* oocyte (Figure 1.4). More recently, unnatural amino acids are site-specifically expressed into neuroreceptors expressed in mammalian cells [60]. Other labs have previously reported the application of this method *in vitro*, when translation mixtures from *E. coli* and rabbit reticulocyte were used.

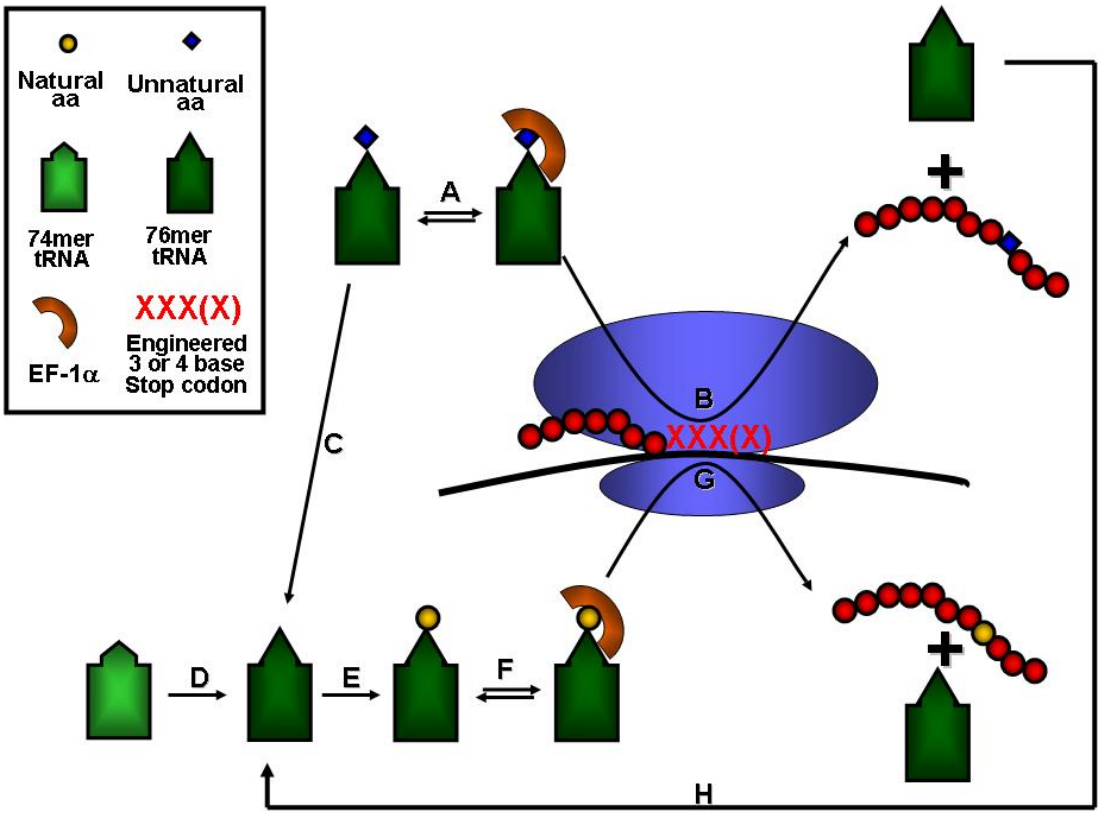

Figure 1.3 Unnatural amino acid incorporation by nonsense suppression (adapted from [55]). A: 76mer tRNA chemically ligated with an unnatural amino acid binds components of the translational machinery (represented by elongation factor EF-1α). B: An unnatural amino acid is incorporated at the desired position engineered as a 3 or 4 base stop codon. C: Undesired loss of the unnatural amino acid. D: Addition of dinucleotide CA to the injected 74mer tRNA (Chapter 3, control experiments for nonsense suppression). E: Undesired amino acylation of the tRNA with a natural amino acid. F: Undesired natural amino acid acylated tRNA binds to the translational machinery. G: Undesired incorporation of a natural amino acid. H: Used tRNA from nonsense suppression could be reacylated by a natural amino acid.

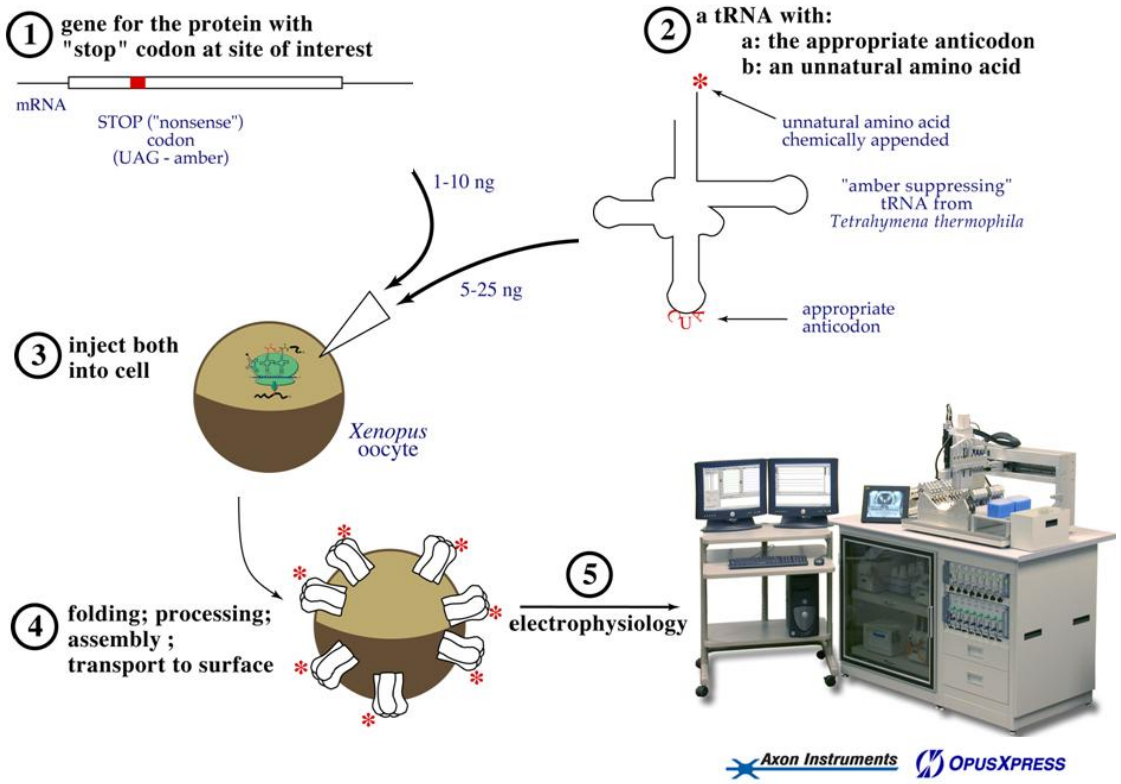

Fig 1.4 Expression system mostly used in our lab for structure-function studies of ion channels. 1: Mutating the gene at the site of interest into a stop codon. Amber (UAG) codon is the most widely used but four base condons and Opal (UGA) are also used. 2: A chemically synthesized amino acid is enzymatically ligated to an engineered tRNA carrying the appropriate anti-codon. 3: Microinjections into the *Xenopus* oocyte of both the tRNA and mRNA. 4: The translational machineries of the *Xenopus* oocyte synthesize, fold, assemble, and transport to the cell surface the mutant ion channels incorporated with the unnatural amino acid at the desired position. 5: Although patch clamp experiments are also carried out in our lab, most electrophysiology characterization experiments are performed on OpusXpress 6000A (Molecular Devices Axon Instruments) which allows simultaneous recording of 8 oocytes.

One requirement of this methodology is that the tRNA is strictly orthogonal so that it is not recognized by any of the endogenous aaRSs, which could result in delivering a natural amino acid at the site of interest. In different expression systems, a variety of such tRNAs have been developed. In the *E. coli* translation system, the Schultz group developed different tRNAs from the

yeast system or from *E.coli* [61, 62]. Chamberlin and co-workers engineered an *E. coli* tRNA suppressor in a rabbit reticulocyte system [63]. In our lab, great nonsense efficiency increase was seen after a mutation U73G was engineered into *a Tetrahymena thermophila* amber suppressor tRNA, producing THG73 and reducing recognition by the oocyte's endogenous glutamine acyltransferease [64].

Suppressor tRNAs that recognize the amber stop codon (UAG) have been the most widely used both *in vitro* and *in vivo* [59, 65]. In the Chamberlin group [62, 63], the Schultz group [62], RajBhandary group [66] and in our group [55, 67], opal (UGA) and ochre (UAA) suppressor have been explored. Four-base codons and corresponding frame shift suppressor tRNAs have also been developed [54, 68, 69] This frameshift suppression method can avoid the competition between the suppressor tRNA and endogenous release factors. It has also enabled the ability to incorporate multiple unnatural amino acids simultaneously. In our lab, we established the simultaneous incorporation of three amino acids *in vivo* by frameshift suppression [54].

Our most recent developments in nonsense suppression include the development of a *Tetrahymena thermophila* Gln amber suppressor (TQAS) tRNA library with increased orthogonality and nonsense suppression efficiency, which allows for screening in eukaryotic cells. The creation of a *T. thermophila* opal suppressor TQOpS' shows about 50 percent suppression efficiency relative to THG73, allowing for multiple incorporation of unnatural amino acids [55, 67].

1.5 Thesis summary

Nicotinic acetylcholine receptors (nAChR) are an important family of ligand gated ion channels found throughout the CNS and the PNS. They have been indicated in a series of

physiological functions and pathological states. nAChRs have received extensive study in the past as a prototype of the Cys loop LGIC member. Growing interest in developing subtype-specific agents targeting nAChRs to treat neurological diseases require more detailed structural and functional information in the numerous members of the nAChR family.

This thesis contains structure-function studies on the chemical scale of several of the most important members of this family: the muscle type $(\alpha_1)_2\beta\gamma\delta$, which has been the representative receptor of the family (Chapter 2); the most prevalent neuronal types $\alpha4\beta2$ and $\alpha7$ (Chapter 3); and a relatively newly characterized neuronal receptor $\alpha4\beta4$ (Chapter 4). A large amount of research has been performed on other Cys loop receptors which share significant structural resemblance to the nicotinic receptors. Using a powerful combination of conventional mutagenesis and unnatural amino acid incorporations, we aim to look at the potential conservation of important channel functions, particularly ligand binding mechanism (Chapter 3 and 4) and channel opening mechanism (Chapter 2). We found that homology in amino acid sequences and structures does not translate into a shared functional mechanisms. In fact, different sets of chemical interactions are adopted between ligands and the receptor, and between amino acids within the ion channel proteins both in ligand binding and channel gating.

Ion channels are membrane-bound multi-subunit macromolecules. We are able to carry out such exhaustive detailed structure-function studies due to the fast-developing methodology of unnatural amino acid incorporation by nonsense suppression. This thesis also describes our effort to improve the efficiency of nonsense suppression. In particular, we designed multiple 21nt small interfering RNA (siRNA) targeting release factor 1 (eRF1) in both HEK cells and *Xenopus*

oocytes, and monitored the nonsense suppression efficiency change *in vivo* and *in vitro* by RNA PCR, western blotting, fluorescence, and electrophysiology (Chapter 5).

1.6 References

1. Kandel, E.R.S., J. H.; Jessell, T. M., The McGraw-Hill Companies, Inc, *Principles of Neural Science.* . 2000.
2. Nestler, E.J.H., S. E.; Malenka, R. C., The McGraw-Hill Companies, Inc.: . *Molecular Neuropharmacology: A Foundation for Clinical Neuroscience.* . 2001.
3. Boehm, S. and H. Kubista, *Fine tuning of sympathetic transmitter release via ionotropic and metabotropic presynaptic receptors.* Pharmacol Rev. 2002 Mar;54(1):43-99.
4. Ghijsen, W.E. and A.G. Leenders, *Differential signaling in presynaptic neurotransmitter release.* Cell Mol Life Sci. 2005 May;62(9):937-54., 2005.
5. Wonnacott, S., et al., *Nicotinic receptors modulate transmitter cross talk in the CNS: nicotinic modulation of transmitters.* J Mol Neurosci. 2006;30(1-2):137-40.
6. Romanelli, M.N., et al., *Central Nicotinic Receptors: Structure, Function, Ligands, and Therapeutic Potential.* ChemMedChem. 2007 Jun 11;2(6):746-767.
7. Keller, S.H. and P. Taylor, *Determinants responsible for assembly of the nicotinic acetylcholine receptor.* J Gen Physiol. 1999 Feb;113(2):171-6.
8. Corringer, P.J., N. Le Novere, and J.P. Changeux, *Nicotinic receptors at the amino acid level.* Annu Rev Pharmacol Toxicol, 2000. **40**: p. 431-58.
9. Jensen, A.A., et al., *Neuronal nicotinic acetylcholine receptors: structural revelations, target identifications, and therapeutic inspirations.* J Med Chem. 2005 Jul 28;48(15):4705-45., 2005.
10. Gotti, C. and F. Clementi, *Neuronal nicotinic receptors: from structure to pathology.* Prog Neurobiol. 2004 Dec;74(6):363-96.
11. Le Novere, N., P.J. Corringer, and J.P. Changeux, *The diversity of subunit composition in nAChRs: evolutionary origins, physiologic and pharmacologic consequences.* J Neurobiol. 2002 Dec;53(4):447-56.
12. Gotti, C., M. Zoli, and F. Clementi, *Brain nicotinic acetylcholine receptors: native subtypes and their relevance.* Trends Pharmacol Sci. 2006 Sep;27(9):482-91. Epub 2006 Jul 31.
13. Decker, M.W., L.E. Rueter, and R.S. Bitner, *Nicotinic acetylcholine receptor agonists: a potential new class of analgesics.* Curr Top Med Chem. 2004;4(3):369-84.
14. Dani, J.A., *Overview of nicotinic receptors and their roles in the central nervous system.* Biol Psychiatry. 2001 Feb 1;49(3):166-74.
15. Nashmi, R., et al., *Chronic nicotine cell specifically upregulates functional alpha 4* nicotinic receptors: basis for both tolerance in midbrain and enhanced long-term potentiation in perforant path.* J Neurosci. 2007 Aug 1;27(31):8202-18.
16. Scott, W.K., et al., *Family-based case-control study of cigarette smoking and Parkinson disease.* Neurology, 2005. **64**(3): p. 442-447.
17. Levin, E.D., et al., *Hippocampal alpha 7 and alpha 4 beta 2 nicotinic receptors and working memory.* Neuroscience. 2002;109(4):757-65.
18. Newhouse, P.A., A. Potter, and A. Singh, *Effects of nicotinic stimulation on cognitive performance.* Curr Opin Pharmacol. 2004 Feb;4(1):36-46.
19. Harris, J.G., et al., *Effects of nicotine on cognitive deficits in schizophrenia.* Neuropsychopharmacology. 2004 Jul;29(7):1378-85.

20. Araki, H., K. Suemaru, and Y. Gomita, *Neuronal nicotinic receptor and psychiatric disorders: functional and behavioral effects of nicotine.* Jpn J Pharmacol. 2002 Feb;88(2):133-8.
21. Coe, J.W., et al., *Varenicline: an alpha4beta2 nicotinic receptor partial agonist for smoking cessation.* J Med Chem. 2005 May 19;48(10):3474-7.
22. Hogg, R.C. and D. Bertrand, *Neuronal nicotinic receptors and epilepsy, from genes to possible therapeutic compounds.* Bioorg Med Chem Lett. 2004 Apr 19;14(8):1859-61.
23. Hille, B., *Ion Channels of Excitable Membranes (3rd Edition)* 2001.
24. Colquhoun, D., *Binding, gating, affinity and efficacy: the interpretation of structure- activity relationships for agonists and of the effects of mutating receptors.* Br J Pharmacol, 1998. **125**(5): p. 924-47.
25. Xiu, X., et al., *A unified view of the role of electrostatic interactions in modulating the gating of Cys loop receptors.* J Biol Chem. 2005 Dec 16;280(50):41655-66. Epub 2005 Oct 10.
26. Smit, A.B., et al., *Acetylcholine-binding proteins: functional and structural homologs of nicotinic acetylcholine receptors.* J Mol Neurosci. 2006;30(1-2):9-10.
27. Hansen, S.B., et al., *Structures of Aplysia AChBP complexes with nicotinic agonists and antagonists reveal distinctive binding interfaces and conformations.* EMBO J. 2005 Oct 19;24(20):3635-46. Epub 2005 Sep 29.
28. Celie, P.H., et al., *Crystal structure of nicotinic acetylcholine receptor homolog AChBP in complex with an alpha-conotoxin PnIA variant.* Nat Struct Mol Biol. 2005 Jul;12(7):582-8. Epub 2005 Jun 12.
29. Celie, P.H., et al., *Crystal structure of acetylcholine-binding protein from Bulinus truncatus reveals the conserved structural scaffold and sites of variation in nicotinic acetylcholine receptors.* J Biol Chem. 2005 Jul 15;280(28):26457-66. Epub 2005 May 16.
30. Bourne, Y., et al., *Crystal structure of a Cbtx-AChBP complex reveals essential interactions between snake alpha-neurotoxins and nicotinic receptors.* EMBO J. 2005 Apr 20;24(8):1512-22. Epub 2005 Mar 24.
31. Celie, P.H., et al., *Nicotine and carbamylcholine binding to nicotinic acetylcholine receptors as studied in AChBP crystal structures.* Neuron. 2004 Mar 25;41(6):907-14.
32. Smit, A.B., et al., *Structure and function of AChBP, homologue of the ligand-binding domain of the nicotinic acetylcholine receptor.* Ann N Y Acad Sci. 2003 Sep;998:81-92.
33. Brejc, K., et al., *Crystal structure of an ACh-binding protein reveals the ligand-binding domain of nicotinic receptors.* Nature. 2001 May 17;411(6835):269-76.
34. Mukhtasimova, N., C. Free, and S.M. Sine, *Initial coupling of binding to gating mediated by conserved residues in the muscle nicotinic receptor.* J Gen Physiol. 2005 Jul;126(1):23-39. Epub 2005 Jun 13.
35. Unwin, N., *Refined structure of the nicotinic acetylcholine receptor at 4A resolution.* J Mol Biol. 2005 Mar 4;346(4):967-89. Epub 2005 Jan 25.
36. Unwin, N., *Nicotinic acetylcholine receptor at 9 A resolution.* J Mol Biol. 1993 Feb 20;229(4):1101-24.
37. Unwin, N., *Acetylcholine receptor channel imaged in the open state.* Nature. 1995 Jan 5;373(6509):37-43.
38. Gay, E. and J.L. Yakel, *Gating of nicotinic ACh receptors; new insights into structural transitions triggered by agonist binding that induce channel opening.* J Physiol. 2007 Sep 6;.
39. Dellisanti, C.D., et al., *Crystal structure of the extracellular domain of nAChR alpha1 bound to alpha-bungarotoxin at 1.94 A resolution.* Nat Neurosci. 2007 Aug;10(8):953-62. Epub 2007 Jul 22.
40. Karlin, A. and M.H. Akabas, *Toward a structural basis for the function of nicotinic acetylcholine receptors and their cousins.* Neuron. 1995 Dec;15(6):1231-44.
41. England, P.M., et al., *Backbone mutations in transmembrane domains of a ligand-gated ion channel: implications for the mechanism of gating.* Cell. 1999 Jan 8;96(1):89-98.
42. Sine, S.M. and A.G. Engel, *Recent advances in Cys-loop receptor structure and function.* Nature. 2006 Mar 23;440(7083):448-55.

43. Lummis, S.C., et al., *Cis-trans isomerization at a proline opens the pore of a neurotransmitter-gated ion channel.* Nature. 2005 Nov 10;438(7065):248-52.
44. Lee, W.Y. and S.M. Sine, *Principal pathway coupling agonist binding to channel gating in nicotinic receptors.* Nature. 2005 Nov 10;438(7065):243-7.
45. Schofield, C.M., A. Jenkins, and N.L. Harrison, *A Highly Conserved Aspartic Acid Residue in the Signature Disulfide Loop of the $\alpha 1$ Subunit Is a Determinant of Gating in the Glycine Receptor.* J. Biol. Chem., 2003. **278**(36): p. 34079-34083.
46. Kash, T.L., et al., *Evaluation of a proposed mechanism of ligand-gated ion channel activation in the $GABA_A$ and glycine receptors.* Neurosci Lett, 2004. **371**: p. 230-234.
47. Kash, T.L., et al., *Coupling of agonist binding to channel gating in the GABA(A) receptor.* Nature, 2003. **421**(6920): p. 272-5.
48. Kash, T.L., et al., *Charged Residues in the β_2 Subunit Involved in $GABA_A$ Receptor Activation.* J. Biol. Chem., 2004. **279**(6): p. 4887-4893.
49. Grosman, C., M. Zhou, and A. Auerbach, *Mapping the conformational wave of acetylcholine receptor channel gating.* Nature. 2000 Feb 17;403(6771):773-6.
50. Purohit, P., A. Mitra, and A. Auerbach, *A stepwise mechanism for acetylcholine receptor channel gating.* Nature. 2007 Apr 19;446(7138):930-3.
51. Zhou, Y., J.E. Pearson, and A. Auerbach, *Phi-value analysis of a linear, sequential reaction mechanism: theory and application to ion channel gating.* Biophys J. 2005 Dec;89(6):3680-5. Epub 2005 Sep 23.
52. Chakrapani, S., T.D. Bailey, and A. Auerbach, *Gating dynamics of the acetylcholine receptor extracellular domain.* J Gen Physiol. 2004 Apr;123(4):341-56.
53. Chakrapani, S. and A. Auerbach, *A speed limit for conformational change of an allosteric membrane protein.* Proc Natl Acad Sci U S A. 2005 Jan 4;102(1):87-92. Epub 2004 Dec 23.
54. Rodriguez, E.A., H.A. Lester, and D.A. Dougherty, *In vivo incorporation of multiple unnatural amino acids through nonsense and frameshift suppression.* Proc Natl Acad Sci U S A. 2006 Jun 6;103(23):8650-5. Epub 2006 May 25.
55. Rodriguez, E.A., H.A. Lester, and D.A. Dougherty, *Improved amber and opal suppressor tRNAs for incorporation of unnatural amino acids in vivo. Part 1: Minimizing misacylation.* RNA. 2007 Oct;13(10):1703-14. Epub 2007 Aug 13.
56. England, P.M., *Unnatural amino acid mutagenesis: a precise tool for probing protein structure and function.* Biochemistry. 2004 Sep 21;43(37):11623-9.
57. Dougherty, D.A., *Cys-Loop Neuroreceptors: Structure to the Rescue?* Chemical Reviews, 2008. **In press**.
58. Dougherty, D.A., *Unnatural amino acids as probes of protein structure and function.* Curr Opin Chem Biol. 2000 Dec;4(6):645-52.
59. Nowak, M.W., et al., *Nicotinic receptor binding site probed with unnatural amino acid incorporation in intact cells.* Science, 1995. **268**(5209): p. 439-442.
60. Monahan, S.L., H.A. Lester, and D.A. Dougherty, *Site-specific incorporation of unnatural amino acids into receptors expressed in Mammalian cells.* Chem Biol. 2003 Jun;10(6):573-80.
61. Noren, C.J., et al., *A general method for site-specific incorporation of unnatural amino acids into proteins.* Science, 1989. **244**(4901): p. 182-188.
62. Cload, S.T., et al., *Development of improved tRNAs for in vitro biosynthesis of proteins containing unnatural amino acids.* Chem Biol. 1996 Dec;3(12):1033-8.
63. Bain, J.D., et al., *Site-specific incorporation of nonnatural residues during in vitro protein biosynthesis with semisynthetic aminoacyl-tRNAs.* Biochemistry. 1991 Jun 4;30(22):5411-21.

64. Saks, M.E., et al., *An engineered Tetrahymena tRNAGln for in vivo incorporation of unnatural amino acids into proteins by nonsense suppression.* J Biol Chem. 1996 Sep 20;271(38):23169-75.
65. Noren, C.J., et al., *A general method for site-specific incorporation of unnatural amino acids into proteins.* Science. 1989 Apr 14;244(4901):182-8.
66. Kohrer, C., et al., *Import of amber and ochre suppressor tRNAs into mammalian cells: a general approach to site-specific insertion of amino acid analogues into proteins.* Proc Natl Acad Sci U S A. 2001 Dec 4;98(25):14310-5. Epub 2001 Nov 20.
67. Rodriguez, E.A., H.A. Lester, and D.A. Dougherty, *Improved amber and opal suppressor tRNAs for incorporation of unnatural amino acids in vivo. Part 2: Evaluating suppression efficiency.* RNA. 2007 Oct;13(10):1715-22. Epub 2007 Aug 13.
68. Hohsaka, T., et al., *Incorporation of Nonnatural Amino Acids into Streptavidin through In Vitro Frame-Shift Suppression.* J. Am. Chem. Soc., 1996. **118**(40): p. 9778-9779.
69. Sisido, M. and T. Hohsaka, *Introduction of specialty functions by the position-specific incorporation of nonnatural amino acids into proteins through four-base codon/anticodon pairs.* Appl Microbiol Biotechnol. 2001 Oct;57(3):274-81.

C h a p t e r 2

A UNIFIED VIEW OF THE ROLE OF ELECTROSTATIC INTERACTIONS IN MODULATING THE GATING OF CYS LOOP RECEPTORS

2.1 Abstract

In the Cys loop superfamily of ligand-gated ion channels, a global conformational change, initiated by agonist binding, results in channel opening and the passage of ions across the cell membrane. The detailed mechanism of channel gating is a subject that has lent itself to both structural and electrophysiological studies. Here we defined a gating interface that incorporates elements from the ligand binding domain and transmembrane domain previously reported as integral to proper channel gating. An overall analysis of charged residues within the gating interface across the entire superfamily showed a conserved charging pattern, although no specific interacting ion pairs were conserved. We utilized a combination of conventional mutagenesis and the high-precision methodology of unnatural amino acid incorporation to study extensively the gating interface of the mouse muscle nicotinic acetylcholine receptor. We found that charge reversal, charge neutralization, and charge introduction at the gating interface are often well tolerated. Furthermore, based on our data and a re-examination of previously reported data on γ-aminobutyric acid, type A, and glycine receptors, we concluded that the

* This chapter is reproduced from *A Unified View of the Role of Electrostatic Interactions in Modulating the Gating of Cys Loop Receptors*, by X. Xiu, A. P. Hanek, J. Wang, H. A. Lester, and D. A. Dougherty, *The Journal of Biological Chemistry, 280, 50, 41655-41666 (2005).*

overall charging pattern of the gating interface, and not any specific pairwise electrostatic interactions, controls the gating process in the Cys loop superfamily.

2.2 Introduction

The Cys loop superfamily of neurotransmitter-gated ion channels plays a prominent role in mediating fast synaptic transmission. Receptors for acetylcholine (nicotinic ACh receptor, nAChR), serotonin (5-HT_3 receptor), γ-aminobutyric acid ($GABA_A$ and $GABA_C$ receptors), and glycine are known, and the receptors are classified as excitatory (cation-conducting; nAChR and 5-HT_3) or inhibitory (anion-conducting; GABA and glycine). Malfunctions in these receptors are responsible for a number of "channelopathies", and the receptors are targets of pharmaceutical efforts toward treatments for a wide range of neurological disorders, including Alzheimer's disease, Parkinson's disease, addiction, schizophrenia, and depression [1, 2]. The receptors share a common architecture, are significantly homologous, and are known to have evolved from a single ancestral gene that coded for an ACh receptor.

The gating mechanism for the Cys loop superfamily is one of the most challenging questions in molecular neuroscience. At issue is how the binding of a small-molecule neurotransmitter can induce a structural change in a large, multisubunit, integral membrane protein sufficient to open (gate) a previously closed ion channel contained within the receptor [3, 4]. All evidence indicates that the neurotransmitter binding site is quite remote (50-60Å) from the channel gate, the region that blocks the channel when the neurotransmitter is absent and that must move to open the channel.

The quest for a gating mechanism has been greatly aided by several recent structural advances. First, crystal structures of the soluble acetylcholine binding protein (AChBP) [5-7], which is homologous to

the extracellular domain of the nAChR and, by extension, other members of the superfamily, provide a good sense of the layout of the agonist binding site and its relationship to the rest of the receptor. Second, continued refinement of cryoEM images of the *Torpedo* nAChR by Unwin [8-10], incorporating insights gained from the AChBP structure, has produced a full atomic-scale model, 2BG9, of the nAChR. It is important to appreciate from the outset that 2BG9, while heuristically quite valuable, is not a crystal structure of the nAChR. It is a model built from low-resolution data and homology modeling. Nevertheless, it represents a substantial advance for the field, and all modern attempts to obtain molecular-scale information on the structure and function of Cys loop receptors must consider this as a starting point.

The full 2BG9 model of the nAChR [10] immediately suggested ways in which the agonist binding site could couple to the transmembrane region and thus initiate gating. As summarized in Figure 2.1, loops 2, 7, and 9 from the AChBP structure are oriented toward the transmembrane region, and, indeed, in 2BG9 these loops make contacts with parts of the transmembrane domain. Note that loop 7 is the eponymous Cys loop. The transmembrane region consists of four α helices per subunit, labeled M1-M4. It is accepted that M2 lines all or most of the channel. Helix M1 extends out of the transmembrane region toward the extracellular domain, creating a segment termed preM1. While M4 is somewhat separated from the rest of the protein in 2BG9, recent modeling studies produce a more compact structure in which M4 is more intimately involved [11]. In particular, the C-terminus of M4, a region we will term postM4, can contact the extracellular domain. A key structure is the M2-M3 loop, a short connector between the two transmembrane helices. Topological considerations have long placed this loop at the interface between the transmembrane and extracellular domains. That expectation was resoundingly confirmed by 2BG9, and many workers have anticipated that this loop could play an important role in gating. Indeed, recent work [12] has established that a key proline at

the apex of the M2-M3 loop provides the conformational switch that gates the channel in the 5-HT_3 receptor.

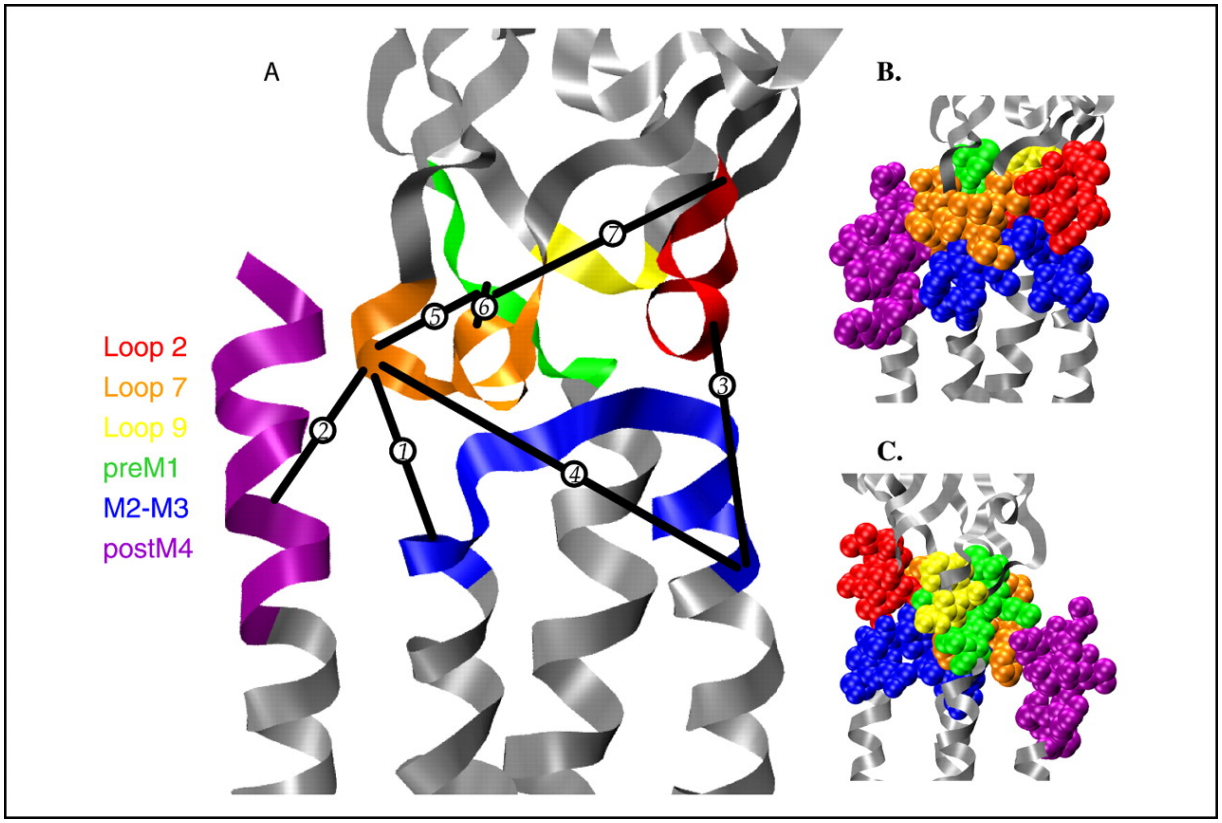

Figure 2.1 Views of the gating interface. Structure is the full model of an α subunit of the *Torpedo* nAChR developed by Unwin [10] (Protein Data Bank code 2BG9). Regions of the gating interface, as defined in text, are color-coded. A: Ribbon diagram, also including pairwise interactions from various studies that have been proposed to contribute to the gating mechanism. Even though they are from different receptors and could be important in different states of the receptor, they are mapped onto the *Torpedo* structure to provide some sense of relative spatial relationships. Distances range from ~ 6 to ~ 20 Å. Interactions are as follows: *1*, Asp-138 to Lys-276 of muscle α nAChR; *2*, Asp-138 to Arg-429 of muscle α nAChR; *3*, Asp-57 to Lys-279 of $GABA_A$ α1 subunit; *4*, Asp-149 to Lys-279 of $GABA_A$ α1 subunit; *5*, Lys-215 to Asp-146 of $GABA_A$ β2 subunit; *6*, Lys-215 to Asp-139 of $GABA_A$ β2 subunit; and *7*, Lys-215 to Asp-56 of $GABA_A$ β2 subunit. Interactions *1*, *2*, *4*, and *5* all involve the same highly conserved Asp residue in loop 7. See text for discussion of these interactions. B: Same view as A but with gating interface residues in space filling. C: View in *B* rotated 180° around vertical axis.

Several groups have attempted to identify key interactions in the interface between the extracellular domain and the transmembrane domain, and we discuss some of these results below. This interface contains a large number of charged residues, and most efforts have focused on these, attempting to find crucial electrostatic interactions that regulate gating. Specific hydrophobic interactions have also been proposed [9, 13]. Several interacting pairs have been identified in various receptors [14, 15], and specific gating models based on critical electrostatic interactions have been proposed [16-19]. We note from the start, however, the curious fact that *none* of the proposed interactions is conserved across the superfamily. We have been puzzled by the notion that in this closely related family of receptors, the mechanism of action of the essential function of the receptors seems to vary from system to system.

In the present work we argue that specific, pairwise electrostatic interactions at the interface between the transmembrane and extracellular domains are not critical to gating. Rather, we argue it is the global charging of this region and the network of interacting ionic residues that are critical to receptor function. We present an overall analysis of charged interfacial residues in the Cys loop superfamily; extensive mutagenesis studies of potential electrostatic interactions in the nAChR; and a reconsideration of previously published data on other receptors to support the model. From such an analysis, a more nearly unified, but less precise, image of the gating mechanism in the Cys loop superfamily emerges.

2.3. Results

2.3.1 Electrostatics at the gating interface

For the purposes of discussion and analysis, we have defined a "gating interface" between the extracellular domain and the transmembrane domain. It is comprised of six segments: three from the extracellular domain (all or parts of loops 2, 7, and 9) and three from the transmembrane domain (preM1, M2-M3, and postM4). The precise residues considered are given in Table 2.1. Unless otherwise noted, we will use the residue numbering system accepted for the nAChR α1 subunit. The selection criterion for the gating interface was geometric; only residues that could reasonably be considered to experience a meaningful electrostatic interaction with another component of the gating interface were included. Because of the low resolution of the nAChR structure and the further uncertainty introduced by extrapolating to other Cys loop receptors, precise distance constraints were not applied. Rather, as illustrated in Figure 2.1, we chose a contiguous belt of residues in the region where the extracellular and transmembrane domains meet. Some leeway must be given in selecting possible interactions, as residues that are not in direct contact in 2BG9 could become so on transit from the closed state to the open, or on going from one receptor to another. We recognize there is some arbitrariness to this assignment, but our studies suggest that extending the definition further out from the interface does not significantly impact the analysis. We will refer to the extracellular component (from loops 2, 7, and 9) and the transmembrane component (from preM1, M2-M3, and postM4) when discussing the gating interface.

To search for patterns of charged residues, we considered the sequences of 124 subunits from the Cys loop superfamily - 74 cationic and 50 anionic channel subunits (see supplementary table S2.1 at the end of this chapter). Table 2.1 shows 22 representative subunits, 11 cationic (excitatory) channels

and 11 anionic (inhibitory) channels, and also serves to define the various segments. Table 2.2 summarizes the analysis of the full collection of the 124 subunits. Shown for each segment of the interface are: the number of cationic residues (K, R); the number of anionic residues (D, E); the net charge (Z); and the number of charged residues (N).

	Loop 2	Loop 7	L9	preM1	M2-M3 linker	postM4
Tor α	DEVNQI	IIVTHFPFDQ	EW	MQIRP	STSSAVPLIGKY	FAGRLIELSQEG
Tor β	NEKIEE	IKVMYFPFDW	QW	IQRKP	ETSLSVPIIIRY	FLDASHNVPPDN
Tor γ	NEKEEA	IAVTYFPFDW	EW	IQRKP	ETSLNVPLIGKY	FLTGHFNQVPEF
Tor δ	KETDET	INVLYFPFDW	EW	IRRKP	ETALAVPLIGKY	FVMGNFNHPPAK
nACh α1	DEVNQI	IIVTHFPFDE	EW	MQRLP	STSSAVPLIGKY	FAGRLIELHQQG
nACh β1	NEKDEE	IQVTYFPFDW	QW	IRRKP	ETSLAVPIIIKY	FLDATYHLPPPE
nACh γ	NEREEA	ISVTYFPFDW	EW	IQRKP	ETSQAVPLISKY	FLMAHYNQVPDL
nACh δ	KEVEET	ISVTYFPFDW	EW	IRRKP	ATSMAIPLVGKF	FLQGVYNQPPLQ
nACh α4	DEKNQM	IDVTFFPFDQ	EW	IRRLP	STSLVIPLIGEY	FLPP--WLAGMI
nACh α7	DEKNQV	IDVRWFPFDV	EW	MRRRT	ATSDSVPLIAQY	LMSAPNFVEAVS
5HT3A	DEKNQV	LDIYNFPFDV	EW	IRRRP	ATAIGTPLIGVY	VMLWSIWQYA--
GABA α1	SDHDME	MHLEDFPMDA	QY	LKRKI	KVAYATAM-DWF	LNREPQLKAPTP
GABA α2	SDTDME	MHLEDFPMDA	QY	LKRKI	KVAYATAM-DWF	LNREPVLGVSP-
GABA α3	SDTDME	MHLEDFPMDV	QY	LKRKI	KVAYATAM-DWF	VNRESAIKGMIR
GABA α4	SDVEME	MRLVDFPMDG	QY	LRRKM	KVSYLTAM-DWF	LSKDTMEKSESL
GABA α5	SDTEME	MQLEDFPMDA	QY	LKRKI	KVAYATAM-DWF	LNREPVIKGAAS
GABA α6	SDVEME	MRLVNFPMDG	QY	LQRKM	KVSYATAM-DWF	LSKDTMEVSSSV
GABA β1	SEVNMD	MDLRRYPLDE	QF	LKRNI	KIPY-VKAIDIY	VN----------
GABA β2	SEVNMD	MDLRRYPLDE	QF	LKRNI	KIPY-VKAIDMY	VN----------
GABA β3	SEVNMD	MDLRRYPLDE	QF	LKRNI	KIPY-VKAIDMY	VN----------
Gly α1	AETTMD	MDLKNFPMDV	QF	LERQM	KVSY-VKAIDIW	KIVRREDVHNQ-
Gly α2	TETTMD	MDLKNFPMDV	QF	LERQM	KVSY-VKAIDIW	KIIRHEDVHKK-
	44 49	130 139	175	207 211	266 277	426

Table 2.1 Selected sequences in the gating interface, highlighting cationic (blue) and anionic (red) residues. The abbreviations used are as follows Tor: nAChR from *Torpedo californica*; nACh: nicotinic ACh receptor; 5-HT_3A: 5-HT_3 receptor, type A. All sequences are from human receptors except: Tor and nACh α1, β1, γ, δ, which are mouse muscle.

	+	–	Z	N
Loop 2	0.5	2.3	-1.8	2.8
Loop 7	0.4	1.9	-1.5	2.4
Loop 9	0.0	0.5	-0.5	0.5
preM1	2.3	0.1	2.2	2.3
M2-M3	1.0	0.8	0.2	1.8
postM4	0.6	0.7	-0.1	1.3
Extracellular	0.9	4.8	-3.9	5.7
Transmembrane	3.9	1.6	2.3	5.5
Gating Interface	4.8	6.4	-1.6	11.1

Table 2.2 Charge characteristics of the gating interface. The abbreviations used are as follows: **+** = number of cationic residues (K, R); **–** = number of anionic residues (D, E); **Z** = overall charge; **N** = number of ionic residues.

Although there is some variation, the typical gating interface contains 47 residues: 18 in the extracellular component and 29 in the transmembrane component. On average, 11.1 or 24% of these residues are charged. This is not significantly different from expectation based on the overall frequencies of occurrence of D, E, R, and K in proteins (July, 2004, Swiss Protein Database). Most of the residues of the gating interface are, or can be easily imagined to be, water exposed to some extent, therefore this global result is not surprising. Of the ~11 charged residues found in the gating interface only two are universally conserved: D138 and R209. So, while all Cys loop receptors have a large number of ionic residues in the gating interface, their locations and absolute charges are variable.

Although the two regions of the gating interface do not have the same number of amino acids, the total number of charges is essentially the same (5.7 vs. 5.5) for the two regions. There is, however, a dramatic difference in the net charge of the two components. The extracellular component has an overall negative charge, averaging -3.9 over the 124 subunits considered. The transmembrane component has an overall positive charge, averaging +2.3. Thus, there is a *global* electrostatic attraction in the interface, holding together the extracellular component and the transmembrane component. This interfacial electrostatic interaction is not created by simply putting anions in the extracellular component and cations in the transmembrane component; typically, there are one cationic and five anionic side chains in the extracellular component, but four cationic and two anionic side chains in the transmembrane component. We propose that it is the balance among all these charges that controls receptor function. With all these charges packed into a fairly compact space, we feel it is more reasonable to consider a network of electrostatic interactions, rather than emphasizing any particular charged pair, as we will discuss below.

There is variability in the charging pattern. Considering only $GABA_A$ subunits, α1 shows Z = -6 in the extracellular component, and Z = +4 in the transmembrane component. In contrast, the α4 subunit shows Z = -4 in the extracellular component and Z = +2 in the transmembrane component. Despite the smaller Z values, the α4 subunit actually has more ionic residues overall than α1 (N = 16 vs. 14).

Looking in more detail, it is clear that loop 2 carries the most negative charge per residue, followed by loop 7. The largest net positive charge is associated with preM1. The total number of charges (N) is slightly larger for the inhibitory channels (average of 11.8 vs. 10.7). The "additional charge" is usually cationic, as the net charge is slightly more positive for the inhibitory channels (-1.1 vs. -1.9).

We propose that Cys loop receptors can function as long as the essential features of the electrostatic network are intact. As we will see below, mutations that alter the charge balance are often well tolerated, apparently because they can be absorbed by the larger collection of charges. In fact full charge reversals (replacing a plus with a minus or vice versa) are often quite acceptable. It appears that the important thing is to have a number of charges in this region, rather than any specific interaction.

2.3.2 Studies of the muscle-type nAChR α subunit

We have evaluated a number of residues in the gating interface by both conventional mutagenesis and unnatural amino acid mutagenesis [20]. Many mutations are meant to parallel studies in other receptors, but, as noted above, conservation is not strong across the family. We study the embryonic mouse muscle nAChR, with a subunit composition of $(\alpha 1)_2\beta 1\gamma\delta$. This receptor shows extremely high homology with and is thus directly comparable to the *Torpedo* receptor modeled by 2BG9. A goal of this work is to conduct an extensive survey of the gating interface, complementing the statistical analysis presented above. As such, we report the results of two-electrode voltage clamp determinations of EC_{50}, rather than the more time-consuming patch clamp studies of single-channel behaviors. Since EC_{50} is a measure of channel function, it reflects contributions from agonist binding and gating. However, the residues studied are not part of the agonist binding site, and so seem unlikely to directly contribute to binding. Furthermore, we show that representative mutations in the gating interface alter the relative efficacy of succinylcholine, a partial agonist of the mouse muscle nAChR [21], supporting a change in the gating of the mutants [14, 22]. In addition, we recently showed that a range of mutations of a key proline at the heart of the gating interface in the M2-M3 loop of the $5HT_{3A}$ receptor significantly affected EC_{50}, but did not alter the binding properties of the receptor, establishing a role in gating [12]. Extensive mutagenesis studies by Auerbach [23] on loops 2 and 7 show that mutations of the sort considered here affect the gating equilibrium. As such, we conclude that the most reasonable interpretation of the changes in EC_{50} reported here is that they reflect alterations in channel gating behavior.

Our primary focus has been on the α subunits, as these make the largest contribution to the agonist binding site and are thought to play a prominent role in the gating mechanism [24]. In this section all

mutations occur in both copies of the mouse muscle α subunit; the results are given in Table 2.3. In a subsequent section we will briefly discuss the non-α subunits.

The 2BG9 model features a particularly intimate interfacial interaction: that between V46 on loop 2 and a portion of the M2-M3 loop [9]. A "pin-into-socket" arrangement was proposed, ascribing a critical gating role to V46. While it was immediately appreciated by many workers that V46 is not conserved in the Cys loop superfamily, the proposal merited investigation. Studies by Harrison, Trudell, and coworkers on analogous residues in the $GABA_A$ α1 and β2 subunits and the glycine receptor α1 subunit (the residue is H, V, and T, respectively) provided no support for the "pin-into-socket" proposal [13].

We have explicitly evaluated V46 in the nAChR (Table 2.3). We wished to determine whether a precise geometrical arrangement of the sort implied by a pin-into-socket interaction was essential for proper receptor function. Not surprisingly, the V46A mutation is substantially deleterious, while the more subtle V46I mutant shows near wild type behavior.

mutant	EC_{50}	nH	mutant	EC_{50}	nH
Wild type	50 ± 2	1.6±0.1	D138K/R429D	50 ± 3	1.45±0.1
D44K	14.3 ± 0.6	1.4±0.1	D138R/R429E	LE	
D44N	20 ± 4	0.80± 0.08	D138E/R429K	63 ± 9	1.31±0.2
E45A	210 ± 20	1.1±0.1	D138K/K276D/R429D	67 ± 10	1.03±0.2
E45W	117 ± 7	1.3±0.1	K276D	45 ± 6	1.39±0.2
E45V	49 ± 4	1.9±0.2	K276E	38 ± 2	1.28±0.07
E45D	19.2 ± 0.5	1.4±0.1	K276D/R429D	51 ± 3	1.52±0.1
E45N	6.3 ± 0.1	1.4±0.1	R429D	57 ± 5	1.46±0.1
E45K	6.5 ± 0.3	1.4±0.1	R429E	69 ± 5	1.29±0.09
E45Q	1.9 ± 0.1	1.3±0.1	R429K	83 ± 4	1.48±0.09
E45R	1.6 ± 0.1	1.0±0.1	R429A	90 ± 4	1.48±0.08
V46A	>1000	1.6±0.1	S266K	62 ± 6	1.54±0.2
V46I	59 ± 7	1.1±0.1	T267A	36 ± 5	1.94±0.4
V46*allo*-I	48 ± 2	1.7 ± 0.1	T267D	24 ± 2	1.21±0.1
V46OMeT	169 ± 9	1.4 ± 0.1	T267K	26 ± 2	1.35±0.05
V46OMe-*allo*-T	32 ± 2	1.5 ± 0.1	T267OMeT	200 ± 10	1.37±0.1
V46T	>1000	1.4±0.1	S268D	0.59 ± 0.02	1.82±0.09
V46K	0.94 ± 0.07	1.5±0.1	S268E	0.18 ± 0.01	1.56±0.1
V46R	120 ± 10	1.4 ±0.1	S268K	7.5 ± 1	1.36±0.2
V46D	>1000		S269D	12 ± 0.5	1.56±0.08
V46E	>1000		S269E	0.08 ± 0.01	1.34±0.2
E45K/V46D	>1000		S269K	9 ± 0.6	1.22±0.08
E45K/V46E	>1000		S269OMeS	23±2	1.79±0.3
E45R/V46D	NE		R209A	NE	
E45R/V46E	NE		R209D	NF	
D138A	NF		R209E	NF	
D138R	NF		R209K	18 ± 1	1.66±0.2
D138K	NF		D138K/R209D	NF	
D138S	NF		D138R/R209D	NS	
D138N	NF		E175R	120 ± 7	1.35±0.08
D138E	28 ± 2	1.45±0.1	E175R/R209E	NS	
D138K/K276D	66 ± 10	1.01±0.1	E45R/R209E	NS	

Table 2.3 Mutations in the nAChR α subunits. EC_{50} in μM. Key: NF: nonfunctional; no response to applied ACh, but surface expression of receptor confirmed by α-bungarotoxin binding; LE: functional; responses to applied ACh are seen, but are too weak to obtain EC_{50}; NS: no signal; no response to applied ACh, surface expression not independently verified; NE: no expression, as judged by lack of α-bungarotoxin binding.

An advantage of the unnatural amino acid methodology is that it allows subtle stereochemical issues to be probed. If a V or, by extension, I side chain at position 46 points into a well-defined

binding pocket, one might anticipate that the isomeric *allo*-I, in which the side chain methyl and ethyl groups swap position relative to I, would show a significantly different interaction. In the event, the difference between I and *allo*-I is insignificant (Table 2.3). The unnatural amino acid O-methyl-threonine (OMeT) is isosteric with I, but inserts a more polar O in place of a CH_2 group [25]. This subtle change is deleterious, raising EC_{50} more than 3-fold. The isomeric OMe-*allo*-T introduces a stereochemical swap that parallels the I/*allo*-I pair, but now the effect is substantial. The difference between OMeT and OMe-*allo*-T is roughly 5-fold, corresponding to 1 kcal/mol at room temperature. This suggests that perhaps the side chain of position 46 is in a sterically well-defined pocket, but one that can only be probed by polar oxygen atoms, not by hydrophobic groups such as CH_2.

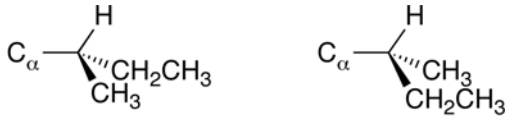

I

allo-I

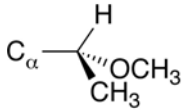

O-Me-T

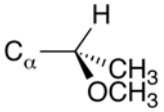

O-Me-*allo*-T

Replacing V46 with much more polar groups like T (essentially isosteric to V) and the anionic D and E seriously compromises receptor function. Radiolabeled α-bungarotoxin binding studies show that V46D and V46E channels are expressed in large enough quantities to detect macroscopic currents, but electrophysiology studies show only small (< 300 nA) currents at 1 mM ACh, suggesting a shift to a much higher EC_{50}. Surprisingly, though, the cationic residues R and K produce, in the first case, only a modest rise in EC_{50}, while the V46K mutant gives an EC_{50} ~50-fold *below* wild type. The V46K

mutation of the nAChR α1 subunit produces a loop 2 pattern equivalent to those of the α7 and α4 nicotinic and 5-HT_3 serotonin receptors, and so perhaps it is not surprising that it can be tolerated.

We have sought a correlation between various physicochemical properties of the mutant side chains and the mutant EC_{50}s at V46 (Figure 2.2) and find that there is no apparent correlation to the side chain hydrophobicity [26, 27] or size [28, 29]. Auerbach *et al*. previously reported single channel recordings on several mutations at V46, and a very rough tendency was observed that more polar side chains have smaller gating equilibrium constants [23]. However, the new mutations that we made, V46K and V46R, do not follow this pattern. Our results suggest that while the side chain of V46 may be docked into a sterically well-defined pocket as implied by the "pin-into-socket" mechanism, a full description of the role V46 plays in gating is more complicated.

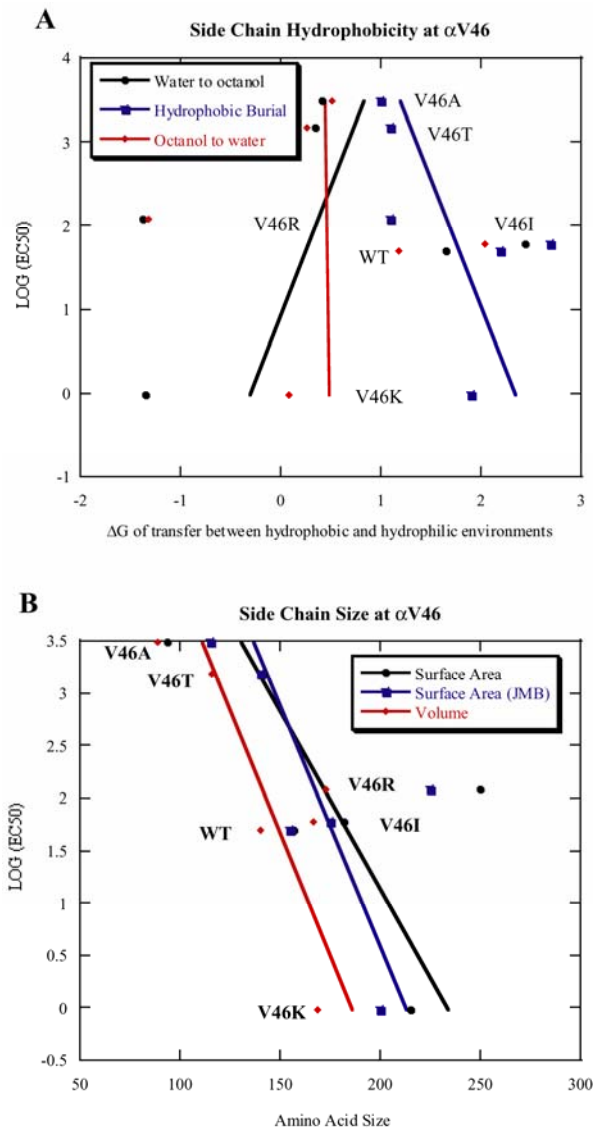

Figure 2.2 Plot of log(EC_{50}) vs. side chain physicochemical properties at site αV46. A: log(EC_{50}) vs. side chain hydrophobicity. B: log(EC_{50}) vs. side chain size. Three hydrophobicity scales were used. Hydrophobicity is measured as the change in free energy upon transfer from water to octanol (R=0.26), hydrophobic burial (R=0.58), and transfer from octanol to water (R=0.011). Attempts to explain EC50 shifts for aV46 mutants by changes in side chain size according to two measures of surface area (R=0.667, 0.674 respectively) as well as volume (R=0.782) resulted in no significant correlation.

As noted above, Loop 2 is highly charged across the Cys loop superfamily, with an overall negative charge. As others have done in different receptors within the superfamily, we have evaluated some of these charged residues. Position 45 is very highly conserved as anionic (D or E), and our studies of E45 in the muscle α subunit are summarized in Figure 2.3. Quite surprisingly, we find that full charge reversal (E45K or E45R) substantially *lowers* EC_{50}. Substitution by a neutral, but polar residue (E45Q or E45N) also lowers EC_{50}, while conversion to a hydrophobic residue gives a small effect, raising EC_{50}, if anything. The logarithms of the mutant EC_{50} at E45 were plotted against the physicochemical properties of the mutant side chains as done for V46, and no apparent correlation was found (Figure 2.4).

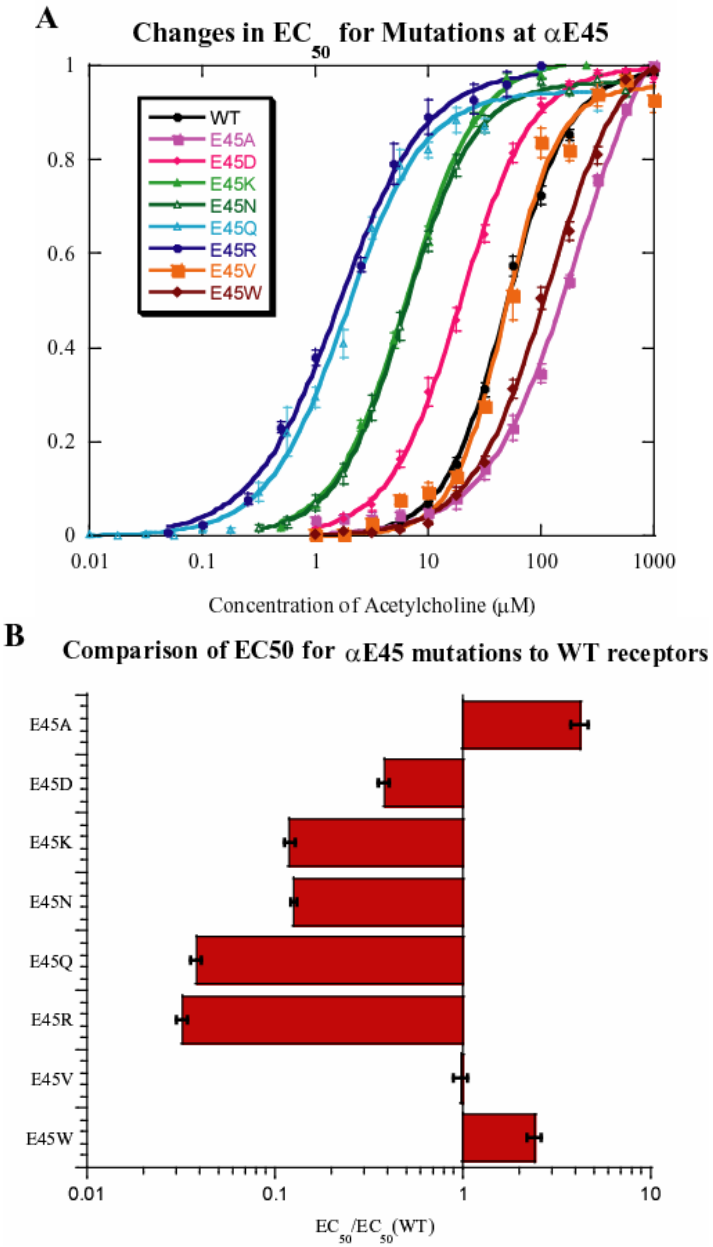

Figure 2.3 A variety of mutations at αE45 are well tolerated. Charge neutralization (N,Q) and charge reversal (K,R) both lower EC_{50} substantially, while mutations to hydrophobic residues (A,W,V) leave EC_{50} little changed. A: Dose-response curves. B: Ratios of mutant to wild type EC_{50}s plotted for comparison.

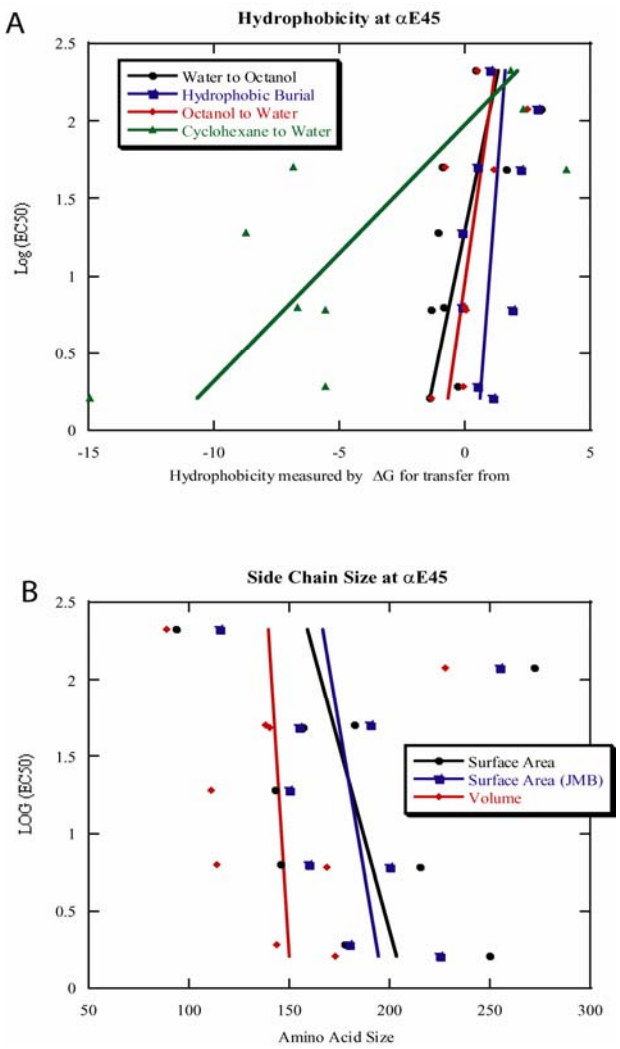

Figure 2.4 Plot of log(EC_{50}) vs. side chain physicochemical properties at site αE45. A: log(EC_{50}) vs. side chain hydrophobicity. B: log(EC_{50}) vs. side chain size. Four hydrophobicity scales were utilized: transfer from water to octanol (R=0.64), octanol to water (R=0.63), cyclohexane to water (R=0.78), and hydrophobic burial (R=0.36). Two measures of surface area (R=0.29, 0.24) as well as a volume scale (R=0.09) were used.

D44 is conserved in nicotinic α subunits, and position 44 is generally a polar residue in other nicotinic subunits and other receptors. Although the D44 side chain points in the opposite direction to the E45 side chain in 2BG9, the mutation pattern is similar. Both charge reversal and introducing a neutral but polar side chain lower EC_{50}.

N47 in loop 2 of the nAChR α subunit aligns with D57 of the $GABA_A$ α1 subunit, which, as discussed below, has been proposed to experience important electrostatic interactions [15]. Auerbach and co-workers have studied mutations at this site in the nAChR, including extensive single-channel measurements [23]. Auerbach found that N47K shows a decrease in EC_{50}, but N47D shows an increase. As noted above, Auerbach's single-channel studies of this and other loop 2 residues establish a role in setting the gating equilibrium for residues in this region.

Thus, at four consecutive residues in loop 2 – D44, E45, V46, and N47 – introducing a positive charge lowers EC_{50}. At N47 and V46 it has also been shown that introducing a negative charge has the opposite effect. These various side chains point in quite different directions in 2BG9. While is it possible that all make specific electrostatic contacts that are being modulated in similar ways by the mutations introduced, we conclude instead that it is the global negative charge of loop 2, not any specific pairwise interaction, that is essential to proper receptor function.

D138 on loop 7 is completely conserved in the Cys loop superfamily. Others have investigated this site in other receptors [14, 15, 23]. In the nAChR α subunit, charge reversal at this site incapacitates the receptor. Both D138K and D138R give non-functional receptors, in that no response to ACh is seen but labeling with radioactive α-bungarotoxin shows that properly assembled receptors have reached the surface. Furthermore, milder disruptions of D138 such as mutation to N, A, or S also give non-functional receptors. The charge-conserving mutation D138E, however, gives near wild type behavior. All evidence shows that a negative charge at this site is essential to form a functional receptor.

A classic test for a specific ion pair interaction is the charge swapping experiment. That is, if D138 experiences an electrostatic interaction with a specific cationic residue, then the non-functional mutant often can be "rescued" by converting the cationic partner to an anion. In the nAChR, we considered

two possible cationic partners to D138: K276 on M2-M3 and R429 on postM4 (pairwise interactions 1 and 2, respectively, in Figure 2.1 A). Both are reasonably close to D138 in 2BG9. Interestingly, the non-functional D138K mutant can be returned to essentially wild type behavior by combination with *either* K276D or R429D (Tables 2.1, and 2.3, Figure 2.5). This suggested that perhaps the 138/276/429 grouping should be considered as a charge triad, rather than a collection of pairwise interactions. As such, we evaluated all eight possible charge combinations for these three residues. The wild type is -/+/+ (138/276/429); the nonfunctional D138K/R mutants are +/+/+. The described double mutants that rescue the channel are +/+/- and +/-/+. In fact, all seven combinations other than the +/+/+ mutant give near wild type behavior (Figure 2.5). It appears that the 138/276/429 grouping can compensate for a range of charge patterns, as long as +/+/+ is avoided. It may seem surprising that the -/-/- combination is viable. If these residues are physically close, we can anticipate that having three negative charges in proximity would alter the effective pK_a of one or more residues. This could lead to protonation of a carboxylate side chain, and lessening of the electrostatic interaction. It is also possible that one or more water molecules mediate the interactions among 138/276/429. As will be discussed below, D138 appears to be associated with a different charge triad in the $GABA_A$ receptor.

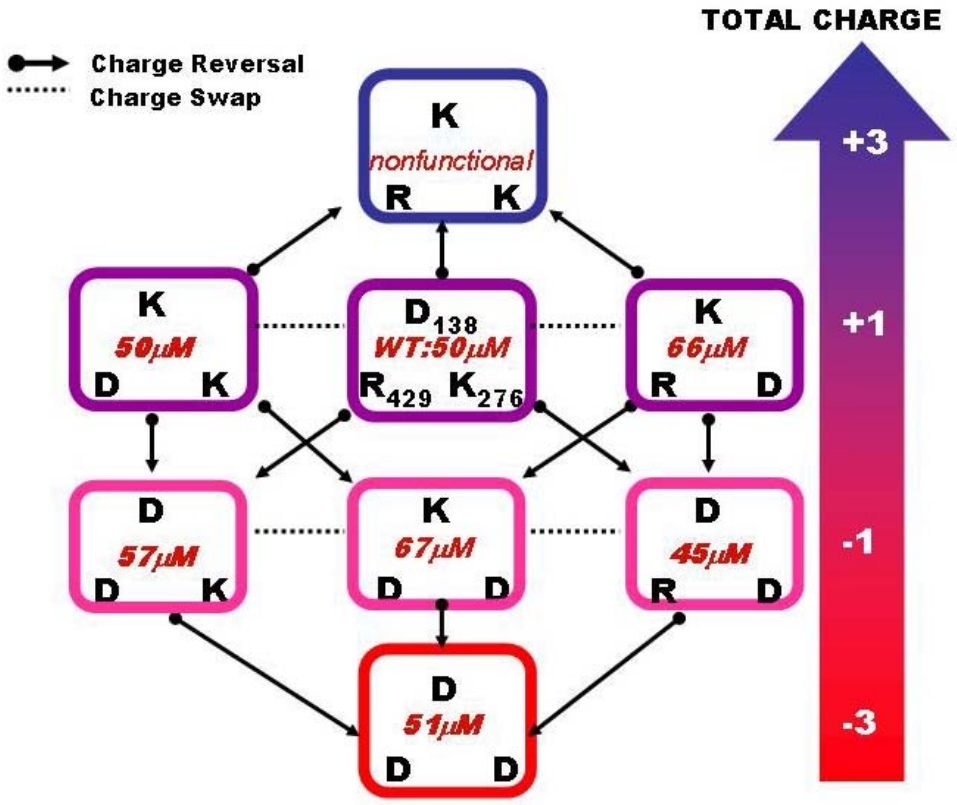

Figure 2.5 Charge reversal at αD138 of the nAChR is rescued by charge swap at either of two sites: R429 (postM4) or K276 (M2-M3). A charge triad is examined. Of the eight possible combinations, seven give near wild type behavior. Only the all-positive triad is deleterious.

Position 276 is conserved as a charged residue, either positive or negative, in the majority of ACh receptor subunits, but not in other members of the superfamily. Position 429 is often, but not always charged, being anionic in GABA receptors, cationic in glycine receptors, but neutral in nicotinic, non-α subunits. Thus, the triad considered here is most likely specific to nAChR α subunit. The M4 transmembrane helix is the furthest separated from the rest of the protein. In 2BG9, the C terminus of M4 is roughly 10 Å from the tip of loop 7. However, as mentioned above, computational studies move M4 closer to the rest of the protein and explicitly identify contacts between M4 and loop 7 [11]. Also, it has been proposed from the computational work that during channel opening, M4 of the α7 receptor moves closer to the other three transmembrane helices. In Auerbach's linear free energy relation (LFER) analysis, the movement of α M4 precedes that of α M2 [30]. Based on the observations reported here, we conclude that in the open state of the nAChR, R429 on postM4 is one of the electrostatic interaction partners of D138.

We have also studied other positions of the M2-M3 linker. Four consecutive hydroxyl-containing residues, STSS, appear at positions 266 to 269 of the nAChR α1 subunit. Various mutations at S266 and T267 do not shift EC_{50} significantly (Table 2.3). This includes mutations that would typically be considered fairly dramatic, in that a neutral residue is changed to an ionic residue. At T267, conversion to a positive charge or a negative charge both result in halving EC_{50}.

Position S269 has been probed previously by Auerbach, who reported that an S269I mutation causes an EC_{50} decrease of approximately 10-fold, mainly by increasing the channel opening rate constant [31]. Based on this observation, it was proposed that position 269 moves from a polar to a non-polar environment on channel opening, and so increasing hydrophobicity should favor the open state and

lower EC_{50}. To probe this further, we incorporated the unnatural amino acid O-methyl serine at position 269, an arguably more subtle way to reduce polarity than S269I. The mutant channel shows a 2-fold drop in EC_{50}, consistent with the expectation that an increase in hydrophobicity lowers EC_{50}, and the less perturbing Ser/OMeSer has a smaller effect.

Against this background, we were surprised to find that a change in the opposite direction - introducing either a positive or a negative charge at 269 – also lowers EC_{50}; S269D and S269K show 4-5-fold drops, while S269E shows an astonishing 600-fold drop in EC_{50}. Certainly, D, E, and K are more polar than S, and so these results contradict the just reached conclusion that hydrophobicity controls the behavior at 269. We see the same pattern for S268; S268D, S268E, and S268K all show lower EC_{50}s, with the E mutant again showing a very large drop. It is remarkable that at two consecutive sites in the M2-M3 loop, a region universally accepted to be involved in the gating transition, a serine can be converted to a cationic or an anionic residue and the result is the same – EC_{50} drops.

PreM1 provides the covalent connection between the extracellular and transmembrane domains in the primary sequence, and there are 1 to 4 positive charges in this region throughout the LGIC family. One R (R209 in the nAChR α1 subunit) is completely conserved. Mutation to glutamine at the analogous arginine in the glycine receptor α1 subunit causes hyperekplexia, an inherited neurological channelopathy, and greatly diminishes receptor function [32]. Among all the mutations at this site in the nAChR, only a charge-conserving mutation, R209K, gave a functional channel; charge reversal mutants were nonfunctional. In 2BG9 the R209 side chain projects between E175 on loop 9 and E45 on loop 2. Charge swapping experiments at this triad, however, show that the non-functional mutant R209E cannot be “rescued” by either E175R or E45R.

Loop 9 is located close to the transmembrane domain, between preM1 and loop2. Chimera studies in Cys loop family members have characterized it as an indispensable contributor to proper channel coupling and functioning [33]. In 2BG9 loop 9 has moved significantly closer to the transmembrane domain compared to the AChBP structure, suggesting that it is arranged differently when the transmembrane domain is present. Position 175 is located very close to the transmembrane domain and is counted as part of the charged interface. E175 is conserved in the majority of excitatory channel subunits, while in inhibitory channels it is frequently replaced by a Q. Mutation studies at this site show that a charge reversal increased the EC_{50}, but by a modest factor.

2.3.3 Studies of the muscle-type nAChR non-α subunits

We have evaluated a large number of charged residues in the non-α subunits (data not shown, but can be found in [34]). Typically, the changes seen in non-α subunits are not as dramatic as those seen in α. For instance, in loop 2, most of the charged residues are fairly tolerant of substitution, producing changes in EC_{50} usually 2-fold or less, in contrast to the 10-30-fold changes often seen in α. At almost every site charge reversal/neutralization is generally tolerated

While αD138K gives nonfunctional receptors that can be rescued by compensating charge-reversal mutations, D138K in β or δ subunits gives functional receptors with no large change in EC_{50}. The γD138K mutant gave very low currents in response to acetylcholine. Similarly, charge reversals in pre-M1 at R208, R209, or K210 are generally well tolerated in non-α subunits. Finally, charge reversal/neutralization is well tolerated throughout the M2-M3 region in non-α subunits. Almost all changes lower EC_{50}, but the effects are all less than 3-fold.

It is clear that, functionally, the non-α gating interfaces play a less important role than the α interfaces. Auerbach and coworkers concluded that, in the M2-M3 loop, homology in sequence does not coincide with homology in function [31], and mutations in the δ subunit do not affect gating, consistent with our observations [30, 35, 36]. From a structural perspective, however, the overall results from studies of non-α subunits highlight the remarkable tolerance of the gating interface. Dozens of charge reversal/neutralization perturbations are well tolerated, with the most common outcome being a small drop in EC_{50}. No evidence for highly specific, structurally or functionally important ion pair interactions is seen.

2.3.4 Studies of a partial agonist

To support our contention that mutations at the gating interface perturb the gating of the receptor rather than the agonist binding site, we measured the relative efficacy (ε) of succinylcholine (SuCh), an nAChR partial agonist [21], for wild type receptor as well as for several representative mutants. The relative efficacy is defined as the ratio of the maximal current elicited by the partial agonist to the maximal current elicited by a full agonist (ACh) (equation 1). Equation 2 shows a highly simplified model of the agonist binding and receptor gating process (R: receptor; c: closed; o: open; A: agonist, β and α are the opening and closing rate constants, respectively). At saturating doses of agonist, all the receptors are forced into a diliganded state (RA_2), so differences in I_{max} for the two agonists are due to differences in P_{open}. As such, ε reflects the ratio of P_{open} values for the partial and full agonists (equation 1). If a mutation has not altered the gating, but only the ligand binding of the receptor, the relative efficacies should be identical for the wild type and mutant receptors [14, 22]

$$\varepsilon = \frac{I_{max,PA}}{I_{max,FA}} = \frac{P_{open,PA}}{P_{open,FA}} \quad (1)$$

$$R^C \underset{-A}{\overset{A}{\rightleftharpoons}} R^CA \underset{-A}{\overset{A}{\rightleftharpoons}} R^CA_2 \underset{\alpha}{\overset{\beta}{\rightleftharpoons}} R^OA_2 \quad (2)$$

$$P_{open} = \frac{\beta}{\alpha + \beta} \quad (3)$$

For the wild type nAChR, P_{open} for ACh is very nearly 1 but P_{open} for succinylcholine is only 7.5% of that for acetylcholine ($\varepsilon = 0.075$). As a control, we examined a previously studied mutant known to affect gating. Mutation of a universally conserved leucine at the 9' position of M2 to a more polar residue such as serine (βL251S) substantially reduces EC_{50} [25, 37, 38]. This residue forms part of the hydrophobic gate of the channel and is quite remote from the agonist binding site, establishing it as a gating residue. As shown in Figure 2.6, the relative efficacy of βL251S is substantially increased over that of wild type. This indicates that P_{open} for SuCh has increased in the mutant, as expected for a mutation that substantially affects gating.

In the α subunit, the loop 2 mutations E45R and E45Q and the M2-M3 mutation S268E all decrease EC_{50} more than 25-fold. All three mutations greatly increase ε, giving values near 1 (Figure 2.6). This indicates that these mutations ease receptor opening, allowing SuCh to act as a full agonist. Importantly, the mutation E45V, which has no affect on EC_{50}, does not alter the efficacy of SuCh. The K210Q mutation in preM1 of the δ subunit shows only a small increase in the relative efficacy. We evaluated this mutation both in the context of the otherwise wild type receptor, and in receptors that contain the βL251S mutation, which moves the EC_{50} values into a more manageable range. The small change in efficacy at this site supports the idea that the non-α subunits are less of a factor in channel gating.

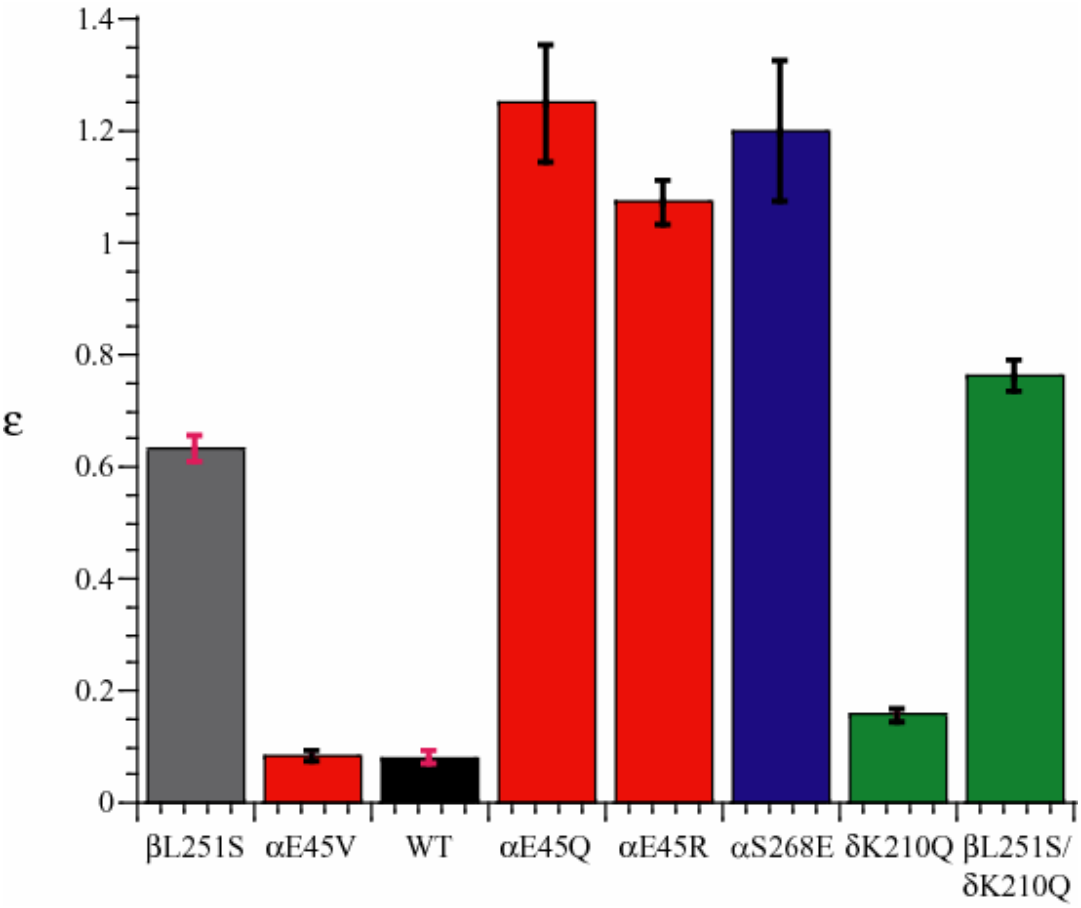

Figure 2.6 Relative efficacy (ε) of succinylcholine for several variants of the nAChR.

2.3.5 Previous work on the $GABA_A$ and Glycine receptors

Several important studies of possible electrostatic interactions in Cys loop receptors have appeared from Harrison, Trudell, and coworkers [14, 15] and Schofield and co-workers [18]. In each case, a specific electrostatic interaction was identified by mutagenesis studies, emphasizing charge-reversal/charge-rescue strategies. While we do not disagree with the fundamental observations of these efforts, we feel the results can be reinterpreted in the context of the charged interface model proposed here.

In the $GABA_A$ receptor α1subunit, Harrison, Trudell, and coworkers propose ion pair interactions between K279 on the M2-M3 loop and two aspartates: D57 on loop 2 and D149 on loop 7 (pairwise interactions 3 and 4, respectively, in Figure 2.1A) [15]. Here we use the $GABA_A$ numbering. The analogous residues in the nAChR α subunit are: S266, N47, and the previously discussed D138; the proposed electrostatic interactions are not conserved. In the $GABA_A$ receptor it is proposed that these "specific electrostatic interactions provide an intramolecular coupling mechanism" for the receptor. The K279D mutation results in a ~10-fold increase in EC_{50}. However, full receptor function is regained when K279D is coupled with *either* D57K or D149K. In addition, it is proposed that D149 and K279 move closer to one another during the transition from closed to open state, presumably strengthening the ion paring interaction.

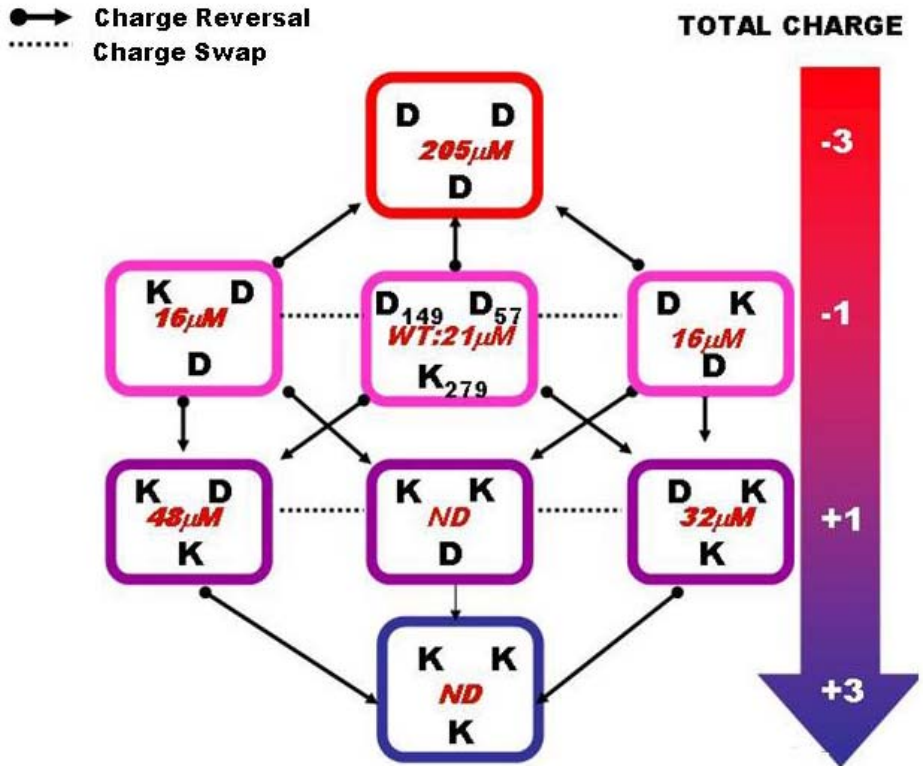

Figure 2.7 Analysis of previously published results for the $GABA_A$ receptor α1 subunit [15] in the same manner as in Figure 2.5, suggesting a charge triad interaction. ND = not determined.

In Figure 2.7 we present these results in the same format as in our discussion of the charge triad of the nAChR given in Figure 2.5. The mutation data, and the generally accepted notion that loop 2 and loop 7 straddle M2-M3, imply a triangular relationship between D57, D149, and K279. Thus, the K279D mutation puts three negative charges in an array, which is apparently unfavorable. What is initially surprising, however, is that K279D is *fully* rescued by the single D/K mutations at either site 57 or site 149, producing receptors that actually function "better" (lower EC_{50}) than wild type. That is, while the D57K compensating mutation does rescue the 57•••279 interaction, 149•••279 is still a repulsive D•••D interaction, yet the receptor shows EC_{50} below wild type. The exact same situation holds with the single D149K mutation. Also, if 149 and 279 move closer to each other during gating, how could a structure in which they are both aspartates (D57K/K279D) gate more efficiently than wild type? If the key interactions are D57•••K279 and D149•••K279, the highly efficient gating of the D47K/K279D and D149K/K279D double mutants is difficult to understand.

We propose that no specific ion pair interaction influences gating, but instead a cluster of charges similar to that described in Figure 2.5 is important. The single K279D mutation puts three negative charges in a cluster, and that is apparently unfavorable. In contrast, the wild type has a –/–/+ pattern (57/149/279), while the double mutants are +/–/– and –/+/–. Any pattern of three charges adding up to –1 gives wild type behavior (or better). Other mutants were also evaluated (Figure 2.7). Apart from –/–/– (the original K279D mutant), the only severely deleterious cluster is –/–/0 (K279A), with a charge of –2. Clusters with three charges that sum to +1 are not overly harmful. The +/–/+ mutant (D57K) shows only a 10% increase in EC_{50}, and –/+/+ (D149K) is much less than 2-fold higher. Surely these models are not of high enough precision to interpret such small differences. It seems the important thing is simply to have a cluster of charges that are not all the same, with specific ion pairing interactions being nonessential. Note the parallel behaviors of the 57/149/279 triad in the $GABA_A$ $\alpha 1$

subunit and the 138/276/429 triad in the nAChR α1 subunit (recall that nAChR 138 and $GABA_A$ 149 are aligned residues). Great variation in the charging pattern is tolerated, with nonfunctional receptors resulting only from clusters with very high overall charge.

Evidence for a cluster can also be seen in the $GABA_A$ β2 subunit [14]. The mutation K215D (pre-M1; aligns with nAChR α1 Q208) is deleterious; EC_{50} goes up 6.1-fold relative to wild type, corresponding to a penalty of 1.1 kcal/mol. This is substantially rescued by a compensating D146K mutation (loop 7; aligns with nAChR α1 D138; pairwise interaction 5 in Figure 2.1A); EC_{50} is only 1.5-fold higher than wild type, corresponding to a 0.25 kcal/mol penalty. Thus, 77% ((1.1-0.25)/1.1) of the K215D penalty is rescued by D146K. However, other charge reversal mutations in the interfacial region also significantly rescue K215D. D139K (aligns with nAChR α1 D131; pairwise interaction 6 in Figure 2.1A) rescues 64%; D56K (loop 2; aligns with nAChR α1 I49; pairwise interaction 7 in Figure 2.1A) rescues 49%; E147K (aligns with nAChR α1 Q139) rescues 29%; and E52K (aligns with nAChR α1 E45) rescues 25%. Stated differently, the range of EC_{50} values for the three best rescue mutants (D146K, D139K, and D56K) is substantially less than 2-fold. It seems risky to ascribe a special relationship to the 146•••215 pair. Again, an image of K215 as presenting a positive charge to a cluster of negative charges, such that it cannot itself be a negative charge, seems more sensible.

Studies of the glycine receptor from Schofield and coworkers [18] identified several charged residues on loops 2 and 7 that appeared to be important for gating. However, no particular pairwise relationships were uncovered, leading to the conclusion that these residues played a key role, but not through a “direct electrostatic” interaction.

2.4. Discussion

We have defined for the Cys loop superfamily of receptors a "gating interface" comprised of segments from the extracellular domain and the transmembrane domain that, based on mutagenesis data and the best available structural information, can reasonably be assumed to be juxtaposed. Analysis of representative subunits from the superfamily indicates that there are a large number of ionic residues in the interface, but for the most part their precise locations and particular charges are not conserved. Many workers, including ourselves, have sought specific ion pair interactions that exert precise control over the gating process. However, we have come to believe that, with such a large number of charges clustered in a fairly compact region, it is not meaningful to isolate specific ion pairs. Rather, the global charging pattern of the gating interface is what controls gating. Receptors have evolved to create a compatible collection of charged residues that allow the receptor to assemble and also facilitates the existence of and interconversions among multiple states.

Although specific ionic residues are generally not conserved, overall charging patterns are. Within the gating interface the extracellular component carries a net negative charge and the transmembrane component carries a net positive charge. This creates a global electrostatic attraction at the interface that maintains the integrity of the receptor as it transitions from the mostly β-sheet, relatively polar extracellular domain to the α-helical, nonpolar transmembrane domain.

Several lines of evidence support this way of thinking about the gating interface. We have studied a number of mutations that reverse, neutralize, or introduce charges. Typically, these are considered to be dramatic mutations, and they might be expected to be disruptive at a functionally important interface. However, one of the more remarkable features of the mutagenesis data of Tables 2.3 is the tolerance of the gating region to such charge disruptions. In fact, very often EC_{50} is *lowered* by such strong

perturbations. It seems hard to imagine that dramatic mutations involving the introduction or reversal of charge just happen to lead to a viable ion pair that is tolerated by the receptor. Rather, we believe the entire gating interface is tolerant of charge up to a point. A delicate balancing act is in operation. By distributing a large number of charges across an interface, it is possible to have movement along that interface without creating adverse situations of like charges interacting strongly or a single charge in isolation in a poorly solvated environment. Consider T267. Introducing charge is not deleterious at this site. In fact, converting the neutral T to a cation (T267K) or an anion (T267D) has the same effect: EC_{50} is halved. It appears that it is the number of charges, not their particular identities, that matters. The same pattern is seen at S268 and S269. These residues are on the M2-M3 loop, a region that is universally accepted to be important in gating in the Cys loop superfamily of receptors [15, 31, 33, 39, 40]. Loop 2 always carries a significant negative charge, and we showed here that introducing a positive charge at any of four locations (D44-N47) lowers EC_{50}. It thus appears that the negative charge stabilizes the closed state of the nicotinic receptor by interacting with a positive region. Based on 2BG9 [8, 9], the M2-M3 loop seems the likely candidate for the positive region, but again the precise positioning of residues may be different.

A few charge reversals have been shown to be deleterious, and they can often be rescued by compensating charge reversals. The universally conserved D138 is one such residue. In the nAChR α1, the $GABA_A$ α1 [15] (where it is D149), and $GABA_A$ β2 [14] (where it is D146) compensating charge reversals can rescue the initial mutant (pairwise interactions 1, 2, 4, and 5 in Figure 2.1A). However, the systems use completely different residues from apparently very different regions of the interface. There is certainly no universal pattern, and it appears that rather than conserving some specific pairwise interaction, it is the global charging pattern of the trio of residues that is most

important. At another site, D139 of $GABA_A$ β2 [14] (I131 of nAChR α1), as many as 5 different sites can contribute to compensating a charge reversal, with a gradation of efficiencies.

We conclude that no one ion pair interaction is crucially important to gating across the entire Cys loop superfamily; clearly each receptor is different. However, it may be that there is a consistent mechanism across the superfamily, but one that does not single out any particular ion pair. Several groups have suggested that the extracellular domain and the transmembrane domain change relative positions on going from the closed to the open state. Harrison and Trudell propose that a residue on loop 7 moves closer to a residue on M2-M3 in the $GABA_A$ receptor α1 subunit (D149 and K279, $GABA_A$ numbering; pairwise interaction 4 in Figure 2.1A). Unwin's detailed gating model emphasizes differential interactions between loops 2/7 (extracellular domain) and M2-M3 (transmembrane domain) along the gating pathway. We have recently proposed [12] that loop 2 and especially loop 7 interact with a specific proline on M2-M3 differentially in the open and closed states. In order to accommodate the structural rearrangement at the gating interface, the many charges involved must be comfortable in the environments provided by both the open and closed states and must also experience no highly adverse interactions in the transition state separating the two. With a large number of charges distributed throughout the interface, the extracellular domain and the transmembrane domain can slide past one another (or twist or turn or unclamp…) while maintaining an acceptable network of compensating charges throughout the process. During the movement, some ion pair interactions will strengthen, some will weaken, but crucial on/off interactions seem less critical. There are clearly many ways to achieve the proper balance, and each system has evolved an ionic array that supports the desired gating behavior. The essential mechanism is universal across the Cys loop superfamily, but the precise details vary from system to system.

2.5 Materials and methods

2.5.1 Mutagenesis and mRNA synthesis

The mRNA that codes for the muscle type nAChR subunits (α, β, γ, and δ) was obtained by linearization of the expression vector (pAMV) with Not 1, followed by *in vitro* transcription using mMessage mMachine kit purchased from Ambion (Austin, TX). The mutations in all subunits were made following the QuickChange mutagenesis protocol (Stratagene).

2.5.2. Electrophysiology and data analysis

mRNAs of α, β, γ, and δ subunits were mixed in the ratio of 2:1:1:1 and microinjected into stage VI oocytes of *Xenopus laevis*. Electrophysiology recordings were performed 24-48 h after injection in two-electrode voltage clamp mode using the OpusXpress 6000A (Molecular Devices Axon Instruments). The holding potential was -60mV and agonist was applied for 15 s [41]. Acetylcholine chloride and succinylcholine chloride dihydrate were purchased from Sigma/Aldrich/RBI (St. Louis, MO). All drugs were diluted to the desired concentrations with calcium-free ND96 buffer. Dose-response data were obtained for at least 8 concentrations of agonists and for a minimum of 5 oocytes. Mutants with I_{max} equal to or greater than 100 nA were defined as functional. EC_{50} and Hill coefficient were calculated by fitting the dose response relation to the Hill equation. All data are reported as mean ± S.E.

If saturation was not reached at 1000 μM concentrations of acetylcholine, the EC_{50} could not be calculated. For two mutations, αV46A and αV46T, a second mutation was incorporated at the 9' position of the β subunit (βL251S). This mutation is known to reduce the wild type EC_{50} to 1.2 μM [25]. The EC_{50} of the double mutant was then determined as described. For scatter plots (Figure 2.2

and 2.4) the EC_{50} of the double mutant was multiplied by 41.7 (50/1.2) to get a corrected $EC_{50.}$ The corrected EC_{50} was used for the linear regression analysis.

EC_{50}s for succinylcholine were measured in the same manner. Maximal currents elicited by acetylcholine $I_{max(acetylcholine)}$ and by succinylcholine $I_{max(succinylcholine)}$ were measured sequentially at saturating concentrations on the same cells. The ratio of $I_{max(succinylcholine)}/ I_{max(acetylcholine)}$ was calculated for each cell and is reported as mean ± S.E.

2.5.3 Unnatural amino acid suppression

The preparation of the unnatural amino acid O-methyl threonine is described elsewhere [25]. O-methyl serine was purchased from Sigma/Aldrich/RBI (St. Louis, MO) and was protected and activated as described [42]. Unnatural amino acids were conjugated to the dinucleotide dCA and ligated to truncated 74 nt tRNA THG73. The aminoacyl tRNA was deprotected by photolysis immediately prior to co-injection with mRNA containing an *amber* (TAG) stop codon at the site of interest. Negative and positive controls were employed as previously reported [41].

2.5.4 Bungarotoxin binding

48-72 h after injection, oocytes were prewashed with calcium-free ND96 buffer with 1 mg/mL bovine serum albumin, then transferred to the same buffer with the addition of 10 nM [^{125}I] α-bungarotoxin (Perkin Elmer), and incubated for 1 h at room temperature [43]. Oocytes were then washed four times and counted individually in a gamma counter. Oocytes injected with 50 nL of water were used to determine background. Mutants with more than 5 times the background reading are regarded to have sufficient expression.

2.6 References

1. Leite, J.F., N. Rodrigues-Pinguet, and H.A. Lester, *Insights into channel function via channel dysfunction.* J Clin Invest, 2003. **111**(4): p. 436-7.
2. Paterson, D. and A. Nordberg, *Neuronal nicotinic receptors in the human brain.* Prog Neurobiol, 2000. **61**(1): p. 75-111.
3. Changeux, J.P. and S.J. Edelstein, *Allosteric mechanisms in normal and pathological nicotinic acetylcholine receptors.* Current Opinion In Neurobiology, 2001. **11**(3): p. 369-377.
4. Lester, H.A., et al., *Cys-loop receptors: new twists and turns.* Trends In Neurosciences, 2004. **27**(6): p. 329-336.
5. Brejc, K., et al., *Crystal structure of an ACh-binding protein reveals the ligand-binding domain of nicotinic receptors.* Nature, 2001. **411**(6835): p. 269-76.
6. Celie, P.H.N., et al., *Crystal Structure of Acetylcholine-binding Protein from Bulinus truncatus Reveals the Conserved Structural Scaffold and Sites of Variation in Nicotinic Acetylcholine Receptors.* J. Biol. Chem., 2005. **280**(28): p. 26457-26466.
7. Celie, P.H.N., et al., *Nicotine and Carbamylcholine Binding to Nicotinic Acetylcholine Receptores as Sutdied in AChBP Crystal Structures.* Neuron, 2004. **41**: p. 907-914.
8. Unwin, N., et al., *Activation of the nicotinic acetylcholine receptor involves a switch in conformation of the α subunits.* J Mol Biol, 2002. **319**(5): p. 1165-76.
9. Miyazawa, A., Y. Fujiyoshi, and N. Unwin, *Structure and gating mechanism of the acetylcholine receptor pore.* Nature, 2003. **423**: p. 949-955.
10. Unwin, N., *Refined Structure of the Nicotinic Acetylcholin receptor at 4 A Resolution.* J Mol Biol, 2005. **346**: p. 967-989.
11. Taly, A., et al., *Normal mode analysis suggests a quaternary twist model for the nicotinic receptor gating mechanism.* Biophysical Journal, 2005. **88**(6): p. 3954-3965.
12. Lummis, S.C., et al., *Cis-trans isomerization at a proline opens the pore of a neurotransmitter-gated ion channel.* Nature. 2005 Nov 10;438(7065):248-52.
13. Kash, T.L., et al., *Evaluation of a proposed mechanism of ligand-gated ion channel activation in the $GABA_A$ and glycine receptors.* Neurosci Lett, 2004. **371**: p. 230-234.
14. Kash, T.L., et al., *Charged Residues in the β_2 Subunit Involved in $GABA_A$ Receptor Activation.* J. Biol. Chem., 2004. **279**(6): p. 4887-4893.
15. Kash, T.L., et al., *Coupling of agonist binding to channel gating in the GABA(A) receptor.* Nature, 2003. **421**(6920): p. 272-5.
16. Schofield, C.M., A. Jenkins, and N.L. Harrison, *A Highly Conserved Aspartic Acid Residue in the Signature Disulfide Loop of the α1 Subunit Is a Determinant of Gating in the Glycine Receptor.* J. Biol. Chem., 2003. **278**(36): p. 34079-34083.
17. Kash, T.L., J.R. Trudell, and N.L. Harrison, *Structural elements involved in activation of the γ-aminobutyric acid type A ($GABA_A$) receptor.* Biochem. Soc. T., 2004. **32**(3): p. 540-546.
18. Absalom, N.L., et al., *Role of Charged Residues in Coupling Ligand Bindig and Channel Activation in the Extraceullular Domain of the Glycine Receptor.* J. Biol. Chem., 2003. **278**(50): p. 50151-50157.
19. Schofield, C.M., J.R. Trudell, and N.L. Harrison, *Alanine-Scanning Mutagenesis in the Signature Disulfide Loop of the Glycine Receptor α1 Subunit: Critical Residues for Activation and Modulation.* Biochemistry, 2004. **43**: p. 10058-10063.

20. Nowak, M.W., et al., *In vivo incorporation of unnatural amino acids into ion channels in a Xenopus oocyte expression system.* Methods Enzymol, 1998. **293**: p. 504-529.
21. Placzek, A.N., et al., *A single point mutation confers properties of the muscle-type nicotinic acetylcholine receptor to homomeric alpha 7 receptors.* Molecular Pharmacology, 2004. **66**(1): p. 169-177.
22. Colquhoun, D., *Binding, gating, affinity and efficacy: the interpretation of structure- activity relationships for agonists and of the effects of mutating receptors.* Br J Pharmacol, 1998. **125**(5): p. 924-47.
23. Chakrapani, S., T.D. Bailey, and A. Auerbach, *Gating Dynamics of the Acetylcholine Receptor Extracellular Domain.* J Gen Physiol, 2004. **123**: p. 341-356.
24. Corringer, P.J., N. Le Novere, and J.P. Changeux, *Nicotinic receptors at the amino acid level.* Annu Rev Pharmacol Toxicol, 2000. **40**: p. 431-58.
25. Kearney, P.C., et al., *Determinants of nicotinic receptor gating in natural and unnatural side chain structures at the M2 9?position.* Neuron, 1996. **17**(6): p. 1221-1229.
26. Karplus, P.A., *Hydrophobicity regained.* Protein Science, 1997. **6**(6): p. 1302-1307.
27. Radzicka, A. and R. Wolfenden, *Comparing The Polarities Of The Amino-Acids - Side-Chain Distribution Coefficients Between The Vapor-Phase, Cyclohexane, 1-Octanol, And Neutral Aqueous-Solution.* Biochemistry, 1988. **27**(5): p. 1664-1670.
28. Chothia, C., *The nature of the accessible and buried surfaces in proteins* Journal of Molecular Biology, 1975. **105**(1): p. 1-12.
29. Zamyatnin, A.A., *Protein volume in solution* 1972. **24** p. 107-123
30. Mitra, A., T.D. Bailey, and A. Auerbach, *Structural Dynamics of the M4 Transmembrane Segment during Acetylcholine Receptor Gating.* Structure, 2004. **12**: p. 1909-1918.
31. Grosman, C., et al., *The extracellular linker of muscle acetylcholine receptor channels is a gating control element.* J Gen Physiol, 2000. **116**(3): p. 327-40.
32. Castaldo, P., et al., *A novel hyperekplexia-causing mutation in the pre-transmembrane segment 1 of the human glycine receptor alpha1 subunit reduces membrane expression and impairs gating by agonists.* J Biol Chem. 2004 Jun 11;279(24):25598-604. Epub 2004 Apr 5.
33. Bouzat, C., et al., *coupling of agonist binding to channel gating in an ACh-binding protein linked to an ion channel.* Nature, 2004. **430**: p. 896-900.
34. Xiu, X., et al., *A Unified View of the Role of Electrostatic Interactions in Modulating the Gating of Cys Loop Receptors.* J. Biol. Chem., 2005. **280**(50): p. 41655-41666.
35. Grosman, C. and A. Auerbach, *Asymmetric and independent contribution of the second transmembrane segment 12' residues to diliganded gating of acetylcholine receptor channels. A single-channel study with choline as the agonist.* J Gen Physiol, 2000. **115**(637-651).
36. Grosman, C., M. Zhou, and A. Auerbach, *Mapping the conformational wave of acetylcholine receptor channel gating.* Nature, 2000. **403**(6771): p. 773-6.
37. Filatov, G.N. and M.M. White, *The role of conserved leucines in the M2 domain of the acetylcholine receptor in channel gating.* Mol Pharmacol, 1995. **48**(3): p. 379-384.
38. Labarca, C., et al., *Channel gating governed symmetrically by conserved leucine residues in the M2 domain of nicotinic receptors.* Nature. 1995 Aug 10;376(6540):514-6.
39. Campos-Caro, A., et al., *A Single Residue in the M2-M3 Loop is a Major Determinant of Coupling Between Binding and Gating in Neuronal Nicotinic Receptors.* Proc. Natl. Acad. Sci. USA, 1996. **93**: p. 6118-6123.
40. Lummis, S.C.R., *The transmembrane domain of the 5-HT3 receptor: its role in selectivity and gating.* Biochemical Society Transactions, 2004. **32**: p. 535-539.

41. Cashin, A.L., et al., *Using physical chemistry to differentiate nicotinic from cholinergic agonists at the nicotinic acetylcholine receptor.* Journal Of The American Chemical Society, 2005. **127**(1): p. 350-356.
42. Kearney, P.C., et al., *Dose-Response Relations for Unnatural Amino Acids at the Agonist Binding Site of the Nicotinic Acetylcholine Receptor: Tests with Novel Side Chains and with Several Agonists.* Mol. Pharmacol., 1996. **50**(5): p. 1401-1412.
43. Tong, Y., et al., *Tyrosine decaging leads to substantial membrane trafficking during modulation of an inward rectifier potassium channel.* J Gen Physiol, 2001. **117**(2): p. 103-18.

Supplementary Table S 2.1: Sequences in the gating interface of the whole LGIC family, highlighting cationic (blue) and anionic (red) residues.

	Loop2	Loop7	L9	preM1	M2-M3	postM4	D	E	K	R	+	-	N	Z
ACH4_HUMAN	DEKNQM	IDVTFFPFDQ	EW	IRRLP	STSLVIPLIGEY	FLPP WLAGMI	3	3	1	2	3	6	-3	9
ACH4_RAT	DEKNQM	IDVTFFPFDQ	EW	IRRLP	STSLVIPLIGEY	FLPP WLAAC	3	3	1	2	3	6	-3	9
ACH4_CHICK	DEKNQM	IDVTFFPFDQ	EW	IRRLP	STSLVIPLIGEY	FLPP WLAGMI	3	3	1	2	3	6	-3	9
ACH2_CHICK	DEKNQM	IDVTYFPFDQ	EW	IRRLP	STSLVIPLIGEY	FLPP YLAGMI	3	3	1	2	3	6	-3	9
ACH2_RAT	DEKNQM	IDVTFFPFDQ	EW	IRRLP	STSLVIPLIGEY	FLPP FLAGMI	3	3	1	2	3	6	-3	9
ACH2_HUMAN	DEKNQM	IDVTFFPFDQ	EW	IRRLP	STSLVIPLIGEY	FLPP FLAGMI	3	3	1	2	3	6	-3	9
ACH3_CARAU	DEVNQI	MDITYFPFDY	EW	IRRLP	STSLVIPLIGEY	FLQP LIGFFS	3	3	0	2	2	6	-4	8
ACH3_HUMAN	DEVNQI	IDVTYFPFDY	EW	IRRLP	STSLVIPLIGEY	FLQP LMARED	4	4	0	3	3	8	-5	11
ACH3_BOVIN	DEVNQI	IDVTYFPFDY	EW	IRRLP	STSLVIPLIGEY	FLQP LMTRDD	5	3	0	3	3	8	-5	11
ACH3_RAT	DEVNQI	IDVTYFPFDY	EW	IRRLP	STSLVIPLIGEY	FLQP LMARDD	5	3	0	3	3	8	-5	11
ACH3_CHICK	DEVNQI	IDVTYFPFDY	EW	IRRLP	STSLVIPLIGEY	FLQP LMTGDD	5	3	0	2	2	8	-6	10
ACH6_HUMAN	DEVNQI	MDITFFPFDH	EW	IRRLP	STSLVVPLVGEY	FLQP LLGNTG	3	3	0	2	2	6	-4	8
ACH6_RAT	DEVNQI	MDITFFPFDH	EW	IRRLP	STSLVIPLVGEY	FLQP LLGNTG	3	3	0	2	2	6	-4	8
ACH6_CHICK	DEVNQI	MDITFFPFDH	EW	IRRLP	STSLVIPLVGEY	FIQP LIADT	4	3	0	2	2	7	-5	9
ACH6_RAT	HEREQI	IEVKHFPFDQ	EW	IRRKP	PTSLDVPLVGKY	FLQP LFQNYT	2	4	3	3	6	6	0	12
ACHN_HUMAN	HEREQI	IEVKHFPFDQ	EW	IRRKP	PTSLDVPLVGKY	FLQP LFQNYT	2	4	3	3	6	6	0	12
ACHN_CHICK	HEREQI	IEVKHFPFDQ	EW	IRRKP	PTSLDVPLVGKY	FLQP LFQNYA	2	4	3	3	6	6	0	12
ACHP_CHICK	NEREQI	IEVKHFPFDQ	EW	IKRKP	PTSLDVPLIGKY	FLQP LFQNHI	2	4	4	2	6	6	0	12
ACHP_RAT	NEREQI	IEVKHFPFDQ	EW	IKRKP	PTSLDIPLIGKY	FLPP LFQIHA	2	4	4	2	6	6	0	12
ACHN_CARAU	NEREQI	IEVRNFPFDQ	EW	IKRKP	PTSLAVPLIGKY	FVQP LFQSYN	1	4	3	3	6	5	1	11
ACH2_DROME	NLKDQI	IDVRYFPFDQ	EW	LRRKT	STSLALPLLGKY	ILG EAPSL	3	2	3	3	6	5	1	11
ACH1_SCHGR	NLKDQI	IDVRYFPFDQ	EW	LRRKT	STSLALPLLGKY	ILC EAPAL	3	2	3	3	6	5	1	11
ACH1_DROME	NLKNQI	IDVEYFPFDE	EW	LRRKT	PTSLTVPLLGKY	IIL QAPSL	2	3	3	2	5	5	0	10
ACH4_DROME	NLKNQV	MNVEYFPYDE	EW	MRRKT	PTSLAVPLLGKY	IDRQLSEIPLRK	2	4	4	4	8	6	2	14
ACHO_RAT	DEKNQL	MDVTFFPFDR	EW	LRRLP	SSSKVIPLIGEY	FI P ALKMW	3	3	3	3	6	6	0	12
ACHO_CHICK	DEKNQL	MELTFFPFDR	EW	LRRLP	SSSKVIPLIGEY	F TPALQMWLNS	2	4	2	3	5	6	-1	11
ACHP_CARAU	DEKNHL	MDVTFFPFDR	EW	LKRLP	SSSKVIPLIGEY	F TPALHMYLST	3	3	3	2	5	6	-1	11
ACHO_CARAU	DEKNQL	MDVTFFPFDR	EW	LKRLP	SSSKVIPLIGEY	F TPALKMFLRT	3	3	4	3	7	6	1	13
ACH5_CHICK	DEKNQL	IDVTFFPFDL	EW	IRRLP	SSSKVIPLIGEY	WASIIVPVHIGS	3	3	2	2	4	6	-2	10
ACH5_HUMAN	DEKNQL	IDVTFFPFDL	EW	IKRLP	SSSKVIPLIGEY	WANILIPVHIGN	3	3	3	1	4	6	-2	10
ACH5_RAT	DEKNQL	IDVTFFPFDL	EW	IKRLP	SSSKVIPLIGEY	WANIIVPVHIGN	3	3	3	1	4	6	-2	10
ACH3_DROME	NEKNQV	IDVTYFPFDQ	TW	IRRKT	PTSLVLPLIAKY	LMDAPHIFEYVD	4	2	3	2	5	6	-1	11
ACHA_BOVIN	DEVNQI	IIVTHFPFDE	EW	MQRLP	STSSAVPLIGKY	FAGRLIELNQQG	2	4	1	2	3	6	-3	9
ACHA_HUMAN	DEVNQI	IIVTHFPFDE	EW	MQRLP	STSSAVPLIGKY	FAGRLIELNQQG	2	4	1	2	3	6	-3	9
ACHA_MOUSE	DEVNQI	IIVTHFPFDE	EW	MQRLP	STSSAVPLIGKY	FAGRLIELHQQG	2	4	1	2	3	6	-3	9
ACHA_RAT	DEVNQI	IIVTHFPFDE	EW	MQRLP	STSSAVPLIGKY	FAGRLIELHQQG	2	4	1	2	3	6	-3	9
ACHA_CHICK	DEVNQI	IIVTYFPFDQ	EW	MQRLP	STSSAVPLIGKY	FAGRLIELNQQG	2	3	1	2	3	5	-2	8
ACH2_XENLA	DEVNQI	IIVTYFPFDQ	EW	LQRLP	STSSAVPLIGKY	FAGRIIEMNMQE	2	4	1	2	3	6	-3	9
ACH1_XENLA	NEVNQI	MIVTYFPFDL	EW	LQRLP	STSSAVPLIGKY	FAGRLIELHMQG	1	3	1	2	3	4	-1	7

```
ACHA_TORCA DEVNQI IIVTHFPFDQ EW MQRIP STSSAVPLIGKY   FAGRLIELSQEG   2  4  1  2  3  6  -3  9
ACHD_RAT   KEVEET ISVTYFPFDW EW IRRKP ATSMAIPLVGKF   FLQGVYNQPPPQ   1  4  3  2  5  5  0  10
ACHD_MOUSE KEVEET ISVTYFPFDW EW IRRKP ATSMAIPLVGKF   FLQGVYNQPPLQ   1  4  3  2  5  5  0  10
ACHD_HUMAN KEVEET ISVTYFPFDW EW IRRKP ATSMAIPLIGKF   FLQGVYNQPPPQ   1  4  3  2  5  5  0  10
ACHD_BOVIN KEVEET ISVTYFPFDW EW IRRKP ATSMAIPLIGKF   FLQGAYNQPPPQ   1  4  3  2  5  5  0  10
ACHD_CHICK KEVDET INVNFFPFDW EW IKRKP ATSHAIPLIGKY   FLMGIYNHPPPL   2  3  4  1  5  5  0  10
ACHD_XENLA KEADET INVNYFPFDW EW IERKP ETSFAIPLISKY   FLGGAYNLPPSL   2  5  3  1  4  7  -3 11
ACHD_TORCA KETDET INVLYFPFDW EW IRRKP ETALAVPLIGKY   FVMGNFNHPPAK   2  4  4  2  6  6  0  12
ACHG_CHICK NEREET IHVTYFPFDW EW IQRKP ETSQAVPLIGKY   FLMAHFNQAPAL   1  5  2  2  4  6  -2  10
ACHG_XENLA NEKEEA VVVTYFPFDW EW IQRKP ETSTSVPLIVKY   FLAGHFNQAPAH   1  5  3  1  4  6  -2  10
ACHG_MOUSE NEREEA ISVTYFPFDW EW IQRKP ETSQAVPLISKY   FLMAHYNQVPDL   2  5  2  2  4  7  -3  11
ACHG_RAT   NEREEA ISVTYFPFDW EW IQRKP ETSQAVPLISKY   FLMAHYNQVPDL   2  5  2  2  4  7  -3  11
ACHG_BOVIN NEREEA VSVTFFPFDW EW IQRKP ETSQAVPLISKY   FLMAHYNRVPAL   1  5  2  3  5  6  -1  11
ACHG_HUMAN NEREEA ISVTYFPFDW EW IQRKP ETSQAVPLISKY   FLMAHYNRVPAL   1  5  2  3  5  6  -1  11
ACHG_TORCA NEKEEA IAVTYFPFDW EW IQRKP ETSLNVPLIGKY   FLTGHFNQVPEF   1  6  3  1  4  7  -3  11
ACHE_XENLA NEKEET IEITYFPFDW EW IQRKP ETSLSVPLIGKY   FLMGHFNTAPEH   1  7  3  1  4  8  -4  12
ACHE_RAT   NEKEET VEVTYFPFDW EW IRRKP ETSLSVPLLGRY   FLGGYFNQVPDL   2  6  2  3  5  8  -3  13
ACHE_MOUSE NEKEET VEVTYFPFDW EW IRRKP ETSLSVPLLGRY   FLGGYFNQVPDL   2  6  2  3  5  8  -3  13
ACHE_HUMAN NEKEET VEVTYFPFDW EW IRRKP ETSLSVPLLGRF   FLGAYFNRVPDL   2  6  2  4  6  8  -2  14
ACHE_BOVIN NEKEET VEVTYFPFDW EW IRRKP ETSLSVPLLGRY   FLGAYFNRVPQL   1  6  2  4  6  7  -1  13
ACHB_MOUSE NEKDEE IQVTYFPFDW QW IRRKP ETSLAVPIIIKY   FLDATYHLPPPE   3  5  3  2  5  8  -3  13
ACHB_RAT   NEKDEE IQVTYFPFDW QW IRRKP ETSLAVPIIIKY   FLDATYHLPPPE   3  5  3  2  5  8  -3  13
ACHB_HUMAN NEKDEE IQVTYFPFDW QW IRRKP ETSLSVPIIIKY   FLDATYHLPPPD   4  4  3  2  5  8  -3  13
ACHB_BOVIN NEKDEE IQVTYFPFDW QW IRRKP ETSLSVPIIIKY   FLDATYHLPPAD   4  4  3  2  5  8  -3  13
ACHB_TORCA NEKIEE IKVMYFPFDW QW IQRKP ETSLSVPIIIRY   FLDASHNVPPDN   3  4  3  2  5  7  -2  12
ACH8_CHICK DEKNQV IDVRWFPFDV EW MRRRT ATSDSVPLIAQY   LMSAPNFIEAVS   4  3  1  4  5  7  -2  12
ACH7_CHICK DEKNQV IDVRWFPFDV EW MRRRT ATSDSVPLIAQY   LMSAPNFVEAVS   4  3  1  4  5  7  -2  12
ACH7_HUMAN DEKNQV IDVRWFPFDV EW MRRRT ATSDSVPLIAQY   LMSAPNFVEAVS   4  3  1  4  5  7  -2  12
ACH7_MOUSE DEKNQV IDVRWFPFDV EW MRRRT ATSDSVPLIAQY   LMSAPNFVEAVS   4  3  1  4  5  7  -2  12
ACH7_RAT   DEKNQV IDVRWFPFDV EW MRRRT ATSDSVPLIAQY   LMSAPNFVEAVS   4  3  1  4  5  7  -2  12
ACH7_BOVIN DEKNQV IDVRWFPFDV EW IRRRT ATSDSVPLIAQY   LMSAPNFVEAVS   4  3  1  4  5  7  -2  12
ACH9_RAT   DERNQI VDVTYFPFDS EW LKRRS A SENVPLIGKY   IARAD          4  3  2  4  6  7  -1  13
5HT3_RAT   DEKNQV LDIYNFPFDV EW IRRRP ATAIGTPLIGVY   LWSIWHYS       3  2  1  3  4  5  -1  9
5HT3_MOUSE DEKNQV LDIYNFPFDV EW IRRRP AT IGTPLIGVY   LWSIWHYS       3  2  1  3  4  5  -1  9
5HT3_HUMAN DEKNQV LDIYNFPFDV EW IRRRP ATAIGTPLIGVY   LWSIWQYA       3  2  1  3  4  5  -1  9
GAA4_BOVIN SDVEME MRLVDFPMDG QY LRRKM KVSYATAM DWF   LSKDTMEKSESL   5  4  4  3  7  9  -2  16
GAA4_HUMAN SDVEME MRLVDFPMDG QY LRRKM KVSYLTAM DWF   LSKDTMEKSESL   5  4  4  3  7  9  -2  16
GAA4_RAT   SDVEME MRLVDFPMDG QY LRRKM KVSYATAM DWF   LSKDTMEKSESL   5  4  4  3  7  9  -2  16
GAA6_HUMAN SDVEME MRLVNFPMDG QY LQRKM KVSYATAM DWF   LSKDTMEVSSSV   4  3  3  2  5  7  -2  12
GAA6_RAT   SDVEME MRLVNFPMDG QY LQRKM KVSYATAM DWF   LSKDTMEVSSTV   4  3  3  2  5  7  -2  12
GAA3_RAT   SDTDME MHLEDFPMDV QY LKRKI KVAYATAM DWF   VNRESAIKGMIR   5  3  4  3  7  8  -1  15
```

```
GAA3_HUMAN SDTDME MHLEDFPMDV QY LKRKI KVAYATAM DWF   VNRESAIKGMIR  5  3  4  3  7  8  -1  15
GAA3_BOVIN SDTDME MHLEDFPMDV QY LKRKI KVAYATAM DWF   VNRESAIKGMIR  5  3  4  3  7  8  -1  15
GAA5_RAT   SDTEME MQLEDFPMDA QY LKRKI KVAYATAM DWF   LNREPVIKGATS  4  4  4  2  6  8  -2  14
GAA5_HUMAN SDTEME MQLEDFPMDA QY LKRKI KVAYATAM DWF   LNREPVIKGAAS  4  4  4  2  6  8  -2  14
GAA2_BOVIN SDTDME MHLEDFPMDA QY LKRKI KVAYATAM DWF   LNREPVLGVSP   5  3  3  2  5  8  -3  13
GAA2_HUMAN SDTDME MHLEDFPMDA QY LKRKI KVAYATAM DWF   LNREPVLGVSP   5  3  3  2  5  8  -3  13
GAA2_RAT   SDTDME MHLEDFPMDA QY LKRKI KVAYATAM DWF   LNREPVLGVSP   5  3  3  2  5  8  -3  13
GAA1_CHICK SDHDME MHLEDFPMDV QY LKRKI KVAYATAM DWF   LNREPQLKAPTP  5  3  4  2  6  8  -2  14
GAA1_HUMAN SDHDME MHLEDFPMDA QY LKRKI KVAYATAM DWF   LNREPQLKAPTP  5  3  4  2  6  8  -2  14
GAA1_BOVIN SDHDME MHLEDFPMDA QY LKRKI KVAYATAM DWF   LNREPQLKAPTP  5  3  4  2  6  8  -2  14
GAA1_RAT   SDHDME MHLEDFPMDA QY LKRKI KVAYATAM DWF   LNREPQLKAPTP  5  3  4  2  6  8  -2  14
GAC2_BOVIN NAINME LQLHNFPMDE QF LSRRM KVSYVTAM DLF   LYL           2  2  1  2  3  4  -1  7
GAC2_HUMAN NAINME LQLHNFPMDE QF LSRRM KVSYVTAM DLF   LYL           2  2  1  2  3  4  -1  7
GAC2_RAT   NAINME LQLHNFPMDE QF LSRRM KVSYVTAM DLF   LYL           2  2  1  2  3  4  -1  7
GAC2_CHICK NAINME LQLHNFPMDA QF LSRRM KVSYVTAM DLF   LYL           2  1  1  2  3  3   0  6
GAC1_RAT   DPINME LQLHNFPMDE QF LSRRM KVSYVTAM DLF   LYL           3  2  1  2  3  5  -2  8
GAC3_RAT   SSINME LQLHNFPMDA QF LSRRM RVSYVTAM DLF   LYL           2  1  0  3  3  3   0  6
GAC4_CHICK SVIQME LQLQNFPMDT QF LSRRM RVSYITAM DLF   LYL           2  1  0  3  3  3   0  6
GAB_DROME  SEVLMD MNLQYFPMDR QF FVRSM KISY VKSIDVY   ILE           3  2  2  2  4  5  -1  9
GAB4_CHICK SEVNMD MDLRRYPLDQ QF IKRNI KIPY VKAIDVY                 4  1  3  3  6  5  1  11
GAB3_RAT   SEVNMD MDLRRYPLDE QF LKRNI KIPY VKAIDMY   VN            4  2  3  3  6  6  0  12
GAB3_HUMAN SEVNMD MDLRRYPLDE QF LKRNI KIPY VKAIDMY   VN            4  2  3  3  6  6  0  12
GAB3_CHICK SEVNMD MDLRRYPLDE QF LKRNI KIPY VKAIDMY   VN            4  2  3  3  6  6  0  12
GAB2_RAT   SEVNMD MDLRRYPLDE QF LKRNI KIPY VKAIDMY   VN            4  2  3  3  6  6  0  12
GAB2_HUMAN SEVNMD MDLRRYPLDE QF LKRNI KIPY VKAIDMY   VN            4  2  3  3  6  6  0  12
GAB1_BOVIN SEVNMD MDLRRYPLDE QF LKRNI KIPY VKAIDIY   VH            4  2  3  3  6  6  0  12
GAB1_RAT   SEVNMD MDLRRYPLDE QF LKRNI KIPY VKAIDIY   VH            4  2  3  3  6  6  0  12
GAB1_HUMAN SEVNMD MDLRRYPLDE QF LKRNI KIPY VKAIDIY   VN            4  2  3  3  6  6  0  12
GAB_LYMST  SEVDMD MDLHNYPLDH QF LQRNI RISY VKAIDIY   LLT           5  1  1  2  3  6  -3  9
GAD_RAT    SEANME MDLAKYPMDE QF LRRNR RAS AIKALDVY   TM            3  3  2  4  6  6   0  12
GAR2_HUMAN SEVDMD MDFSHFPLDS QF LRRHI RVSY VKAVDIY   S             5  1  1  3  4  6  -2  10
GAR2_RAT   SEVDMD MDFSHFPLDS QF LRRHI RVSY IRAVDIY   S             5  1  0  4  4  6  -2  10
GAR1_RAT   SEVDMD MDFSRFPLDT QF LRRHI RVSY IKAVDIY   S             5  1  1  4  5  6  -1  11
GAR1_HUMAN SEVDMD MDFSRFPLDT QF LRRHI RVSY IKAVDIY   S             5  1  1  4  5  6  -1  11
GAR3_RAT   SEVNMD MDFSRFPLDT QF LRRHI QVSY VKAVDVY   V             4  1  1  3  4  5  -1  9
GRB_HUMAN  QETTMD LDLTLFPMDT QF LRRQV KVSY VKALDVW   L             4  1  2  2  4  5  -1  9
GRB_RAT    QETTMD LDLTLFPMDT QF LRRQV KVSY VKALDVW                 4  1  2  2  4  5  -1  9
GRA3_RAT   AETTMD MDLKNFPMDV QF LERQM KVSY VKAIDIW   KILRHEDIHHQQ  5  3  4  2  6  8  -2  14
GRA1_RAT   AETTMD MDLKNFPMDV QF LERQM KVSY VKAIDIW   KIVRREDVHNK   5  3  5  3  8  8   0  16
GRA1_HUMAN AETTMD MDLKNFPMDV QF LERQM KVSY VKAIDIW   KIVRREDVHNQ   5  3  4  3  7  8  -1  15
GRA2_HUMAN TETTMD MDLKNFPMDV QF LERQM KVSY VKAIDIW   KIIRHEDVHKK   5  3  6  2  8  8   0  16
```

```
GRA2_RAT   TETTMD MDLKNFPMDV QF LERQM KVSY VKAIDIW   KIIRHEDVHKK    5  3  6  2  8  8   0  16
GluCl-alph DVVNME MYLQYYPMDV SF LKREF PVSY IKAIDVW        RFGQQNV   3  2  2  2  4  5  -1  9
GluCl-beta DVVNME MRLQLYPLDY NF FKRQF PVSY VKVVDVW   LIMSANASTPES   3  2  2  2  4  5  -1  9
```

Key: **+** = number of cationic residues (K, R); **–** = number of anionic residues (D, E); **Z** = overall charge; **N** = number of ionic residues.

	CATION CHANNELS		
	XC	TM	TOT
+	1.0	3.4	4.4
-	4.9	1.4	6.3
Z	-3.9	2.0	-1.9
N	6.0	4.8	10.7

	ANION CHANNELS		
	XC	**TM**	**TOT**
+	0.7	4.6	5.3
-	4.6	1.9	6.4
Z	-3.9	2.8	-1.1
N	5.3	6.5	11.8

XC: extracellular part of the gating interface, containing loop2, loop 7 and loop 9. TM: trasmembrane part of the gating interface, containg preM1, M2-M3 linker and postM4. TOT: the total gating interface.

Chapter 3

NICOTINE IN THE CNS VS. THE NEUROMUSCULAR JUNCTION: A CATION-π INTERACTION AND A HYDROGEN BOND MAKE THE DIFFERENCE

3.1 Abstract

The launching point for nicotine addiction is the activation by nicotine of a family of neuroreceptors in the CNS that normally respond to the neurotransmitter acetylcholine (ACh). The same family of neuroreceptors also governs the fast electric signal transmission at the neuromuscular junction. The long standing puzzle has been the mechanism underlining a significant increase of affinity for nicotine in the CNS compared with that at the neuromuscular junction. Here, by incorporating unnatural amino acids, we report a cation-π interaction and a hydrogen bond employed by nicotine with the α4β2 receptor specifically. These two key interactions are absent or significantly diminished in both the muscle type receptors and in the α7 form of neuronal receptor. These results provide unprecedented details regarding nicotine binding in the nervous system, with significant implications for efforts in drug discovery targeting nAChRs.

3.2 Introduction

The addictive properties of nicotine lead to over 4,000,000 smoking-related deaths annually and produce the largest source of preventable mortality in the western world. Nicotine activates a family of neuroreceptors that normally respond to the

neurotransmitter acetylcholine (ACh). These aptly named nicotinic acetylcholine receptors (nAChR) are ligand-gated ion channels that mediate fast synaptic transmission throughout the central and peripheral nervous systems.[1] Therapeutic strategies targeting nAChRs have been proposed for Alzheimer's disease, schizophrenia, Parkinson's disease, pain, attention deficit-hyperactivity disorder, epilepsy, depression, autism, Tourette's syndrome, and smoking cessation[2-4]. Along with these central nervous system (CNS) indications, the nAChR also controls the neuromuscular junction, where ACh released from a motor neuron activates postsynaptic nAChRs in the muscle. Dysfunctions of nAChRs at the neuromuscular junction of the peripheral nervous system are associated with a number of myasthenic syndromes.[5, 6]

An important and curious feature of the nAChR is that sensitivity to nicotine is substantially reduced at the neuromuscular junction relative to receptors found in the CNS. Of course, the cognitive and addictive effects of nicotine occur in the CNS, and it is the relative lack of activity at the neuromuscular junction that allows smokers to experience the CNS effects of nicotine without acute motor abnormalities[4]. This unfortunate differential sensitivity to nicotine occurs despite the fact that the nAChRs of the CNS and neuromuscular junction are very highly homologous throughout their structures and are essentially identical in the immediate vicinity of the agonist binding site. (Figure 3.1)

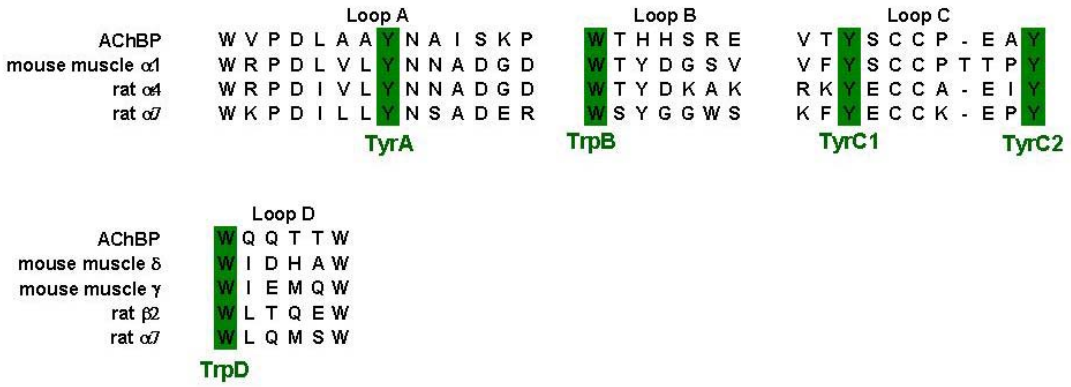

Figure 3.1 Sequence alignments in the immediate vicinity of the agonist binding sites from AChBP, mouse muscle type, rat α4β2 and rat α7 nAChR.

Here we describe studies of agonist activation of two prominent nAChRs of the CNS. Using the powerful tool of unnatural amino acid mutagenesis, we establish a strong cation-π interaction between nicotine and a conserved tryptophan in the α4β2 receptor, the nAChR type most strongly associated with nicotine addiction[7-10]. Importantly, this potent binding interaction is absent in the nAChR of the neuromuscular junction. In addition, we find that a hydrogen bond between nicotine and a backbone carbonyl of the agonist binding site is substantially strengthened in the α4β2 receptor compared to the comparable interaction with the muscle-type receptor. Taken together, these two observations provide a molecular rationale for the differential sensitivities to nicotine of the two receptors.

Surprisingly, we find that a second CNS nAChR (α7) displays a different binding pattern. While a cation-π interaction is still important, it is made to a different aromatic amino acid of the receptor than is employed by the α4β2 or muscle-type receptors. In addition, the strong hydrogen bond seen in the α4β2 receptor is significantly diminished in α7. Along with providing a molecular

understanding of the differential actions of nicotine in the CNS and neuromuscular junction, these findings have significant implications for efforts in drug discovery targeting nAChRs.

3.3 Results

3.3.1 Background and approach

nAChRs are pentameric, integral membrane, ligand-gated ion channels, whose overall layout and gross structural features have been established by cryoelectron microscopy[11]. There are 17 known human genes that code for nAChR subunits, termed α1-α10, β1-β4, γ, δ, and ε. Not all possible pentameric combinations of subunits are viable, but as many as 20 different nAChRs have been established to be important in humans[3, 7]. The nAChR of the postsynaptic membrane of the neuromuscular junction is unique. This "muscle-type" receptor has a precise stoichiometry of $(\alpha1)_2\beta1\gamma\delta$ (fetal form; the adult form is $(\alpha1)_2\beta1\delta\varepsilon$). The "neuronal" nAChRs of autonomic ganglia and cholinergic neurons throughout the CNS are formed from various combinations of α2-α10 and β2-β4 subunits[12] (Figure 1.2)

Of the neuronal receptors, two appear to play especially prominent roles in the pathology of the diseases mentioned above: the α4β2 and α7 receptors. The α4β2 receptors account for over 90% of the high affinity nicotine binding sites in the brain[3]. Activation of receptors containing α4 is known to be necessary and sufficient for nicotine-induced reward, tolerance, and sensitization[13]. Knocking out the β2 subunit in mice results in complete abolishment of nicotine self-administration[3]. Unlike the muscle-type receptor, with its precise stoichiometry,

the α4β2 receptor exists in at least two forms: $(\alpha4)_2(\beta2)_3$ and $(\alpha4)_3(\beta2)_2$.[14, 15]

Another prominent CNS nAChR is the homopentameric receptor formed from α7 subunits. This receptor has been implicated in schizophrenia and is considered a treatment target for Alzheimer's disease and other cognitive disorders[16, 17]. It has a pharmacology that is distinct from that of α4β2.

In previous work we have performed extensive studies of the muscle-type receptor. Our primary tool has been a structure-function study using the subtle and precise tool of unnatural amino acid incorporation, made possible by nonsense suppression technology[18-28]. Through such studies, we established that the quaternary ammonium ion of ACh makes a cation-π interaction with Trp149 of the α1 subunit. This was established through a fluorination plot. A cation-π interaction is a stabilizing interaction between a cation and the face of a simple aromatic, and it is broadly utilized in stabilizing both protein secondary structure & receptor-ligand binding interactions[29-32]. It is well established that fluorine is deactivating in a cation-π interaction, and that multiple fluorines have an additive effect. By successively replacing the wild type Trp with monofluoro, difluoro, trifluoro… analogues, we can probe for a cation-π interaction. A positive result manifests as a linear "fluorination plot", as shown in Figure 3.2.

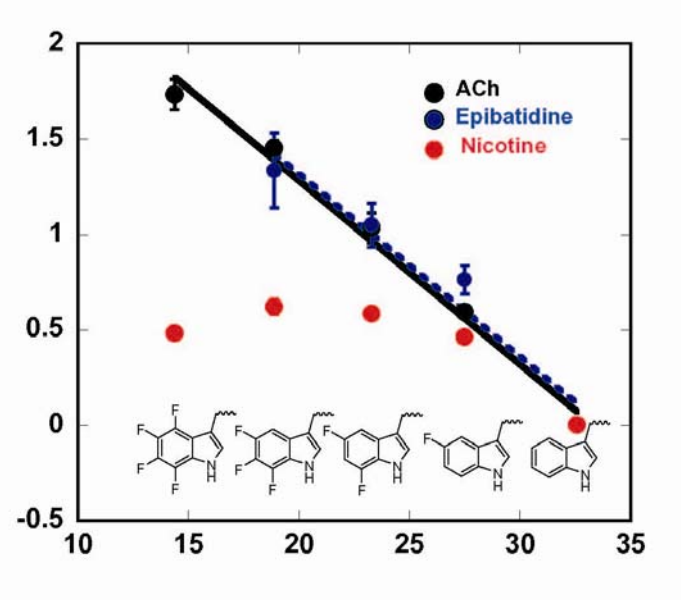

Figure 3.2 Fluorination plots demonstrating a cation-π interaction of TrpB in the muscle nAChR with the cationic centers of ACh and Epibatidine, but not with nicotine.

The fluorination plot established van der Waals contact between the quaternary ammonium of ACh and the side chain of α1Trp149. Another useful probe of a potential cation-π interaction is the cyano/bromo (CN/Br) comparison [24]. When appended to an aromatic ring, CN and Br substituents present a similar steric perturbation. However, CN is strongly deactivating in the cation-π interaction, while Br is much less so. As such, a large CN/Br effect, i.e., a much larger rise in EC_{50} for CN than for Br, can also be taken as good evidence for a cation-π interaction. In the muscle-type receptor, the ACh CN/Br effect is roughly a factor of 50 in EC_{50} for α1Trp149.

Subsequent to our structure-function studies, the binding site of the acetylcholine binding proteins (AChBP) - small, soluble, homopentameric proteins that are 20-25% homologous to the extracellular domains of nAChRs - was revealed[33]. As anticipated, the binding site is rich in aromatics and occurs at the interface between

two subunits (the relevant interfaces are α/γ and α/δ in the muscle-type receptor). Gratifyingly, the analogue of α1Trp149 (TrpB) was shown to be a component of the "aromatic box" that forms the agonist binding site. In fact, all five aromatic amino acids of the box – now referred to generically as A, B, C1, C2, and D - had previously been implicated as contributing to binding of ACh in the nAChR, confirming the relevance of AChBP to the nAChRs[34]. Crystallographic images of drugs bound to AChBP[33, 35-37] supported the viability of the cation-π interaction to the homolog to TrpB. (Figure 3.3)

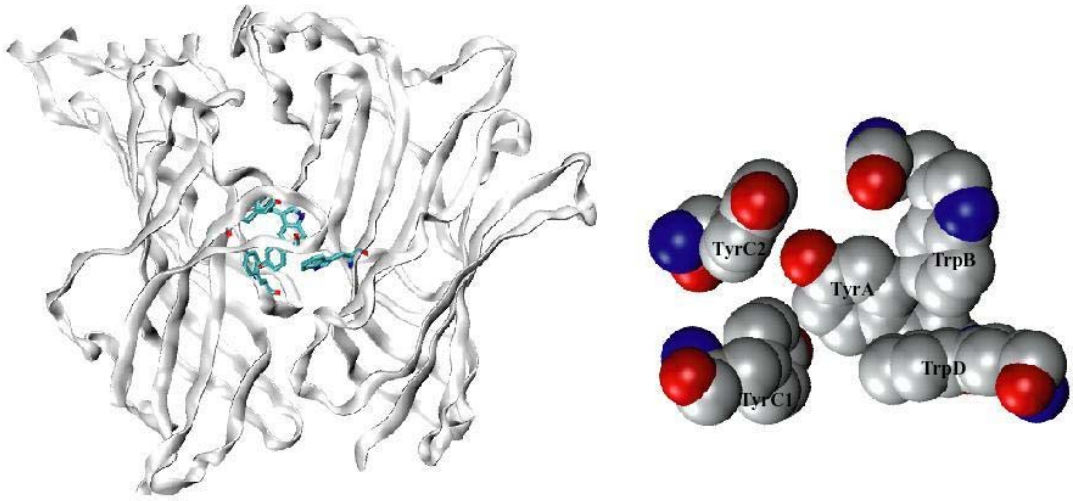

Figure 3.3 The "aromatic box" of the Cys-loop receptor. On the left, the five aromatic residues contributing to ligand binding, four from the principle subunit and one from the complementary subunit are shown as revealed in the AChBP crystal structure. On the right, the five residues are shown in VDW with generic nomenclature used in this thesis. The images are made from the crystal structure of AChBP from *Lymnaea stagnalis* in complex with carbamylcholine[38] . (PDB code 1UV6).

Given the well-established nicotinic pharmacophore, it might be assumed that the positive charge of nicotine – the protonated pyrrolidine nitrogen – would make a cation-π interaction with TrpB. However, the fluorination plot clearly established

that no such interaction occurs in the nAChR of the neuromuscular junction[18] (Figure 3.2).

The AChBP crystal structure also showed that the backbone carbonyl associated with TrpB points into the agonist binding site, and we and others inferred that this could act as a hydrogen bond acceptor for appropriate agonists. To test this hypothesis, we converted the backbone amide carbonyl to a backbone ester by substituting an α-hydroxy acid at the *i+1* position[19].(Figure 3.4) This significantly weakens the hydrogen bonding ability of the carbonyl. In the muscle-type nAChR both nicotine and epibatidine were modestly less potent when the backbone ester was present. Interestingly, the receptor with the backbone ester showed an enhanced sensitivity to ACh, which cannot make such a hydrogen bond. These data supported the hydrogen bonding motif suggested by the AChBP structure, as did subsequent structures of small molecules bound to AChBP[33, 35-38].

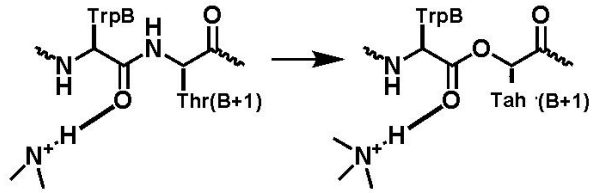

agonists	EC50 (μM)		ratio
	Thr	Tah	Tah/Thr
	muscle		
ACh	0.83	0.25	0.30
Nicotine	57	92	1.6
Epibatidine	0.60	2.2	3.7

Figure 3.4 Establishing a hydrogen bond between the backbone carbonyl and select agonists in the muscle nAChR. The left panel shows that the backbone amide carbonyl of TrpB is replaced with an ester carbonyl upon incorporation of α-hydroxythreonine (Tah) at position B+1. The right table shows EC_{50} values (μM) for testing H-bond interactions at TrpB in the muscle receptor. Data adapted from Cashin et al [19].

The nAChR is the prototype of a larger family of Cys-loop receptors that includes the $GABA_A$ and $GABA_C$ (ρ) receptors, the glycine receptor, and two

receptors for serotonin – the 5-HT_3 receptor that is found throughout the animal kingdom and a novel variant termed MOD-1 that is found in *C. elegans*. We have studied all of these except the glycine receptor, and in each case a fluorination plot reveals a cation-π interaction to the natural agonist[18, 39-41]. Interestingly, the exact location of the cation-π interaction within the aromatic box is variable. It is at position B (like in the muscle-type nAChR) for the 5-HT_3 and $GABA_C$ receptors. However, it has moved to position A in the $GABA_A$ receptor, and it has moved to position C2 in the MOD-1 receptor. To date, every Cys-loop receptor we have probed has employed a cation-π interaction to bind its agonist. However, the variable location of the cation-π interaction within the aromatic box indicates that one cannot assume that a binding interaction seen in one Cys-loop receptor will be observed in another, despite the high conservation in the agonist binding site region.

3.3.2 Challenges in studying neuronal nAChRs

While the nonsense suppression methodology has proven to be quite general, repeated attempts to apply the methodology to neuronal nAChRs were frustrated by several factors. These include poor expression in *Xenopus* oocytes and some intrinsic pharmacological properties of the receptors. We have now overcome these obstacles in both the α4β2 and α7 receptors.

The α4β2 receptors present two challenges: poor expression in *Xenopus* oocytes and ambiguous stoichiometry. Concerning the former, recent studies by Fonck et al. showed that a mutation termed L9'A in the M2 transmembrane helix of the α4 subunit greatly improves expression without altering the pharmacology of the

receptor[42]. Therefore, all studies of α4β2 described here included this mutation. As with other mutations of L9', the L9′A mutation lowers EC_{50} systematically by influencing receptor gating, a factor that does not perturb the present analysis[21, 22].

As noted above, the α4β2 receptor can have variable stoichiometry, but it is essential for the studies here to probe a homogeneous collection of receptors. A recent definitive study by Moroni et al. established that there are two forms of α4β2, $(\alpha4)_2(\beta2)_3$ and $(\alpha4)_3(\beta2)_2$, which we will refer to as A2B3 and A3B2[43]. The A2B3 form is the higher sensitivity form for nicotine, and chronic exposure to nicotine leads to upregulation of this form at the expense of A3B2 in a variety of contexts, including *Xenopus* oocytes[43, 44]. As such, the A2B3 form is most relevant to nicotine addiction, and our studies have focused on it. Several studies established that controlling the ratios of mRNAs injected into the oocyte can control subunit stoichiometry, and we have found similar results. Injection of an mRNA ratio α4(L9'A):β2 of 10:1 or higher produces pure populations of A3B2, while a ratio of 3:1 or lower guarantees a pure population of A2B3(Table 3.1). Note that the α4(L9′A) mutation lowers EC_{50} in a multiplicative fashion, depending on how many α4 subunits are present. As such, our A3B2 receptor (with three L9′A mutations) actually has a lower EC_{50} than our A2B3 receptor (with two L9′A mutations), even though the binding site from the A2B3 stoichiometry is clearly that of the high sensitivity receptor.

	mRNA ratio	ACh EC_{50} (μM)	nH	Stoichiometry
α4L9'Aβ2	**100:1**	0.02 ± 0	1.47 ± 0.18	A3B2
	10:1	0.02 ± 0	1.33 ± 0.14	
	6:1	0.15 ± 0.02	0.67 ± 0.04	mixture
	3:1	0.44 ± 0.03	1.24 ± 0.07	A2B3
	1:1	0.4 ± 0.01	1.22 ± 0.02	
	1:10	0.43 ± 0.02	1.17 ± 0.06	

Table 3.1: Injection of various mRNA ratios α4(L9'A):β2 resulting in receptors of different stoichiometry.

While varying mRNA ratios can control stoichiometry when expressing the wild type receptor, in a nonsense suppression experiment the subunit that contains the stop codon where the unnatural amino acid will be incorporated can experience variable expression levels. As such, we sought a second, independent indicator of the stoichiometry of the α4β2 receptor. We now report that the A2B3 and A3B2 forms of the α4(L9'A)β2 receptor show significantly different rectification behaviors. As indicated by either voltage ramp or voltage jump experiments, A2B3 is substantially more inward rectifying than A3B2. As such, at positive voltages A2B3 receptors pass much less outward current than A3B2 (Figure 3.5). This difference is much less pronounced in fully wild type receptors, as others have seen.

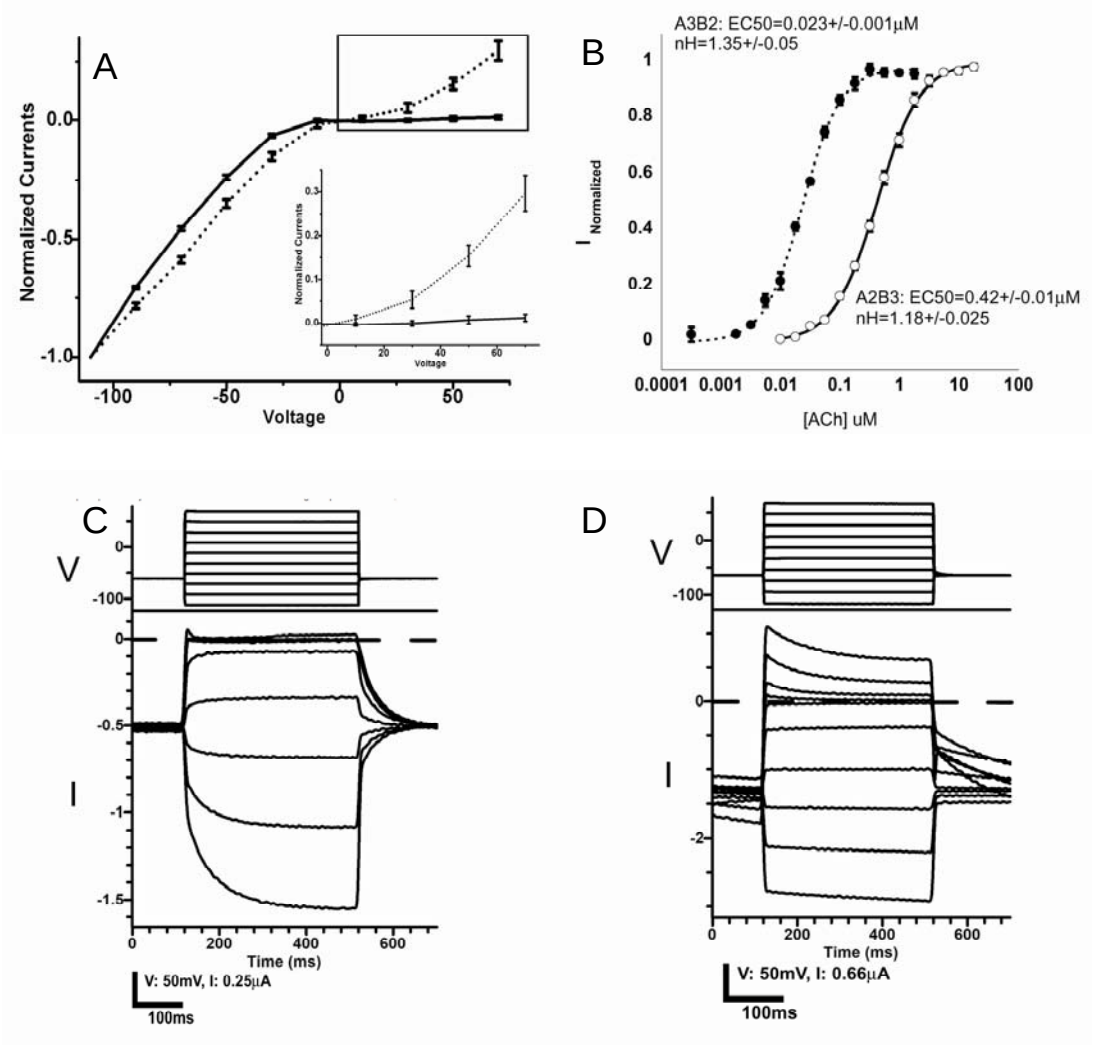

Figure 3.5 Rectification behaviors of A2B3 and A3B2 α4L9'Aβ2 nAChR in *Xenopus* oocytes. A: IV curves for A2B3 (solid line) and A3B2 (dotted line). The inset shows the blowup of the region at positive voltages. B: Corresponding dose response curves and EC_{50}s of the A2B3 (solid line) and A3B2 (dotted line) receptors. Sample traces of voltage jump experiments for A2B3 and A3B2 from which the IV curves (A) are derived are shown in C (A2B3) and D (A3B2).

In all our experiments with unnatural amino acids, the stoichiometries of mutant receptors are closely monitored by performing voltage jumps. For every mutant receptor studied, we report the normalized current size at +70mV normalized to that at -110mV. A value smaller than 0.1 establishes the desired A2B3 stoichiometry. (Table 3.2).

Studies of the α7 nAChR also presented several challenges, including poor expression and agonist concentration-dependent desensitization, which hampers the accurate measurement of dose-response relations. To address the poor expression issue, we co-expressed the human homolog of the RIC-3 protein (hRIC-3), which others have shown enhances surface expression of α7 nAChRs, presumably by aiding the folding, assembly, and/or trafficking of the protein[45-49]. To address desensitization, we introduced an alternative M2 transmembrane helix mutation termed T6'S[50]. Previous studies established that this mutation decreases desensitization without disrupting channel conductance and pharmacology.

Finally, we note that nicotine is not especially potent at α7 receptors expressed in *Xenopus* oocytes, with an EC_{50} on the order of 15-50 μM. In addition, we have found that at concentrations approaching 1mM, nicotine can induce inward currents in naive (uninjected) oocytes. While not a problem for wild type receptors, this complicates analyses of mutant receptors with elevated EC_{50} values. As such, our studies of α7 have primarily employed epibatidine as a "nicotinic" agonist, which has a much lower EC_{50} and poses no special problems.

3.3.3 A cation-π interaction in the α4β2 receptor

Given the results with the muscle-type nAChR, a logical starting point to search for a cation-π interaction in the α4β2 receptor is at TrpB (α4Trp149). With ACh as the agonist, both the CN/Br effect (10-fold ratio of EC_{50}; Table 3.2) and the fluorination effect (Figure 3.6, right panel) clearly establish a cation-π interaction. In fact, an excellent linear correlation is seen when all the data are combined

(fluorination plus CN/Br), giving a straight line with a slope very similar to that seen for the muscle-type receptor.

a4L9'Ab2					
Mutation	**ACh**	**n_H**	**Nicotine**	**n_H**	**Norm. I (+70mV)**
Wild type					
A2B3	**0.42 ± 0.01**	**1.2 ± 0.0**	**0.08 ± 0.01**	**1.2 ± 0.1**	0.041 ± 0.005
A3B2	0.02 ± 0	1.3 ± 0.1	0.01 ± 0	1.7 ± 0.2	0.297 ± 0.041
TyrA (Tyr98) A2B3					
Tyr	0.42 ± 0.03	1.2 ± 0.1	0.08 ± 0.01	1.7 ± 0.3	0.023 ± 0.009
Phe	12 ± 1	1.3 ± 0.1	0.77 ± 0.05	2.1 ± 0.3	0.064 ± 0.011
MeO-Phe	2.3 ± 0.2	1.2 ± 0.1	0.40 ± 0.02	1.7 ± 0.2	0.054 ± 0.032
F-Phe	15 ± 1	1.2 ± 0.1	0.32 ± 0.03	1.4 ± 0.2	−0.076 ± 0.046
F_2-Phe	16 ± 2	1.8 ± 0.3	0.39 ± 0.05	1.8 ± 0.4	0.028 ± 0.005
F_3-Phe	14 ± 1	1.2 ± 0.1	0.53 ± 0.04	1.4 ± 0.1	0.044 ± 0.010
Br-Phe	3.3 ± 0.2	1.2 ± 0.1	0.54 ± 0.04	1.5 ± 0.1	−0.003 ± 0.031
CN-Phe	73 ± 4	1.7 ± 0.1	8.8 ± 0.9	1.5 ± 0.2	0.075 ± 0.008
TrpB (Trp 154) A2B3					
Trp	0.44 ± 0.03	1.3 ± 0.1	0.09 ± 0.01	1.5 ± 0.1	0.006 ± 0.014
F-Trp	1.9 ± 0.1	1.2 ± 0.1	0.26 ± 0.02	1.3 ± 0.1	−0.065 ± 0.047
F_2-Trp	2.0 ± 0.1	1.3 ± 0.1	0.32 ± 0.04	1.3 ± 0.1	0.032 ± 0.025
F_3-Trp	13 ± 1	1.3 ± 0.1	1.2 ± 0.1	1.4 ± 0.2	−0.073 ± 0.029
F_4-Trp	29 ± 2	1.1 ± 0.1	4.2 ± 0.4	1.3 ± 0.2	−0.027 ± 0.023
CN-Trp	12 ± 1	1.2 ± 0.1	0.90 ± 0.07	1.4 ± 0.1	0.009 ± 0.017
Br-Trp	1.1 ± 0.1	1.3 ± 0.1	0.20 ± 0.02	1.3 ± 0.2	0.020 ± 0.005
TyrC1 (Tyr195) A2B3					
Tyr	0.42 ± 0.03	1.5 ± 0.1	0.07 ± 0	1.3 ± 0.1	0.042 ± 0.014
Phe	53 ± 4	1.3 ± 0.1	3.3 ± 0.2	1.2 ± 0.1	0.059 ± 0.014
MeO-Phe	48 ± 5	1.4 ± 0.2	2.8 ± 0.4	1.2 ± 0.2	0.064 ± 0.028
CN-Phe	210 ± 10	1.6 ± 0.1	19 ± 2	1.6 ± 0.2	0.057 ± 0.011
TyrC2 (Tyr202) A2B3					
Tyr	0.42 ± 0.03	1.3 ± 0.1	0.09 ± 0.01	1.6 ± 0.1	0.057 ± 0.016
Phe	0.32 ± 0.02	1.4 ± 0.1	0.14 ± 0.01	1.4 ± 0.1	0.014 ± 0.010
MeO-Phe	0.33 ± 0.02	1.3 ± 0.1	0.097 ± 0.006	1.7 ± 0.2	0.034 ± 0.033
CN-Phe	0.42 ± 0.04	1.4 ± 0.2	0.11 ± 0.01	1.6 ± 0.2	0.066 ± 0.046
Thr (B+1) (Thr 155) A2B3					
Thr	0.41 ± 0.02	1.4 ± 0.1	0.09 ± 0.01	1.6 ± 0.1	0.044 ± 0.007
Tah	0.37 ± 0.02	1.3 ± 0.1	1.71 ± 0.14	1.2 ± 0.1	0.018 ± 0.013

Table 3.2 EC_{50} values (μM), Hill coefficients and normalized current size at +70mV (normalized to current size at -100mV as -1) for selected mutants in α4L9'Aβ2 nAChR A2B3 receptors.

While the ACh results for α4β2 parallel those of the muscle-type receptor, a dramatic change is seen with nicotine. In the α4β2 receptor, nicotine precisely mimics ACh, giving a linear fluorination plot and a strong CN/Br effect (Table 3.2; Figure 3.6, left panel). These observations clearly establish a cation-π interaction between nicotine and TrpB of the α4β2 receptor. Recall that in the nAChR of the neuromuscular junction there is no such cation-π interaction to TrpB, and so this specific noncovalent binding interaction provides a clear discriminator between the neuronal and muscle-type receptors. With nicotine as agonist, the low sensitivity muscle-type nAChR lacks a key noncovalent interaction that evidently increases the nicotine sensitivity of the neuronal receptor.

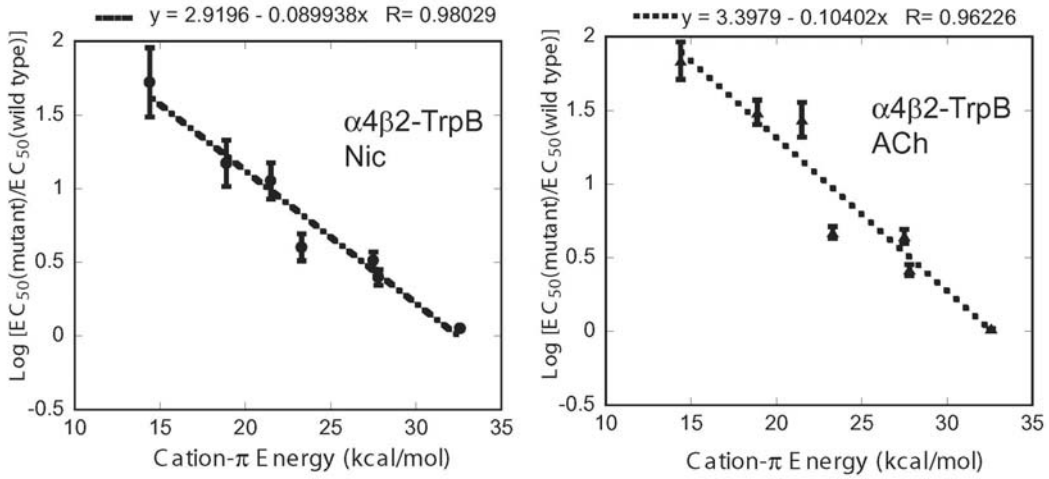

Figure 3.6 Fluorination plots demonstrating cation-π interactions of TrpB in α4β2 nAChR with nicotine (left) and ACh (right). In addition to fluorinated tryptophans, CN-Trp and Br-Trp are also included in these plots, which fitted excellently on the lines. On each plot, from the left to the right, each point represents F_4-Trp, F_3-Trp, CN-Trp, F_2-Trp, F-Trp, Br-Trp and Trp.

We have performed extensive studies of other aromatic residues in and around the aromatic box (Table 3.2). Briefly, when comparing α4β2 to the muscle-type receptor, very similar results are seen. TyrC1 is very sensitive to substitution, establishing a key role for this residue, likely in receptor gating. TyrA appears to be a hydrogen bond donor (large effects for Phe and MeO-Phe substitutions), and while it is generally more sensitive to perturbations in the neuronal receptor, the basic trends are the same. TyrC2 is very permissive in both the muscle-type and α4β2 receptors.

3.3.4 A strong hydrogen bond in the α4β2 receptor

To probe a potential hydrogen bond to a backbone carbonyl we employ the strategy outlined in Figure 3.4. By replacing the amino acid at the *i+1* position with the analogous α-hydroxy acid, the carbonyl associated with residue *i* is converted to an ester carbonyl rather than an amide (peptide) carbonyl. It is well established that ester carbonyls are much poorer hydrogen bond acceptors than amide carbonyls, and so if a hydrogen bond to this carbonyl is essential, the backbone ester mutation should influence agonist potency. In the muscle-type receptor the mutation raised EC_{50} for nicotine and epibatidine by factors of 1.6 and 3.7, respectively. Epibatidine is a much more potent agonist at the muscle-type receptor than nicotine, consistent with the relative magnitudes of the ester effect.

In the α4β2 receptor, a much more dramatic effect is seen (Table 3.2). With nicotine as the agonist, the backbone ester mutation causes a 19-fold increase in EC_{50}. Importantly, the potency of ACh, which can not make a conventional hydrogen bond to the carbonyl, is essentially unperturbed by the backbone ester mutation. This

establishes that the mutation does not globally alter the binding/gating characteristics of the receptor, supporting the notion that we are modulating a potential hydrogen bonding interaction between the receptor and nicotine.

3.3.5. Single channel measurements

The EC_{50} values for the various mutants described here represent a measure of receptor function and are thus a composite of ligand binding and receptor gating properties. We have argued in the past that subtle mutations of residues that are intimately involved in forming the ligand binding site most likely are perturbing ligand binding rather than channel gating. However, comparably subtle mutations of some other residues in or near the agonist binding site have been shown to influence gating. We cannot thus not rule out the possibility that the fluorination effects on EC_{50} result from reductions in agonist efficacy (gating efficiency), rather than agonist binding. As such, we evaluated the gating behaviors of several key mutants using patch clamp techniques.

We recorded single channel traces for the α4L9′Aβ2 receptor with Trp or F_3-Trp at TrpB, the cation-π site (J. A. P. Shanata, personal communication). In each case, nicotine is applied at its EC_{50}. With Trp at position B, nicotine is a partial agonist, with P_{open} ~0.2 at EC_{50}. This is consistent with macroscopic (whole cell) studies, which also show nicotine to be a partial agonist relative to ACh. With F_3-Trp at TrpB, P_{open} *increases* to ~0.4. Thus, it appears that nicotine is slightly more efficacious in the F_3-Trp mutant than in the Trp receptor, and so the rise in EC_{50} cannot be a gating effect. We conclude that fluorination has diminished the binding

affinity of nicotine for the receptor.

3.3.6 Different behavior in the α7 receptor

Again, the logical starting point in searching for a cation-π interaction in α7 was TrpB. However, it is clear that there is no cation-π interaction to TrpB of the α7 receptor with either ACh or epibatidine as agonist. (Table 3.3) Both CN-Trp and F_2-Trp give essentially wild type behavior. As noted above, nicotine can be problematical with the α7 receptor, but we were able to obtain convincing data to establish that EC_{50} is also unperturbed by the CN-Trp mutant with nicotine as the agonist.

Since other Cys-loop receptors have employed site A or site C2 in cation-π interactions, we probed those locations in α7; both residues are natively tyrosines. We note that tyrosines have proven to be more challenging than tryptophans when probing for a cation-π interaction. Directly fluorinating tyrosine will progressively lower the pK_a of the side chain OH, such that the pK_a for tetrafluorotyrosine is ~5.3. This could lead to ionization of the OH in substituted tyrosines, which would complicate the analysis. To circumvent this potential problem in other systems, we considered the phenylalanine mutant as our starting point, since it can be fluorinated with no complications. However, at site A of the α7 receptor, the Phe mutant is significantly compromised (factor of almost 50 in EC_{50} for ACh). Interestingly, 4-MeO-Phe, 4-Br-Phe, 4-Ac-Phe and, to a lesser extent, 4-Me-Phe rescue the wild type EC_{50}. It thus appears that in α7, the 4-substituent of TyrA is an essential steric placeholder. This is a very different pattern from what is seen at TyrA in α4β2 or

muscle-type receptors, for which the OH appears to be a hydrogen bond donor, not a steric placeholder.

We find strong evidence for a cation-π interaction between ACh and TyrA (Tyr92). (Figure 3.7, left panel) There is a clear correlation in the fluorination plot, and the slope is comparable to that seen for other cation-π plots involving ACh. There is more scatter than in most other fluorination plots we have seen, but the steric impact of the 4-substituent is overlaid on this plot. Note the large CN/Br ratio, which compensates to a considerable extent for that steric effect.

The TyrA plot for epibatidine shows more scatter and a smaller slope. (Figure 3.7, right panel) There appears to be an interaction, but it may be weaker than normal.

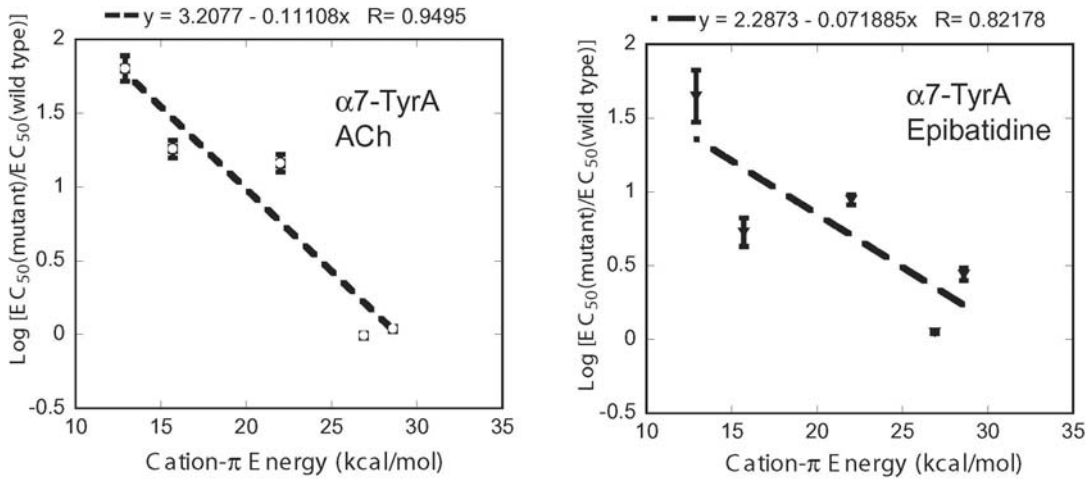

Figure 3.7 Fluorination plots demonstrating cation-π interactions of TyrA in α7 nAChR with ACh (left) and epibatidine (right). On each plot, from the left to the right, each point represents F_3-Phe, CN-Phe, F-Phe, Tyr, and MeO-Phe.

At TyrC2 (Y194) a different story emerges. There is no cation-π interaction involving ACh. (Table 3.3) However, epibatidine shows a clear correlation, with a

larger slope than seen at TyrA and less scatter. (Figure 3.8) We conclude there is a significant cation-π interaction to TyrC2 for epibatidine, but not for ACh.

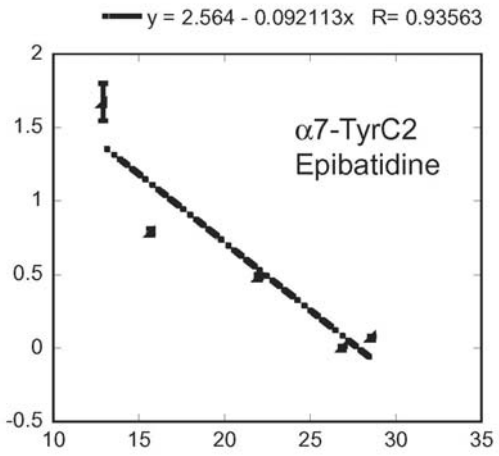

Figure 3.8 Fluorination plots demonstrating cation-π interactions of TyrC2 in α7 nAChR with epibatidine. On the plot, from the left to the right, each point represents F_3-Phe, CN-Phe, F-Phe, Tyr, and MeO-Phe.

We also evaluated the potential hydrogen bond to the backbone carbonyl of TrpB. The results are much different than seen for α4β2. For epibatidine, the backbone ester substitution raises EC_{50} only 2.1-fold. Also, EC_{50} for ACh actually drops by a factor of 4. This is precisely the pattern that was seen in the muscle-type receptor, and the implications of the ACh effect have been discussed previously (Table 3.3).

α7 T6'S				
Mutation	**ACh**	**n_H**	**Epibatidine**	**n_H**
Wild type	**94 ± 3**	**1.8 ± 0.1**	**0.34 ± 0.01**	**2.5 ± 0.1**
		TyrA (Tyr92)		
Tyr	93 ± 10	1.5 ± 0.2	0.38 ± 0.05	2.2 ± 0.5
Phe	4500 ± 200	3.1 ± 0.4	3.0 ± 0	3.4 ± 0.2
MeO-Phe	100 ± 0	2.3 ± 0.1	0.94 ± 0.09	2.2 ± 0.4
CN-Phe	1700 ± 100	2.1 ± 0.1	1.8 ± 0.2	1.7 ± 0.3
F-Phe	1400 ± 100	3.3 ± 0.4	3.0 ± 0.1	3.5 ± 0.4
F_3-Phe	6000 ± 200	2.2 ± 0.2	15 ± 2	3.2 ± 0.7
Me-Phe	330 ± 30	1.8 ± 0.2	2.7 ± 0.1	2.8 ± 0.1
Ac-Phe	95 ± 9	2.2 ± 0.7	0.26 ± 0.01	3.0 ± 0.3
Br-Phe	78 ± 3	2.5 ± 0.2	0.34 ± 0.04	1.4 ± 0.1
3-MeO-Phe	>5000		33 ± 1	3.1 ± 0.2
mTyr	4700 ± 300	2.0 ± 0.1	no signal	
COOH-Phe	4500 ± 200	2.3 ± 0.3	5.1 ± 0.1	2.8 ± 0.1
CHA	no signal		signal too small	
F_2-Phe	4100 ± 200	2.6 ± 0.3	18 ± 1	2.0 ± 0.2
		TrpB (Trp148)		
Trp	93 ± 9	1.7 ± 0.3	0.38 ± 0.02	2.1 ± 0.2
CN-Trp	63 ± 4	1.7 ± 0.2	0.14 ± 0.03	3.1 ± 1.4
F_2-Trp	87 ± 5	1.7 ± 0.1	0.62 ± 0.04	2.4 ± 0.3
		TyrC1 (Tyr187)		
Tyr	98 ± 5	2.2 ± 0.2		
Phe	8600 ± 600	2.7 ± 0.4		
MeO-Phe	no signal			
F_3-Phe	no signal			
F-Phe	no signal			
		TyrC2 (Tyr194)		
Tyr	94 ± 2	2.3 ± 0.1	0.35 ± 0.04	2.6 ± 0.6
Phe	560 ± 20	2.6 ± 0.2	3.8 ± 0.4	1.6 ± 0.3
MeO-Phe	160 ± 10	2.1 ± 0.2	0.41 ± 0.01	3.2 ± 0.2
CN-Phe	150 ± 10	2.3 ± 0.2	2.1 ± 0	2.4 ± 0.2
F-Phe	86 ± 5	2.0 ± 0.2	1.1 ± 0	2.8 ± 0.1
F_3-Phe	1300 ± 100	2.4 ± 0.3	16 ± 1	3.0 ± 0.4
Me-Phe	99 ± 7	2.7 ± 0.5	0.70 ± 0.04	2.2 ± 0.2
Br-Phe	51 ± 2	1.7 ± 0.1	0.32 ± 0.02	1.5 ± 0.1
3-MeO-Phe	no signal		no signal	
mTyr	780 ± 80	1.7 ± 0.2	signal too small	
F_2-Phe	870 ± 40	2.9 ± 0.4	13 ± 1	2.3 ± 0.2
		TrpD (Trp54)		
Trp	92 ± 4	2.1 ± 0.2		
CN-Trp	130 ± 10	2.4 ± 0.3		
		Trp153		
CN-Trp	56 ± 4	1.5 ± 0.2		
		Tyr150		
Phe	430 ± 10	2.6 ± 0.1	1.6 ± 0.1	2.2 ± 0.3
F_3-Phe	420 ± 40	1.4 ± 0.1	1.9 ± 0.1	3.1 ± 0.2
MeO-Phe	140 ± 20	1.4 ± 0.2	0.61 ± 0.09	1.4 ± 0.2
Me-Phe	110 ± 0	1.9 ± 0.1	0.75 ± 0.03	1.9 ± 0.2
Br-Phe	160 ± 0	2.1 ± 0.1	0.86 ± 0.04	2.1 ± 0.2
		Phe103		
F_3-Phe	120 ± 0	2.0 ± 0.1	0.37 ± 0.01	2.6 ± 0.1
		Phe145		
F_3-Phe	170 ± 20	1.6 ± 0.5	0.44 ± 0.02	2.8 ± 0.4
		Phe186		
F_3-Phe	140 ± 30	1.4 ± 0.4		
		Ser (B+1) (Ser 149)		
Thr	47 ± 2	2.2 ± 0.1	0.45 ± 0.01	2.1 ± 0.12
Tah	11 ± 1	1.9 ± 0.3	0.95 ± 0.03	2.7 ± 0.2

Table 3.3 EC_{50} values (μM) and Hill coefficients for selected mutants in α7 T6'S nAChR.

3.4 Discussion

The diverse family of nAChRs provides an array of targets for pharmaceutical development. In addition, an understanding of the physiological effects of nicotine requires insights into the differential actions of this powerful drug on the various forms of nAChR. How is it that nicotine and nicotinic analogues can target specific types of nAChRs, when the sequence similarity is considerable, especially in the region of the agonist binding site? The powerful tool of unnatural amino acid mutagenesis is ideal for addressing such questions. The subtle and systematic modifications that the method enables can isolate specific binding interactions and provide compelling evidence for their absence or existence, as well as qualitative guidance on the relative magnitudes of specific interactions.

The primary goal of the present work was to understand why nicotine is potent at the CNS receptor most associated with nicotine addiction, α4β2, but not at the neuromuscular junction. Concerning the binding of ACh, the muscle-type nAChR and α4β2 show very similar behaviors. The quaternary ammonium ion of ACh makes van der Waals contact to the side chain of TrpB, providing an unambiguous anchor point for ACh docking. The roles of the other components of the aromatic box also seem to be similar in the muscle-type and α4β2 receptors when binding ACh.

When considering the binding of nicotine, however, a dramatic difference was seen. In α4β2 nicotine makes the same cation-π interaction as ACh, consistent with the long-accepted nicotinic pharmacophore. At the muscle-type receptor, however, this important interaction is absent. Thus, a cation-π interaction to TrpB is a

clear-cut discriminator between receptors with high sensitivity to nicotine (α4β2) and those with lower sensitivity (muscle-type).

Whenever EC_{50} is used to evaluate mutant receptors, it can be difficult to deconvolute binding effects from gating effects. In previous efforts we have argued that the subtlety of the fluorination mutations, the proximity of the residues to the agonist binding site, and the strong correlation with what is clearly a binding phenomenon (a cation-π interaction) argue strongly that we are modulating binding, not gating. Still, this is not an incontrovertible argument, and other subtle mutations in the agonist binding site region clearly impact gating.

Here we have used single channel measurements to convincingly establish that the fluorination approach we have applied is modulating nicotine binding, not channel gating. Consider, for example, the F_3-Trp mutation at TrpB of α4β2, which shows an increase in EC_{50} over wild type of ~13-fold. If this EC_{50} increase was caused by changes in channel gating, the gating equilibrium would have changed over 100 fold, and thus the P_{open} would have decreased significantly compared with the wild type. Our measurements show that at EC_{50} nicotine, F_3-Trp at TrpB has a P_{open} higher than the wild type; therefore, the rise in EC_{50} must be caused by diminished binding affinity of nicotine for the receptor.

We have also identified another discriminating factor in the binding of nicotine at α4β2 vs. muscle-type receptors. Based on the AChBP structures it was proposed that nicotine makes a hydrogen bond to the backbone carbonyl associated with TrpB. To test this hypothesis, we employed a backbone ester strategy, converting the

carbonyl in question to a weaker hydrogen bond acceptor (ester vs. amide). As with the fluorination strategy employed to evaluate a cation-π interaction, the advantages of the unnatural amino acid methodology are evident here. To probe a potential hydrogen bonding interaction we do not ablate it, we simply modulate it in a controlled and predictable manner. Importantly, in the present case when the agonist was ACh – a molecule that can not make a conventional hydrogen bond to a carbonyl – essentially wild type receptor behavior was seen. This indicates that the backbone mutation did not alter receptor function, i.e., gating.

In the muscle-type receptor nicotine is a very weak agonist, and it shows a modest 1.6-fold rise in EC_{50} due to the backbone ester mutation. The more potent agonist epibatidine, which is clearly a "nicotinic" agonist, shows a larger 3.7-fold shift in the muscle-type receptor. In contrast, at α4β2 nicotine shows a 19-fold increase in EC_{50} in response to the ester mutation. To appreciate the significance of this difference, if we put these shifts on an energy scale, the effects are 0.28 kcal/mol at the muscle-type vs. 1.7 kcal/mol at α4β2. We conclude that while nicotine is able to make a hydrogen bond to the carbonyl in question in both receptors, the interaction is much stronger in the α4β2 receptor than in the muscle-type, and that this is an additional contributor to the enhanced potency of nicotine at α4β2.

We also considered a second neuronal nAChR, the homopentameric α7 receptor. Along with being an intrinsically interesting target, our previous experience with Cys-loop receptors established that it is risky to assume that a binding interaction seen in one member of a family will carry over to other members. Indeed, we find a

dramatic change in the binding mode on going from α4β2 to α7. Remarkably, the strong cation-π interaction that ACh and nicotine make to TrpB in α4β2 is completely absent in α7. This result is quite unambiguous; both CN substitution and difluoro substitution have no effect on EC_{50} for ACh and epibatidine, and nicotine is oblivious to CN substitution (the stronger perturbation of the two). So, despite complete identity among the five residues that form the aromatic box, ACh adopts two different binding modes in the neuronal nAChRs.

To date, every Cys-loop receptor we have studied makes a cation-π interaction, so we assumed one must be present in α7. For ACh as agonist, that site is now TyrA. Fluorination has a strong, additive effect, and given the complications associated with modulating this tyrosine site, the fit to the fluorination plot is good. Also, the CN/Br ratio is large.

The situation with epibatidine is more complicated, and, to some extent, unprecedented. It is clear that fluorination at TyrA impacts epibatidine potency, and more fluorines have a bigger effect. However, the correlation is not nearly as compelling as in other systems, and the slope is less than any other we have seen. We propose that the diminished slope indicates a weaker than usual cation-π interaction. A weaker cation-π interaction would make the fluorination plot more susceptible to other variations such as steric effects, accounting for the generally poorer quality of the fit.

At TyrC2, however, a much more compelling plot is obtained with epibatidine. The fit is better, and the slope is well within the normal range for a cation-π

interaction. It thus appears that epibatidine interacts with two contributors to the aromatic box: strongly with TyrC2 and less strongly with TyrA. While we have not seen such behavior before in a Cys-loop receptor, these two tyrosines are quite near each other,(Figure 3.3) and the epibatidine molecule is large enough to contact both residues simultaneously. Note that the energetic fall off of the cation-π interaction with distance between the cation and the aromatic is not especially steep, and so even a cation that is not in direct van der Waals contact with an aromatic can experience a significant stabilization.

The α7 receptor is also different from α4β2 with regard to hydrogen bonding. The very strong interaction to the TrpB backbone carbonyl seen in α4β2 is greatly diminished in α7. In fact, with regard to hydrogen bonding (but not the cation-π interaction), α7 is qualitatively similar to the muscle-type receptor.

We have now studied three members of the nAChR family: muscle-type, α4β2, and α7. The pharmacologies of these vary, and we have identified structural features of the receptor that discriminate among the three. The three receptors make different use of the cation-π interaction to recognize agonists. In the muscle-type receptor, TrpB makes a cation-π interaction to ACh, but not to nicotine. In α4β2, the TrpB cation-π interaction to ACh remains, but now nicotine also makes a strong cation-π interaction. Finally, the α7 receptor eschews the cation-π interaction to TrpB, and agonists have moved their cationic center across the aromatic box to TyrA and TyrC2. As we have seen with other Cys-loop receptors, there is considerable risk in extrapolating too heavily from one model structure, AChBP, to a large family of

receptors. Such a model structure provides extremely valuable guidance, but not definitive answers.

A second discriminating feature of the family is the hydrogen bonding interaction to the backbone carbonyl of TrpB. While this interaction is modest in the muscle-type and α7 receptors, it is much stronger in α4β2, the most sensitive of the receptors studied here.

What features of the nAChRs produce these differing binding behaviors? As noted above, the five aromatic residues, three tyrosines and two tryptophans that form the aromatic box are completely conserved in the nAChR family. Clearly, one must think outside of the box to find the answers. It must be that other features of the receptor are reshaping the box, facilitating interactions with particular agonists and discouraging others. The beautiful aromatic box of AChBP must in fact be deformable and adaptable to specific receptor requirements. There is considerable variability in loop C among the three receptors probed here. Also, many workers have proposed that the "non-α" subunit is more responsible for subtype specificity. Here, that would be subunits δ and γ in the muscle-type, β2, and α7 in the neuronals. Loop D and other non-α regions (loops E and F) do show significant sequence variability among the various subtypes.

In summary, we have identified key noncovalent binding interactions that contribute to the differential pharmacology of three nAChRs. The critical factor that makes nicotine potent in the brain but not at the neuromuscular junction can be traced to a cation-π interaction that is strong in the α4β2 neuronal receptor but absent in the

muscle-type receptor. Additionally, a hydrogen bond to the agonist that is present in all receptors is significantly enhanced in the high sensitivity α4β2 receptor. A cation-π interaction is also important in another neuronal receptor, α7, but the interaction has moved across the agonist binding site to a different aromatic residue(s). These results provide valuable insights into the molecular basis of nicotine addiction and should provide useful guidance to efforts to develop subtype-selective drugs that target nAChRs.

3.5 Experimental procedures

3.5.1 mRNA synthesis and mutagenesis

Rat α4, β2 and α7 mRNA were obtained from linearizations of the expression vector pAMV with Not1, followed by *in vitro* transcription using the mMessage mMachine T7 kit from Ambion (Austin, TX). The mutations for each subunit were introduced according to the QuikChange mutagenesis protocol (Stratagene). The cDNA for hRIC-3 was obtained from Dr. Miller Treinin at Hebrew University and the mRNA was *in vitro* transcribed from XhoI linearized expression vector pGEM.

3.5.2 Ion channel expression

To express the ion channels with a wild type ligand binding box, α4L9'A mRNA was coinjected with β2 mRNA at various ratios (total mRNA 10-25ng/cell). 10-25ng α7 T6'S mRNA was coinjected with 20ng of hRIC-3 mRNA per cell. Stage V-VI oocytes of *Xenopus Laevis* were employed and the injected cells were allowed 24-48 hour incubation at 18°C before characterization.

3.5.3 Unnatural amino acid / α-hydroxy acid incorporation

Nitroveratryloxycarbonyl (NVOC) protected cyanomethyl ester form of unnatural amino acids and α-hydroxythreonine cyanomethyl ester were synthesized, coupled to dinucleotide dCA, and enzymatically ligated to 74-mer THG73 $tRNA_{CUA}$ as detailed previously. The unnatural amino acid-conjugated tRNA was deprotected by photolysis immediately before co-injection with mRNA containing the TAG mutation at the site of interest. Typically, about 10-25 ng mRNA and 25 ng tRNA-amino acid or tRNA-hydroxy acid were injected into stage V–VI oocytes in a total volume of 50 nL. For all the α7 T6'S mutant channels, 20ng of hRIC-3 mRNA was coinjected with the mRNA/tRNA mixture.

The fidelity of unnatural amino acid incorporation is confirmed at each site with a so-called "wild type recovery" experiment and a read-through test. In the "wild type recovery" experiment, TAG mutant mRNA was coinjected with tRNA charged with the amino acid that is present at this residue in the wild type protein. Generation of receptors that are indistinguishable from the wild type protein indicates that the residue carried by the suppressor tRNA is successfully and exclusively integrated into the protein. In a read-through test, the TAG mutant mRNA was introduced with no tRNA or with tRNA THG73 that is not charged with any amino acid or with tRNA THG73 enzymatically ligated with dinucleotide dCA. Lack of currents in these experiments validates the reliability of the nonsense suppression experiments.

3.5.4 Electrophysiological characterizations of the channels

Agonist induced currents were recorded in two-electrode voltage clamp mode using the OpusXpress 6000A (Molecular Devices Axon Instruments) at a holding potential of -60mV. In the case of α4L9'Aβ2 receptors, agonists were prepared in ND96 Ca^{2+} free buffer, applied for 12s, and followed by a 2 minute wash with ND96 Ca^{2+} free buffer between each concentration. For α7 T6'S receptors, agonists were prepared in ND96 buffer and applied for 30s or 12s. 5 minutes of wash with ND96 buffer was allowed between each concentration. Acetylcholine chloride, (-)-nicotine tartrate, and (±)-epibatidine dihydrochloride were purchased from Sigma/Aldrich/RBI (St. Louis, MO). Dose-response data were obtained for at least 6 concentrations of agonists and for a minimum of 5 oocytes. Mutants with I_{max} of at least 100 nA of current were defined as functional. EC_{50} and Hill coefficient were calculated by fitting the dose-response relation to the Hill equation. All data are reported as means ± S.E.

Voltage jump experiments were performed in the absence of ACh and at EC_{50} concentration of ACh. The membrane potential was held at -60mV, and stepped to 10 test potentials at 20mV increments between +70mV and -110mV for 400ms each. 600ms at -60mV holding potential was allowed between each test potential. Background subtracted traces were used to measure the steady-state amplitudes of the ACh-induced currents near the end of the test pulses. Normalized I-V curves were generated using current amplitudes normalized to that at -110mV. For each α4L9'Aβ2 mutant, normalized I_{+70mV} ± S.E. from at least 5 cells was reported.

3.6 References

1. Wonnacott, S., N. Sidhpura, and D.J. Balfour, *Nicotine: from molecular mechanisms to behaviour.* Curr Opin Pharmacol, 2005. **5**(1): p. 53-9.
2. Lester, H.A., et al., *Cys-loop receptors: new twists and turns.* Trends Neurosci. 2004 Jun;27(6):329-36.
3. Jensen, A.A., et al., *Neuronal nicotinic acetylcholine receptors: structural revelations, target identifications, and therapeutic inspirations.* J Med Chem. 2005 Jul 28;48(15):4705-45.
4. Romanelli, M.N., et al., *Central Nicotinic Receptors: Structure, Function, Ligands, and Therapeutic Potential.* ChemMedChem, 2007. **2**(6): p. 746-767.
5. Grosman, C., et al., *The extracellular linker of muscle acetylcholine receptor channels is a gating control element.* J Gen Physiol. 2000 Sep;116(3):327-40.
6. Sine, S.M., et al., *Mutation of the acetylcholine receptor alpha subunit causes a slow-channel myasthenic syndrome by enhancing agonist binding affinity.* Neuron. 1995 Jul;15(1):229-39.
7. Gotti, C., M. Zoli, and F. Clementi, *Brain nicotinic acetylcholine receptors: native subtypes and their relevance.* Trends Pharmacol Sci. 2006 Sep;27(9):482-91. Epub.
8. Laviolette, S.R. and D. van der Kooy, *The neurobiology of nicotine addiction: bridging the gap from molecules to behaviour.* Nat Rev Neurosci, 2004. **5**(1): p. 55-65.
9. Mansvelder, H.D., J.R. Keath, and D.S. McGehee, *Synaptic Mechanisms Underlie Nicotine-Induced Excitability of Brain Reward Areas.* Neuron, 2002. **33**(6): p. 905.
10. Mansvelder, H.D. and D.S. McGehee, *Cellular and synaptic mechanisms of nicotine addiction.* J Neurobiol. 2002 Dec;53(4):606-17.
11. Unwin, N., *Refined structure of the nicotinic acetylcholine receptor at 4A resolution.* J Mol Biol. 2005 Mar 4;346(4):967-89.
12. Gotti, C. and F. Clementi, *Neuronal nicotinic receptors: from structure to pathology.* Prog Neurobiol. 2004 Dec;74(6):363-96.
13. Tapper, A.R., et al., *Nicotine activation of alpha4* receptors: sufficient for reward, tolerance, and sensitization.* Science. 2004 Nov 5;306(5698):1029-32.
14. Zhou, Y., et al., *Human alpha4beta2 acetylcholine receptors formed from linked subunits.* J Neurosci. 2003 Oct 8;23(27):9004-15.
15. Nelson, M.E., et al., *Alternate Stoichiometries of alpha 4beta 2 Nicotinic Acetylcholine Receptors.* Mol Pharmacol, 2003. **63**(2): p. 332-341.
16. Harris, J.G., et al., *Effects of nicotine on cognitive deficits in schizophrenia.* Neuropsychopharmacology. 2004 Jul;29(7):1378-85.
17. Newhouse, P.A., A. Potter, and A. Singh, *Effects of nicotinic stimulation on cognitive performance.* Curr Opin Pharmacol. 2004 Feb;4(1):36-46.
18. Beene, D.L., et al., *Cation-pi interactions in ligand recognition by serotonergic (5-HT3A) and nicotinic acetylcholine receptors: the anomalous binding properties of nicotine.* Biochemistry. 2002 Aug 13;41(32):10262-9.

19. Cashin, A.L., et al., *Using physical chemistry to differentiate nicotinic from cholinergic agonists at the nicotinic acetylcholine receptor.* J Am Chem Soc. 2005 Jan 12;127(1):350-6.
20. England, P.M., et al., *Backbone mutations in transmembrane domains of a ligand-gated ion channel: implications for the mechanism of gating.* Cell. 1999 Jan 8;96(1):89-98.
21. Kearney, P.C., et al., *Dose-response relations for unnatural amino acids at the agonist binding site of the nicotinic acetylcholine receptor: tests with novel side chains and with several agonists.* Mol Pharmacol. 1996 Nov;50(5):1401-12.
22. Kearney, P.C., et al., *Determinants of nicotinic receptor gating in natural and unnatural side chain structures at the M2 9′ position.* Neuron. 1996 Dec;17(6):1221-9.
23. Nowak, M.W., et al., *In vivo incorporation of unnatural amino acids into ion channels in Xenopus oocyte expression system.* Methods Enzymol. 1998;293:504-29.
24. Zhong, W., et al., *From ab initio quantum mechanics to molecular neurobiology: a cation-pi binding site in the nicotinic receptor.* Proc Natl Acad Sci U S A. 1998 Oct 13;95(21):12088-93.
25. Beene, D.L., D.A. Dougherty, and H.A. Lester, *Unnatural amino acid mutagenesis in mapping ion channel function.* Curr Opin Neurobiol. 2003 Jun;13(3):264-70.
26. Rodriguez, E.A., H.A. Lester, and D.A. Dougherty, *Improved amber and opal suppressor tRNAs for incorporation of unnatural amino acids in vivo. Part 1: Minimizing misacylation.* RNA. 2007 Oct;13(10):1703-14.
27. Rodriguez, E.A., H.A. Lester, and D.A. Dougherty, *In vivo incorporation of multiple unnatural amino acids through nonsense and frameshift suppression.* Proc Natl Acad Sci U S A. 2006 Jun 6;103(23):8650-5.
28. Rodriguez, E.A., H.A. Lester, and D.A. Dougherty, *Improved amber and opal suppressor tRNAs for incorporation of unnatural amino acids in vivo. Part 2: Evaluating suppression efficiency.* RNA. 2007 Oct;13(10):1715-22.
29. Dougherty, D.A., *Cation-pi interactions in chemistry and biology: a new view of benzene, Phe, Tyr, and Trp.* Science. 1996 Jan 12;271(5246):163-8.
30. Zacharias, N. and D.A. Dougherty, *Cation-pi interactions in ligand recognition and catalysis.* Trends Pharmacol Sci. 2002 Jun;23(6):281-7., 2002.
31. Gallivan, J.P. and D.A. Dougherty, *Cation-pi interactions in structural biology.* Proc Natl Acad Sci U S A. 1999 Aug 17;96(17):9459-64.
32. Ma, J.C. and D.A. Dougherty, *The Cation-Pi Interaction.* Chem. Rev., 1997. **97**(5): p. 1303-1324.
33. Brejc, K., et al., *Crystal structure of an ACh-binding protein reveals the ligand-binding domain of nicotinic receptors.* Nature. 2001 May 17;411(6835):269-76., 2001.
34. Corringer, P.J., N. Le Novere, and J.P. Changeux, *Nicotinic receptors at the amino acid level.* Annu Rev Pharmacol Toxicol, 2000. **40**: p. 431-58.

35. Sixma, T.K. and A.B. Smit, *Acetylcholine binding protein (AChBP): a secreted glial protein that provides a high-resolution model for the extracellular domain of pentameric ligand-gated ion channels.* Annu Rev Biophys Biomol Struct. 2003;32:311-34. Epub 2003 Feb 21.
36. Smit, A.B., et al., *Structure and function of AChBP, homologue of the ligand-binding domain of the nicotinic acetylcholine receptor.* Ann N Y Acad Sci. 2003 Sep;998:81-92.
37. Harel M, R.K., Anne Nicolas, J. Mitchell Guss, Moshe Balass, Mati Fridkin, August B. Smit, Katjua Brejc, Titia K. Sixma, Ephraim Katchalski-Katzir, Joel L. Sussman and Sara Fuchs, *The Binding Site of Acetylcholine Receptor as Visualized in the X-Ray Structure of a Complex between α-Bungarotoxin and a Mimotope Peptide* Neuron, 2001. **32**(2).
38. Celie, P.H., et al., *Nicotine and carbamylcholine binding to nicotinic acetylcholine receptors as studied in AChBP crystal structures.* Neuron. 2004 Mar 25;41(6):907-14.
39. Padgett, C.L., et al., *Unnatural amino acid mutagenesis of the GABA(A) receptor binding site residues reveals a novel cation-pi interaction between GABA and beta 2Tyr97.* J Neurosci. 2007 Jan 24;27(4):886-92.
40. Lummis, S.C., et al., *A cation-pi binding interaction with a tyrosine in the binding site of the GABAC receptor.* Chem Biol. 2005 Sep;12(9):993-7.
41. Mu, T.W., H.A. Lester, and D.A. Dougherty, *Different binding orientations for the same agonist at homologous receptors: a lock and key or a simple wedge?* J Am Chem Soc. 2003 Jun 11;125(23):6850-1.
42. Fonck, C., et al., *Novel seizure phenotype and sleep disruptions in knock-in mice with hypersensitive alpha 4* nicotinic receptors.* J Neurosci. 2005 Dec 7;25(49):11396-411.
43. Moroni, M., et al., *alpha4beta2 nicotinic receptors with high and low acetylcholine sensitivity: pharmacology, stoichiometry, and sensitivity to long-term exposure to nicotine.* Mol Pharmacol. 2006 Aug;70(2):755-68. Epub 2006 May 23.
44. Kuryatov, A., et al., *Nicotine acts as a pharmacological chaperone to up-regulate human alpha4beta2 acetylcholine receptors.* Mol Pharmacol. 2005 Dec;68(6):1839-51.
45. Halevi, S., et al., *The C.elegansric-3 gene is required for maturation of nicotinic acetylcholine receptors.* EMBO J., 2002. **21**(5): p. 1012-1020.
46. Ben-Ami, H.C., et al., *RIC-3 Affects Properties and Quantity of Nicotinic Acetylcholine Receptors via a Mechanism That Does Not Require the Coiled-coil Domains.* J. Biol. Chem., 2005. **280**(30): p. 28053-28060.
47. Castillo, M., et al., *Dual Role of the RIC-3 Protein in Trafficking of Serotonin and Nicotinic Acetylcholine Receptors.* J. Biol. Chem., 2005. **280**(29): p. 27062-27068.
48. Cheng, A., N.A. McDonald, and C.N. Connolly, *Cell Surface Expression of 5-Hydroxytryptamine Type 3 Receptors Is Promoted by RIC-3.* J. Biol. Chem., 2005. **280**(23): p. 22502-22507.

49. Williams, M.E., et al., *Ric-3 Promotes Functional Expression of the Nicotinic Acetylcholine Receptor {alpha}7 Subunit in Mammalian Cells*. J. Biol. Chem., 2005. **280**(2): p. 1257-1263.
50. Placzek, A.N., et al., *An alpha7 nicotinic acetylcholine receptor gain-of-function mutant that retains pharmacological fidelity.* Mol Pharmacol. 2005 Dec;68(6):1863-76.

Chapter 4

CONTRASTING DRUG-RECEPTOR INTERACTIONS AT NEURONAL VS. MUSCLE-TYPE NICOTINIC ACETYLCHOLINE RECEPTORS: THE α4β4 NEURONAL RECEPTOR*

This chapter is a brief description of a project in collaboration with Neurion Pharmaceuticals and Eli Lilly & Company, which predated the α4β2 and α7 nAChR research reported in the previous chapter.

4.1 Background

The nicotinic acetylcholine receptors (nAChRs) are members of a superfamily of ligand gated ion channels, which also includes $GABA_A$ and $GABA_C$, glycine, and 5-HT_3 (serotonin) receptors.[1] The nAChRs are found in both the central and peripheral nervous systems, where they mediate fast synaptic transmission and muscular contraction, respectively. Malfunctions of nAChRs have been implicated in a wide variety of "channelopathies", including addiction, Parkinson's disease, schizophrenia, Alzheimer's disease and congenital myasthenic syndromes.[2]

Like other Cys loop receptors, nAChRs are pentameric ion channels, each of the five homologous subunits containing a large extracellular domain and a transmembrane domain. There are 17 known subunits of nAChRs: α1-α10, β1-β4,δ, γ and ε. While the muscle-type is well defined as $(\alpha1)_2\beta1\gamma\delta$ (fetal form; $(\alpha1)_2\beta1\varepsilon\delta$ in adult cells), many different types of neuronal nAChRs can arise from varying combinations of the remaining α2-α10 and β2-β4 subunits[3]. Among the numerous neuronal nAChRs characterized in the mammal brain, α4 and β4 nAChR subunits were recently found to colocalize in different species in various brain

regions [4]. α4β4-containing receptors account partially for the type 4 currents in the mouse brain in the β2 knockout mice[5]. The physiological relevance of this receptor, however, is not known in great detail. The basic pharmacology of the α4β4 receptor differs significantly from that of the muscle type receptor we have probed previously. For example, in the muscle receptor ACh is a much more potent agonist than nicotine, while in α4β4, nicotine is almost 8-fold more potent than ACh, more typical of neuronal receptors.

Among the many tools that have been used to probe the nAChR and related structures, unnatural amino acid mutagenesis using nonsense suppression has proven to be an especially powerful tool for structure function studies of ion channels at the atomic level. [6-8] Well in advance of the crystal structures of AChBP [9, 10], a small protein that is highly homologous to the extracellular domain of the nAChRs, the unnatural amino acid methodology established that ACh binds to the muscle-type nAChR through a cation-π interaction to Trp α149, a residue now identified as TrpB [6]. In subsequent studies of other Cys-loop receptors, it was found that agonists bind the receptors through strong cation-π interactions within the "aromatic box" (Chapter 3). As is shown in Table 4.1, three of these established cation-π interactions involve a homologous tryptophan or tyrosine on loop B[11, 12], but other receptors employ a different aromatic[13, 14]. Interestingly, the same ligand can bind highly homologous receptors differently, as illustrated by serotonin forming cation-π interactions with two different tryptophans in the MOD-1 and 5-HT_3 receptors. Other interactions that are important for ligand binding, e.g., hydrogen bonds, have also been established by unnatural amino acid incorporations[15, 16].

	A	B	C1	C2	D
m-nAChR	Y93	**W149**	Y190	Y198	W55
5-HT$_3$R	E129	**W183**	F226	W234	W90
MOD-1	C120	Y180	Y221	**W226**	F83
GABA$_C$R	F138	**Y198**	Y241	Y247	Y102
GABA$_A$R	**Y97**	Y157	F200	Y205	F65

Table 4.1 Amino acids in the aromatic box of the agonist binding site in five different Cys-loop receptors, including the generic nomenclature of each amino acid according to the structural ”loop” that contains it. Bold and blue residues make a cation-π interaction with the natural agonist. Table adopted from [17]

The “aromatic box” for ligand binding is completely conserved in these and *all* other nAChRs. Here we report the first studies of a neuronal nAChR using unnatural amino acid mutagenesis, probing the agonist binding site of the α4β4 receptor. In addition to ACh and nicotine, we study epibatidine and cytisine, the lead compound for development of the anti-smoking drug varenicline (Figure 4.1).

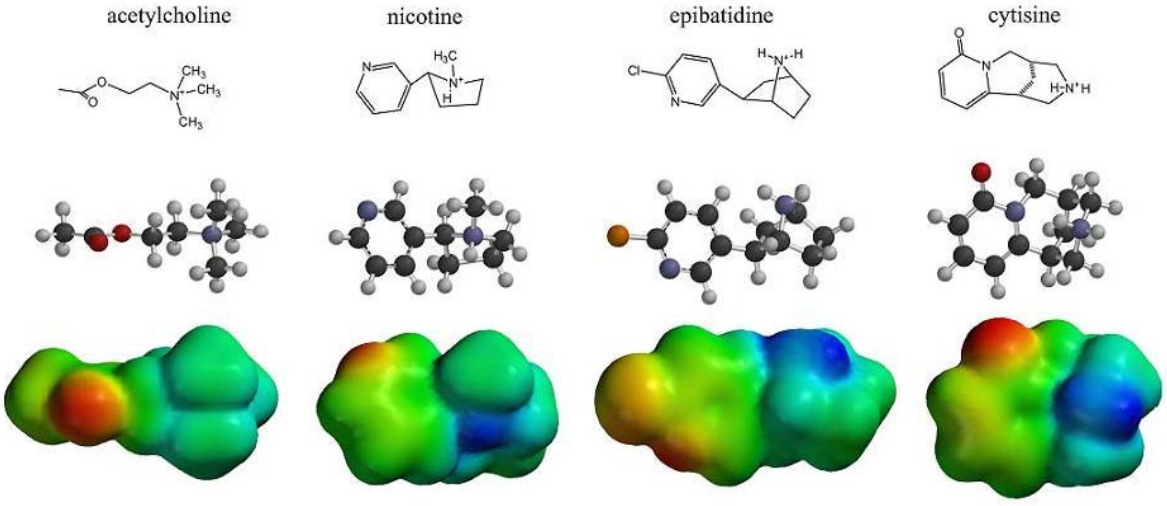

Figure 4.1: Compounds tested in the current study. Shown for each agonist are the chemical formula, ball-and-stick representation, and the electrostatic potential surface. Values for the electrostatic potential range from 0 (red) to +170 (blue) kcal/mol.

4.2 Results

4.2.1 Establishing the viability of unnatural amino acid incorporation in the α4β4 receptor

Human α4β4 nAChR were heterologously expressed in *Xenopus* oocytes by introducing wild type α4 and β4 mRNA at a ratio of 1:1, yielding functional receptors with a Hill coefficient around 1.5. The measured EC_{50}s of four different agonists are shown in Table 4.2 in comparison with the muscle type receptor. Next, unnatural amino acids (Figure 4.2) were introduced at positions of interest in either α4 or β4 subunits. For example, the amber stop codon (TAG) was introduced at position 153 of α4, a Trp site that corresponds to Trp α149 of the muscle-type receptor, the site of the ACh cation-π interaction. This is generically referred to as TrpB. When mutant mRNA was injected into a *Xenopus* oocyte along with the suppressor tRNA THG73 that is charged with Trp, receptors that are indistinguishable from wild type were obtained. Note that the subunit carrying the TAG mutation is usually injected into oocytes in 2 to 3 fold excess to ensure a sufficient incorporation of this subunit. This wild type recovery experiment establishes that nonsense suppression techniques are viable for the α4β4 receptor, and analogous wild type recovery experiments were performed at all sites probed. As negative controls for suppression, mutant mRNA was injected into oocytes without tRNA at all, with tRNA THG73 that is not charged with any amino acid, or with tRNA THG73 ligated with dCA. In no case was any response to agonists detected.

Receptor subtype	ACh	Nicotine	Epibatidine	Cytisine
Muscle-type	50	~2000	26	
α4β4	13	1.7	0.01	0.08

Table 4.2: Comparison of muscle type nAChR $(\alpha 1)_2\beta 1\gamma\delta$ and the neuronal nAChR α4β4 EC_{50}s in *Xenopus* oocytes. EC_{50} in μM.

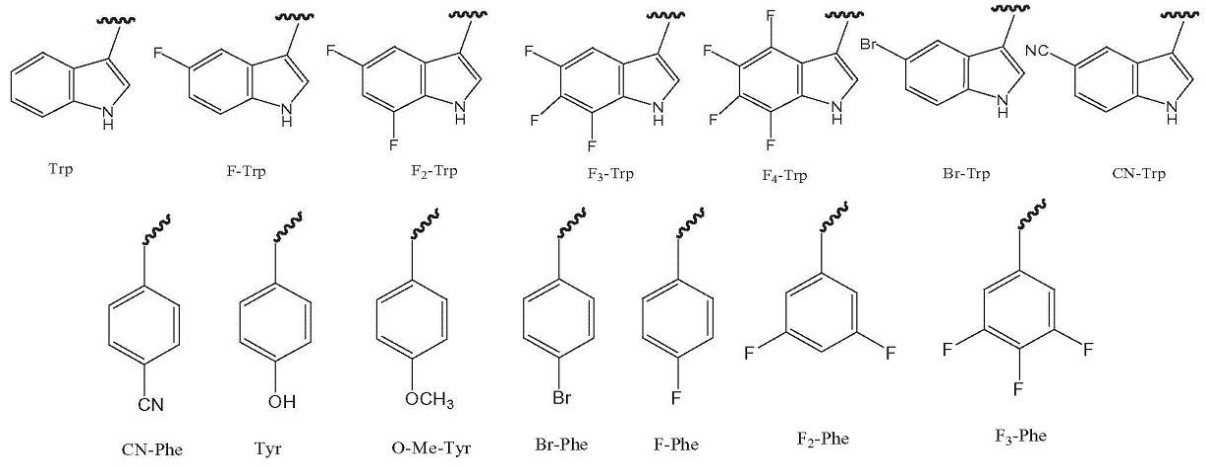

Figure 4.2: Tryptophan and phenylalanine analogs incorporated in the current study.

In this study we measure the EC_{50}s of the mutant α4β4 receptors and compare them with the wild type values. The EC_{50} value represents a functional assay, and as such it is a composite of equilibria for both binding and gating. In residues that define the agonist binding site, when subtle changes are introduced by incorporating unnatural amino acids, we interpret changes in EC_{50} values to reflect changes in agonist affinity rather than influencing gating processes.

4.2.2 TrpB

An aforementioned fluorination plot (chapter 3) is the most accurate indicator of a

cation-π interaction, therefore, progressively fluorinated tryptophan residues were incorporated at site B in the α4β4 receptor (Table 4.3). In the cases of ACh and epibatidine, progressive fluorination did not lead to a systematic increase in EC_{50} as was seen in the muscle-type receptor. The response was "flat", in that adding more electron-withdrawing fluorine atoms on the tryptophan did not correlate with a weakened binding of the agonist to the receptor. In addition, CN-Trp produces only a modest effect when ACh or epibatidine is the agonist.

Nicotine and cytisine are both only minimally affected by fluorination at TrpB, much like ACh and epibatidine. However, in the case of nicotine, CN-Trp produces a 22-fold drop in potency, while Br-Trp produces only a 3-fold drop. While not as dramatic as the effect seen with ACh at the muscle-type receptor[6], these results do suggest a significant electrostatic interaction between nicotine and TrpB in the α4β4 receptor. The CN/Br effect is even more dramatic with cytisine, being roughly comparable to that seen with ACh in the muscle-type receptor. This is the first time the CN/Br and fluorination strategies have not produced consistent results.

4.2.3. TyrA

In the α4β4 receptor, we studied the potential of TyrA to form both cation-π and hydrogen bonds (Table 4.3).

Mutating Tyr to MeO-Phe evaluates the role of a Tyr as a potential hydrogen bond donor. In muscle-type receptor this causes an 8-fold decrease in ACh potency[8]. In α4β4, all agonists show diminished potency in response to this mutation, with effects ranging from 3-

to 11-fold.

As mentioned in Chapter 3, substituted Phe derivatives instead of fluorinated tyrosines were used to evaluate the cation-π interaction at the tyrosine site. Fluorination shows no consistent effect with ACh or epibatidine (remembering that Phe is the proper reference point). CN/Br comparisions are varied. With ACh CN-Phe has a 16-fold bigger effect than Br-Phe, suggesting a possible electrostatic effect, but again the fluorination study is not consistent with this. The CN/Br ratios are relatively modest with the other agonists.

4.2.4. TyrC1 and TyrC2

Consistent with effects seen in the muscle receptor, in the α4β4 receptor the sensitivity of residue C1 persists (Table 4.3), in that for ACh, nicotine and cytisine, replacing the hydroxyl with a methoxy, a bromo or a cyano group causes the EC_{50} to increase over 100 fold. The effects are less dramatic with epibatidine, but still substantial.

In the α4β4 receptor, TyrC2 is again found to be very tolerant to mutagenesis. Replacing the hydroxyl group with either a methoxy, bromo or cyano group doesn't change the EC_{50} for ACh, nicotine or epibatidine significantly. Cytisine appears to be a bit more sensitive to these substitutions, but the effects are still relatively small.

	α4β4			
Mutation	**ACh**	**Nicotine**	**Epibatdine**	**Cytisine**
		TyrA (Tyr 97)		
MeO-Phe	3.5	3	6	11
Br-Phe	2.7	5	3	78
CN-Phe	45	32	9	210
Phe	**20**	**4.3**		
F-Phe	**20**	**2.7**		
F_2-Phe	**12**	**7.1**		
F_3-Phe	**10**	**2.2**		
		TrpB (Trp 153)		
F-Trp	3.4	3	2	4.4
F_2-Trp	2.7	3	3	3.3
F_3-Trp	2.2	7	1	4.4
Br-Trp		**3**		**8**
CN-Trp	7.1	22	4	210
		TyrC1 (Tyr 194)		
MeO-Phe	> 10 mM*	>1 mM*	7	120
Br-Phe	>10 mM*	>1 mM*	30	590
CN-Phe	> 10 mM*	>1 mM*	80	560
		TyrC2 (Tyr 201)		
MeO-Phe	0.8	1	1	2.2
Br-Phe	0.3	0.5	1	1.1
CN-Phe	0.8	1.5	1	5.6

Table 4.3 Ratios of mutant EC_{50} over the wild type EC_{50} for selected mutants in α4β4 receptors. The bold and underlined numbers are from recordings from our lab and the other numbers are from our collaborating labs at Neurion Pharmaceuticals and Eli Lilly and Company. (*approximate EC_{50} values.)

4.2.5 TrpD

The fifth contributor to the "aromatic box" comes from the complementary subunit. In the muscle receptor, this is the Trp 55/57 from γ/δ subunits, and in the α4β4 receptor it is Trp 59 in the β4 subunit. In the muscle-type receptor, the EC_{50} values for both CN-Trp and Br-Trp are very near wild type for ACh and nicotine. Similarly, for the analogous residue in the 5-HT_3 receptor (Trp90), tetrafluorinated tryptophan showed a wild type like EC_{50}. In α4β4

receptor, when CN-Trp is incorporated at this position, no response to agonists (*ACh and Nicotine tested)* could be detected, while wild type recovery is successful. The detailed function of this residue needs further investigation.

4.3 Discussion

The remarkable complexity of the CNS is evident at all levels: anatomical, cellular, and molecular. Dozens of different neurotransmitters target cognate receptors. Even for a single neurotransmitter like ACh, there are nicotinic receptors, studied here, but also muscarinic receptors (GPCRs). And the nicotinic receptors are themselves diverse. The muscle-type is well defined, but many different types of neuronal nAChRs can arise from the α2-α10 and β2-β4 subunits. While certainly not all combinations are viable, it seems likely that a dozen or more neuronal nAChR subtypes play a role in the mammalian CNS. A critical issue, then, in efforts at drug discovery around the nAChR family is targeting specific receptor subtypes.

The present work preceded the work in α4β2 and α7 nAChR reported in Chapter 3, and it describes the first application of the nonsense suppression, unnatural amino acid methodology to a neuronal nAChR, the human α4β4 receptor. Many previous studies of the muscle-type nAChR have established that this approach can provide powerful insights into structure and function. The primary goal of the present work was to establish that nonsense suppression is viable in the neuronal receptors. Secondarily, we wished to determine whether the well-defined structure-function relationships seen in the muscle-type receptor, such as the cation-π interaction between TrpB and ACh, carry over to the neuronal family. Finally, we hoped to begin an investigation of the structural features that produce the

substantially differing pharmacologies of the muscle-type and neuronal receptors. Since there is absolute conservation of the five aromatics that define the agonist binding site "box", and since all models emphasize these residues as providing the sole side chains that contact the agonist, the effects will necessarily be subtle, and these early studies can only hope to provide guidance for future work.

We report that the nonsense suppression approach to unnatural amino acid incorporation for receptors expressed in *Xenopus* oocytes is applicable to a neuronal nAChR, the α4β4 receptor. This receptor was chosen for initial studies because it had been known that receptors expressing the β4 subunit express well in *Xenopus* oocytes. More recently, we have established successful nonsense suppression in homopentameric α7 receptors and α4β2 receptors (Chapter 3). For the α4β4 receptor, expression is robust, and a number of unnatural amino acids have been successfully incorporated and evaluated.

This first round of studies on a neuronal receptor has produced some surprising results. Most remarkably, the compelling cation-π interaction seen between ACh and TrpB of the muscle-type receptor is clearly absent in the α4β4 receptor. No other side chain probed in the α4β4 receptor shows strong evidence for an equally strong cation-π interaction with ACh. Note that the muscle-type result is not an isolated anomaly. Equally compelling results have established cation-π interactions between serotonin and the aligned tryptophan of the 5-HT_3 receptor; between GABA and the aligned tyrosine of the $GABA_C$ receptor; and between serotonin and a Trp at site C2 in the MOD-1 receptor; and more recently, between GABA and TyrA in the $GABA_A$ receptor.

A possibility is that the cation-π site has moved in α4β4 relative to the muscle-type. This

would be precisely analogous to what we have seen with two homologous serotonin receptors. Both receptors bind serotonin with a cation-π interaction and the magnitude of the effect is the same. However, in the 5-HT_3 receptor TrpB is responsible, while in MOD-1 it is TrpC2. The present results indicate that the only possible candidate for a cation-π interaction to ACh in α4β4 is TyrA. An attempted fluorination plot produced no trend. However, the starting point for the experiment was Phe, not Tyr, and the Phe mutant is already 20-fold less potent with ACh. It may be that a substituent at the 4 position of tyrosine is essential, and so the fluorination series is compromised from the start. Consistent with this, Br-Phe is only 3-fold worse than Tyr. The isosteric, but much more deactivating, CN-Phe is 45-fold worse. This CN/Br ratio of ~15 is not as large as seen with TrpB in the muscle-type (57-fold). First, Tyr is an intrinsically weaker cation-π binding site than Trp, so it may be ACh is picking up a moderate cation-π interaction at TyrA. Secondly, as reported in the previous chapter, at TrpB site in α4β2 receptor where ACh and nicotine show an unambiguous cation-π interaction, the CN/Br ratio is 11 fold and 4.5 fold, respectively. For α7 nAChR, epibatidine shows cation-π interactions at both TyrA and TyrC2 sites and the CN/Br ratio is 5.3 fold and 6.6 fold respectively. Therefore, the 15 fold ratio of CN/Br at TyrA in α4β4 may indeed indicate a cation-π interaction.

In other ways, the binding of ACh is similar for the two receptors. TyrC1 is quite sensitive to substitution, while TyrC2 is quite tolerant.

We have also evaluated three other agonists – nicotine, epibatidine, and cytisine – to further compare and contrast the muscle-type and neuronal receptors. A hallmark of the muscle-type receptor is its insensitivity to nicotine. However, epibatidine, clearly a nicotine

analogue, is potent at the muscle-type receptor. In earlier work we showed that the cation-π interaction at TrpB displayed by ACh is absent for the weak agonist nicotine but present for the potent agonist epibatidine[15]. Both nicotine and epibatidine appear to make a hydrogen bond to the backbone carbonyl of TrpB in the muscle-type; an interaction that is not possible for ACh.

In the α4β4 receptor, all three additional agonists are insensitive to progressive fluorination at TrpB. This would appear to rule out a cation-π interaction. However, for nicotine to some extent and definitely for cytisine, CN-Trp causes a very large drop in potency. Coupled in each case with the much smaller drop for Br-Trp, this observation could be interpreted as indicating a cation-π interaction. Alternatively, both nicotine and cytisine have polarized C(sp^2)-H bonds that could experience a π-π interaction with the TrpB side chain. This is much weaker than a cation-π interaction, and perhaps the fluorination series is unable to reveal it, but the strongly perturbing CN substituent is.

Alterations of TyrA in α4β4 have similar consequences for all the additional agonists considered here. MeO-Phe is detrimental, as seen before. Nicotine produces no consistent fluorination effect. CN-Phe has varying effects, but they are tracked by Br-Phe, such that the large CN/Br ratio seen with ACh is absent with the other agonists. We conclude there is no strong interaction to TyrA with nicotine, epibatidine, or cytisine.

As with ACh, all other agonists are significantly impacted by changes to TyrC1 and relatively unaffected by changes to TyrC2.

Taken together, the evaluation of α4β4 leads to several conclusions. Most important is the danger of extrapolating observations from one receptor to another, despite high homology

and absolute identity for the supposedly key residues. The cation-π interaction at TrpB seen for both ACh and epibatidine in the muscle-type receptor is not manifest in α4β4. Both agonists show no fluorination trend, and a ≤7-fold change for CN-Trp, vs. 95-fold for ACh at the muscle-type. The other agonists nicotine and cytisine do show a hint of an interaction in an elevated CN/Br ratio, but that is not mirrored in the fluorination trend. This may indicate a π-π rather than a cation-π interaction.

It may also be that the cation-π interaction for ACh seen in the muscle-type receptor has moved from TrpB to TyrA. The evidence is not as compelling as seen with other systems, but it is suggestive.

Certainly, the four agonists probed here do not experience identical interactions with the α4β4 receptor. Given the somewhat "generic" appearance of the aromatic box, it may not be surprising that different drugs can find different ways to bind to and activate the receptor. An interesting trend is that, in most cases, cytisine is the most sensitive of the agonists to mutation. Cytisine is also the only completely rigid agonist and is fairly large, so perhaps it is more limited in the ways it can adapt to perturbations of the binding site.

The overarching conclusion from these and other studies of the agonist binding site of Cys-loop receptors is that they seem to be much more adaptable than the beautiful but static image from the AChBP structures. Certainly some variation in structure has been implied by different structures and by simulations, but the differences from ligand to ligand and receptor type to receptor type are quite remarkable. The results present an intriguing but cautionary tale for those engaged in efforts to specifically target selected receptors.

4.4 References

1. Corringer, P.J., N. Le Novere, and J.P. Changeux, *Nicotinic receptors at the amino acid level.* Annu Rev Pharmacol Toxicol, 2000. **40**: p. 431-58.
2. Lester, H.A., et al., *Cys-loop receptors: new twists and turns.* Trends Neurosci. 2004 Jun;27(6):329-36.
3. Jensen, A.A., et al., *Neuronal nicotinic acetylcholine receptors: structural revelations, target identifications, and therapeutic inspirations.* J Med Chem. 2005 Jul 28;48(15):4705-45.
4. Wu, J., et al., *Roles of nicotinic acetylcholine receptor beta subunits in function of human alpha4-containing nicotinic receptors.* J Physiol. 2006 Oct 1;576(Pt 1):103-18.
5. Zoli, M., et al., *Identification of Four Classes of Brain Nicotinic Receptors Using beta 2 Mutant Mice.* J. Neurosci., 1998. **18**(12): p. 4461-4472.
6. Zhong, W., et al., *From ab initio quantum mechanics to molecular neurobiology: a cation-pi binding site in the nicotinic receptor.* Proc Natl Acad Sci U S A. 1998 Oct 13;95(21):12088-93.
7. Nowak, M.W., et al., *In vivo incorporation of unnatural amino acids into ion channels in Xenopus oocyte expression system.* Methods Enzymol. 1998;293:504-29.
8. Kearney, P.C., et al., *Dose-response relations for unnatural amino acids at the agonist binding site of the nicotinic acetylcholine receptor: tests with novel side chains and with several agonists.* Mol Pharmacol. 1996 Nov;50(5):1401-12.
9. Celie, P.H., et al., *Nicotine and carbamylcholine binding to nicotinic acetylcholine receptors as studied in AChBP crystal structures.* Neuron. 2004 Mar 25;41(6):907-14.
10. Brejc, K., et al., *Crystal structure of an ACh-binding protein reveals the ligand-binding domain of nicotinic receptors.* Nature. 2001 May 17;411(6835):269-76.
11. Lummis, S.C., et al., *A cation-pi binding interaction with a tyrosine in the binding site of the GABAC receptor.* Chem Biol. 2005 Sep;12(9):993-7.
12. Beene, D.L., et al., *Cation-pi interactions in ligand recognition by serotonergic (5-HT3A) and nicotinic acetylcholine receptors: the anomalous binding properties of nicotine.* Biochemistry. 2002 Aug 13;41(32):10262-9.
13. Padgett, C.L., et al., *Unnatural amino acid mutagenesis of the GABA(A) receptor binding site residues reveals a novel cation-pi interaction between GABA and beta 2Tyr97.* J Neurosci. 2007 Jan 24;27(4):886-92.
14. Mu, T.W., H.A. Lester, and D.A. Dougherty, *Different binding orientations for the same agonist at homologous receptors: a lock and key or a simple wedge?* J Am Chem Soc. 2003 Jun 11;125(23):6850-1.
15. Cashin, A.L., et al., *Using physical chemistry to differentiate nicotinic from cholinergic agonists at the nicotinic acetylcholine receptor.* J Am Chem Soc. 2005 Jan 12;127(1):350-6.
16. Beene, D.L., et al., *Tyrosine residues that control binding and gating in the 5-hydroxytryptamine3 receptor revealed by unnatural amino acid mutagenesis.* J Neurosci. 2004 Oct 13;24(41):9097-104.
17. Padgett, C.L., et al., *Unnatural Amino Acid Mutagenesis of the GABAA Receptor Binding Site Residues Reveals a Novel Cation-{pi} Interaction between GABA and {beta}2Tyr97.* J. Neurosci., 2007. **27**(4): p. 886-892.

Chapter 5

IMPROVING NONSENSE SUPPRESSION BY SUPPRESSING eRF-1 WITH siRNA

5.1 Abstract

Introducing unnatural amino acids into proteins by nonsense suppression has proven to be an effective and powerful tool to study protein structure-function relationships on the chemical scale. In our lab, this strategy has greatly facilitated the structure-function studies of a series of membrane bound ion channels. The research reported here describes efforts to increase nonsense suppression efficiency in *Xenopus laevis* oocytes and human embryonic kidney (HEK) cells using RNA interference to target eukaryotic release factor 1 (eRF1). In particular, we designed multiple 21nt small interfering RNAs (siRNA) targeting both *Xenopus* and human eRF1, and monitored the nonsense suppression efficiency *in vitro* and *in vivo* by RNA PCR, Western blotting, fluorescence and electrophysiology.

5.2 Introduction

5.2.1 Unnatural amino acid incorporation by nonsense suppression

Introducing unnatural amino acids into proteins by nonsense suppression is an effective and powerful tool to study protein structure-function relationships on the chemical scale[1]. By introducing a stop codon into the mRNA at the site of interest, together with a misacylated tRNA chemically ligated with a synthesized unnatural amino acid, proteins can acquire chemical properties that are not represented by any of the 20 natural amino acids (Figure 5.1). This methodology has greatly facilitated our study of

membrane ion channels, a family of physiologically important but structurally complex, multisubunit proteins that are embedded in lipid bilayers.

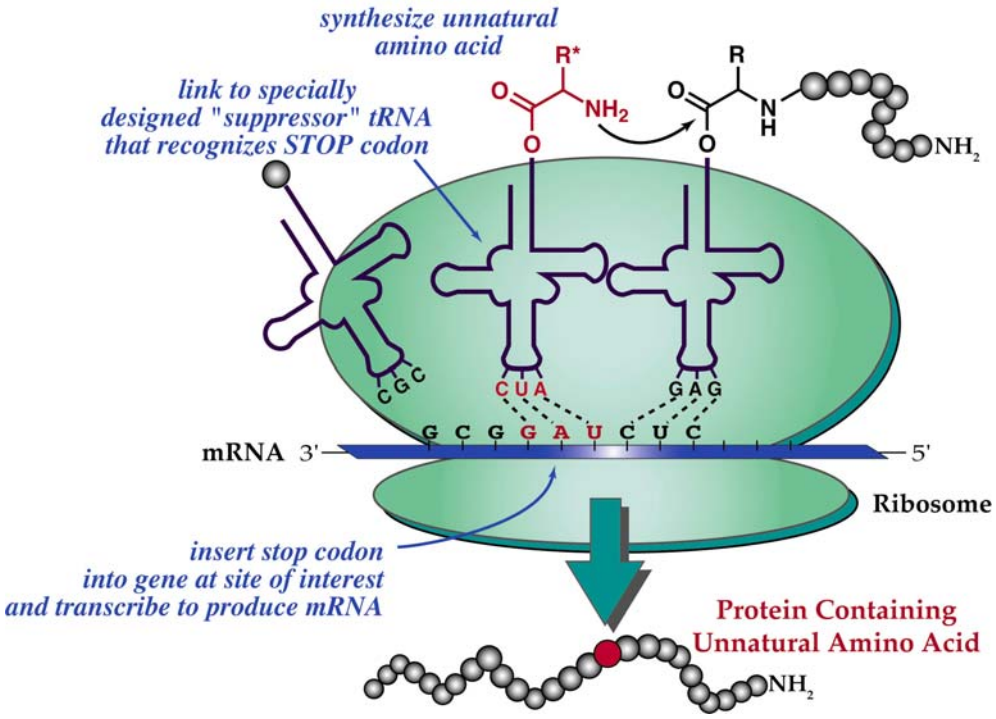

Figure 5.1. Schematics of the unnatural amino acid incorporation *in vivo* by nonsense suppression.

A limitation of nonsense suppression methodology is that the aminoacylated tRNA is stoichiometric, such that each aminoacylated tRNA can be used only once. Therefore, to generate enough proteins for characterization, either large quantities of aminoacylated tRNA is required or a very sensitive assay needs to be adopted. In our lab, we primarily study ion channels that can be assayed by very sensitive electrophysiological recordings. Furthermore, the majority of experiments are performed in *Xenopus laevis* oocytes in which relatively large amounts of aminoacylated tRNA can be injected. Utilizing this system with an engineered orthogonal *Tetrahymena thermophila* tRNA charged with

unnatural amino acids[2], over 20 of ion channels, including the nAChR (nicotinic acetylcholine receptor), serotonin receptor (5-HT_{3A}R)[3], MOD-1[4], Shaker [5] and Kir2.1 potassium channels [6] and so on[7, 8] have been studied, and information on ligand binding and ion channel gating mechanisms has been obtained.

5.2.2 Nonsense suppression efficiency

One complication of the nonsense suppression experiments is that there is great variability of suppression efficiency. Efficiency varies from channel to channel, from residue to residue, and in some cases an amino acid may be replaceable by some unnatural side chains but not by others[9]. Factors associated with this variability include 1) codon context, 2) read-through of the stop codon and 3) the production of truncated proteins when the UAG codon is recognized by protein translation termination machinery instead of the aminoacylated tRNA. These factors are quite difficult to control.

First of all, there have been many reports correlating codon context and suppression efficiency. In our lab, however, no obvious correlation has been found[9].

Secondly, read-through of the engineered stop codon causes the production of full length proteins without incorporation of desired unnatural amino acid. This may result from the recognition of the stop codon by an endogenous tRNA even without a perfect codon:anticodon match, or by the replacement of the unnatural amino acid by a natural amino acid, or by the deletion of the desired incorporation site. It has been difficult to generate systematic rules to predict the likelihood of erroneous full length protein production. In our lab, we control read-through expression by varying the amount of injected mRNA and the ratio of receptor subunits to each other.

Finally, it was found that suppression efficiency can be affected by termination at the introduced stop codon. The resultant truncated protein not only lacks function, but also may have deleterious effects on cell death or possible dominant negative effects. In the case of membrane proteins such as receptors, partial-length proteins may be trafficked to the surface and interfere with experimental results.

Misfolding, misassembly and the failure of trafficking may complicate suppression efficiency too. These can be partially evaluated by Western blotting the membrane fraction of proteins expressed, but are generally difficult to analyze.

5.2.3 Improving nonsense suppression efficiency in *Xenopus* oocytes

Increasing nonsense suppression efficiency of this methodology would be beneficial in multiple ways. First of all, it would facilitate the study on functionally important yet poorly expressed ion channels, such as neuronal ACh receptors α4β2 and α7 (Chapter 3 describes our work on these two receptors later). It would also enable us to explore regions of receptors that are less tolerant of unnatural amino acids, and to incorporate unnatural amino acids with more structural diversity. Furthermore, improved yield of nonsense suppression would allow for characterizations of products using a less sensitive assay than electrophysiology.

A lot of efforts have been put into improving nonsense suppression efficiency in our lab. These included optimizing the expression vector, overexpressing elongation factors, trying to reduce clatherin-mediated endocytosis by co-expression of a dominant-negative dynamin, overexpression of ER-chaperones (BiP), insertion of forward-trafficking signals for greater surface expression, construction of a chimera of the poorly expressed ion channel with a better expressed ion channel, and multiple injections into oocytes. In the

case of α4β2, only multiple injections had a measurable effect, but the whole-cell currents were still too small to generate reliable dose-response relations[9]. Another strategy to improve suppression efficiency is to use a four-base codon instead of an amber stop codon in mRNA to avoid recognition by protein translation stop machinery. Recently, simultaneous incorporation of three amino acids *in vivo* by frame shift suppression has been established in our lab[10].

5.2.4 Improving nonsense suppression efficiency in mammalian cells

In addition to utilizing nonsense suppression in *Xenopus* oocytes, our lab expanded the exploration into mammalian human embryonic kidney (HEK) cells as well. A mammalian cell expression system is a more relevant environment for many proteins of mammalian origin and would allow for studies of cell-specific signal transduction pathways. Therefore there is much interest in our lab to extend the nonsense suppression technology into a mammalian system. However, mammalian cells are much smaller than oocytes, meaning that fewer aminoacylated tRNA will be able to enter the cells. Also, hydrolysis of the aminoacyl-ester bond is quite rapid at the physiological pH which is required for handling of mammalian cells. The first successful mammalian nonsense suppression experiment delivering unnatural amino acid to the nAChR site-specifically was reported in our lab by Dr. Monahan in 2003[11]. However, similar experiments performed on α4β2 had no observable nonsense suppression, although wild type α4β2 subcloned into mammalian expression vector pCO-neo did express. In order to obtain observable nonsense suppression, Dr. Monahan substantially increased the mRNA/tRNA concentration in the trasfection solution, but under no circumstances was any sign of suppression observed[12].

5.2.5 Improving nonsense suppression efficiency by suppressing eRF1

One way to improve suppression efficiency is to decrease the production of the truncated protein, due to translation termination at the incorporated stop codon.

When the ribosome elongation machinery encounters a stop codon, protein synthesis typically terminates (Figure 5.2 A). The eRF1-eRF3 complex binds to the A site of the ribosome, where eRF1 directly interacts with the stop codon (eRF3 has a stimulating effect). This leads to hydrolysis of the peptidyl-tRNA bond, and then the formation of eRF1/eRF3 complex with poly(A) binding protein or PABP. Interaction of PABP with translation initiation factors mediates the ribosome recycling and re-initiation of translation[13].

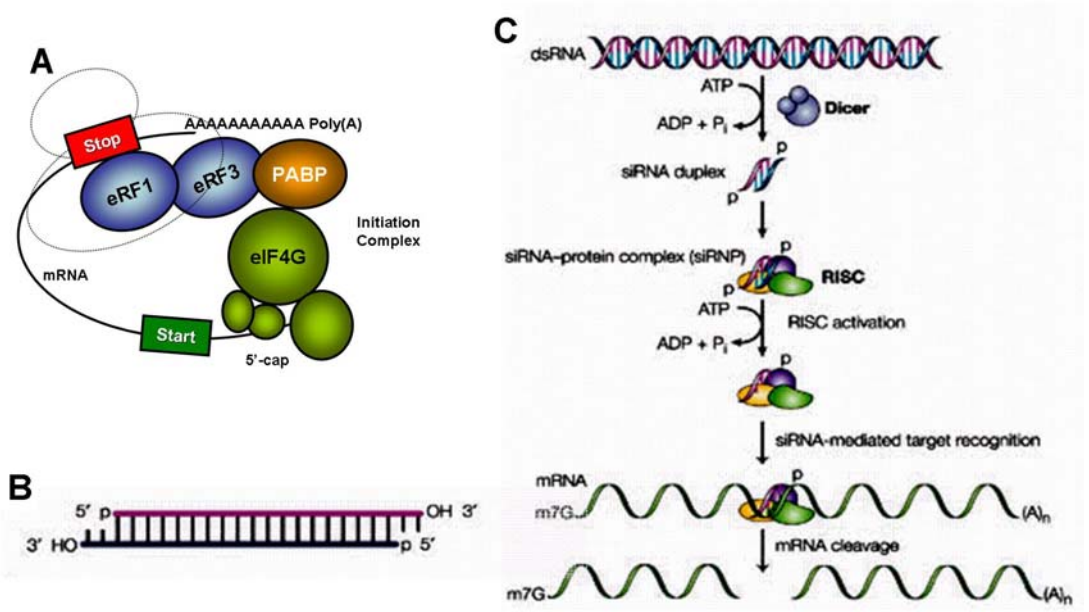

Figure 5.2. A: A general scheme of the translation termination complex. (adapted from[13]). B: siRNA structure. C: A scheme of RNA interference mechanism. (adapted from[14])

UAG stop codon has been chosen to be the nonsense stop codon, and it is recognized by eRF1 only. Therefore diminution of eRF1 could lessen competition with the misacylated suppressor tRNA and thus promote the incorporation of the unnatural amino acid into proteins[15].

In an *in vitro* experiment performed in the Hecht lab, the suppression efficiency was improved 11-fold when release factors were partially inactivated by heat shock in an *E. coli*-derived extract with a thermo sensitive eRF1. Interestingly, along with the great improvement of nonsense suppression efficiency they also reported a decrease of protein translation accuracy, assayed by the specific activity of suppressed HIV-1 protease. They proved that this was due to the increasing ability of endogenous tRNA to read through the engineered stop codon as the eRF1 is depleted[16].

5.2.6 Using RNA interference (RNAi) to suppress eRF1 in mammalian cells

It has also been shown by the Yarus lab that in cultured HEK (human embryonic kidney) cells, RNAi can decrease levels of eRF1 and increase read-through of UAG stop codons. In this experiment, three siRNAs designed to target different positions of human eRF1 were separately transfected into HEK cells. Read-through of a UAG codon was assayed by the expression of a luciferase gene located right after the UAG codon. Although the read-through of the UAG codon was not perfectly correlated with the mRNA level of eRF1 detected by RNA PCR, the largest effect seen was a 90% eRF1 degradation that correlated with a 150% increase of UAG read-through[17].

The success of this experiment suggests that RNAi is potentially an effective way of suppressing endogenous eRF1 in nonsense suppression systems. We decided to use this new yet fast developing technology, RNAi, to improve the suppression efficiency both in *Xenopus* oocytes and in HEK cells.

In 2004, the Vogel lab reported that by suppressing eRF1 in HEK cells, a five-time higher level of unnatural amino acid incorporation, demonstrated by EGFP fluorescence recovery was achieved[18].

5.2.7 Using RNAi to suppress endogenous proteins in *Xenopus laevis* oocytes

Suppressing eRF1 of *Xenopus laevis* has no precedent, but the first siRNA experiment targeting an endogenous protein in *Xenopus* oocytes was reported in 2003 in which the expression of an ion channel xMiRP2 was reduced 5 fold by a chemically synthesized 21nt siRNA[19] (Figure 5.2 B).

The most recent application of siRNA suppressing an endogenous protein in *Xenopus* oocytes is reported by the Boehmer lab[20]. They knocked down an endogenous ubiquitin ligase Nedd4-2 (xNedd4-2) expression to increase the activity of a transporter (EAAT4) mediating glutamate uptake through the action of a serum and glucocorticoid kinase (SGK) 1. The reduction was about 50% as revealed by Western blotting.

5.2.8 RNA interference

RNA interference is a post-transcriptional gene silencing (PTGS) initiated by the introduction of double-stranded RNA. PTGS occurs in both plants and animals and has roles in viral defense and transposon silencing mechanisms.

The understanding of RNA interference mechanism includes two steps (Fig. 5.2 C). 1) Initial step. The long double stranded RNA introduced either directly, via a transgene, or with a virus, is digested into 21-23 nucleotide small interfering RNAs (siRNAs) by an enzyme called Dicer. Dicer belongs to RNase III family of RNA-specific ribonucleases. It cuts the dsRNA in an ATP-dependent processive manner. The structure of siRNA contains 2 nucleotide overhangs at the 3'-end and a phosphate at the 5'-end, which is the typical structure of the digestion products of this family of enzymes. 2) Effecter step. The siRNA binds to a nuclease complex known as the RNA-induced silencing complex, or RISC. An ATP-depending unwinding of the siRNA duplex is required for the activation of the RISC. The active RISC then targets the homologous transcript by base pairing and then cleaves the mRNA 10 nucleotides from the 5'-end of the siRNA[14, 21, 22].

After being discovered as a factor for gene silencing, double stranded RNAs have been used in various organisms. Chemically synthesized small interfering RNA is the most commonly used[23]. Long double stranded RNAs are used also but they need to be

processed into small interfering RNAs by Dicer. It was also found that siRNA based hairpins with perfectly matched or imperfectly matched stem can be cut by Dicers[24].

In recent years, RNA interference has become an almost-standard method for *in vitro* knock down of any target gene of interest. Recent efforts in this area have focused on developing efficient delivery of target gene-specific siRNAs. [25]

Herein, we will use chemically synthesized 21nt siRNAs to decrease eRF1 both in *Xenopus* oocytes and in HEK cells in efforts to improve nonsense suppression efficiency.

5.3. Experimental Design

5.3.1 siRNA molecules designed to target human and *Xenopus laevis* eRF1.

The siRNA Si1187h targeting human eRF1 was reported to reduce human eRF1 mRNA in HEK cells by 90% and to increase UAG readthrough by about 150%[17]. A second siRNA, si36h, reduced human eRF1 mRNA by 40% and increased UAG readthrough by 80%. The numbers in the two names denote the distance from the A of the translation start codon AUG in eRF1 mRNA, and "h" means "human", to distinguish from "x" meaning "*Xenopus*".

These two 21nt sequences were ordered from Dharmacon Research as desalted and deprotected double stranded RNAs with two nucleotide overhangs at the 3'-end. These molecules were dissolved in DEPC water to a concentration of 1 μg/μl.

Xenopus laevis eukaryotic release factor 1 was first sequenced in 1993 and it is highly homologous to human eRF1 sequence. Therefore, two siRNAs targeting the same positions as in human eRF1 were ordered. Si1187x (antisense strand: CACAAGAAGGCUCUCAGUUdTdT) has one nucleotide difference from si1187h

(antisense strand: CACAAGAAGGGUCUCAGUUdTdT) and si36x (antisense strand:GGAGAUCUGGAAGAUCAAGdTdT) has the same sequence as si36h.

Finally, two more siRNA molecules were designed and ordered, si1151x (antisense strand: UUCGGAGCAACACUGGAGAdTdT) and si450x (UUGAUGGGAGUGGAGCACUdTdT). siControl is a 21 nt non-targeting siRNA of comparable GC content as the targeting siRNAs. This serves as a negative control for non-sequence-specific effects. (Figure 5.3 A)

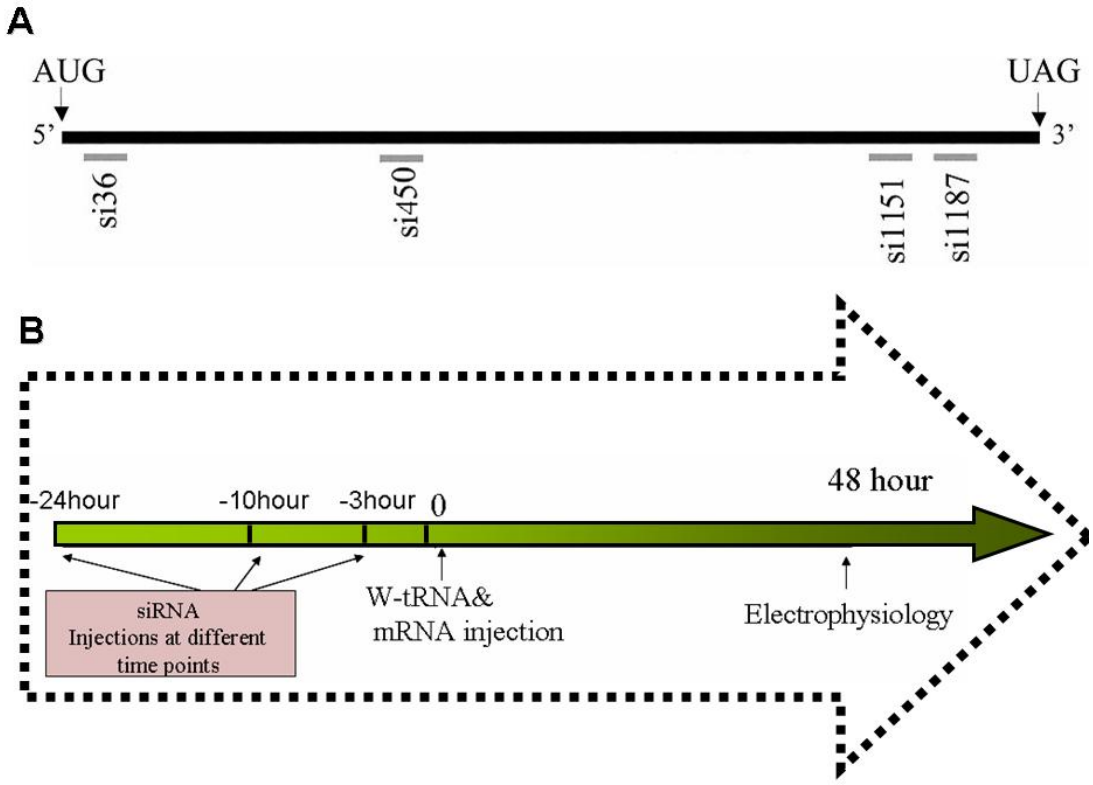

Figure 5.3 A: Different positions of siRNA targets on eRF1 mRNA (both human and *Xenopus* homologs were used, see text) B: Different time delays between the siRNA injection and the mRNA/tRNA injections were applied.

5.3.2 Coinjection of siRNA molecules with nonsense suppression experiments into *Xenopus* oocytes

In order to test if the presence of siRNA could help to increase the nonsense suppression efficiency, siRNA molecules targeting *Xenopus laevis* eRF1 were coinjected into *Xenopus* oocytes.

The nonsense suppression experiment selected here is a wild type recovery experiment where the nicotinic acetylcholine receptor (nAChR) α1 subunit mRNA with a UAG codon at position 149 was suppressed by a suppressor tRNA charged with wild type tryptophan. W149 is located in the extracellular domain of the nAChR (Chapter 3). Successful and efficient suppression should yield wild type nAChR whose function can be monitored using a two electrode voltage clamp electrophysiology.

Specifically, 12.5ng of mRNA with UAG codon, 25ng of tryptophan charged tRNA and 500pg of siRNA (or siControl) are mixed in 0.05 µl of DEPC water and coinjected into *Xenopus* oocytes using a micropipette. mRNA, tRNA and siRNA were either coinjected simultaneously, or injected at different time intervals between the siRNA injection and mRNA/tRNA injection. Experiments were performed where siRNA molecules were injected 24 hours, 10 hours or 3 hours prior to mRNA/tRNA injections (Figure 5.3 B).

The amount of siRNA molecules introduced into oocytes was also varied; 25 ng, 5 ng, 500 pg, 50 pg, 5 pg of si1187 and si36 were injected at different time delays of 3 hours, 10 hours and 24 hours.

5.3.3 Recording currents in *Xenopus* oocytes of nAChR introduced by 50 µM ACh and 250 µM ACh.

The expression of nAChR was tested using two electrode voltage clamp electrophysiology. We use a high throughput OpusXpress system (Axon Instruments) with automated drug delivery, which records simultaneously from 8 oocytes. The currents introduced by 50 μM ACh (EC_{50}) and 250 μM ACh (saturating concentration) were recorded as indications of nAChR expression level. The recordings were always performed 24 hours after the injection of mRNA and tRNA.

5.3.4 RNA PCR on eRF1 both in *Xenopus* oocytes and in HEK cells.

In order to estimate the siRNA efficiency, RNA PCR was performed to look at the mRNA of eRF1 in both oocytes and HEK cells. RNA PCR is also called RT PCR or reverse transcription PCR. It uses RNA as template to perform *in vitro* reverse transcription followed by conventional PCR on the cDNA. In order for RNA PCR to be semi quantitative, a calibration experiment has to be performed to find a point where the reagents in the PCR mixture begin to be saturated by the RNA templates, so that later in the PCR product comparison experiment, the amount of PCR product is solely dependent on the amount of RNA templates, i.e. there is a linear correlation between the mRNA template and PCR product.

5.3.4.1 General strategy

Figure 5.4 shows the two major steps of this strategy. First, in order to achieve a linear correlation between mRNA templates (the total mRNA extracted from cells) and the product, total RNA was extracted from uninjected oocytes or untreated HEK cells. Amplification primers for eRF1 mRNA were 5'-AGCTGGATCCGCTGACTTTAAA-3' and 5'-ATACCTCCAATTCCACCAAATC-3' for HEK cells and were 5'-GGCTGGATCCGCAGATTTTAAA-3' and 5'-ATCCCTCCAATTCCACCAAATC-3'

for *Xenopus laevis*. RNA PCR was performed under the same conditions using a titration of total RNA (1 μg, 0.2 μg, 40 ng, 8 ng, 1.6 ng and etc) as templates. By observing the band intensities of the PCR product on the gel, the amount of mRNA template that is sensitive to a 5 fold decrease was found, which determined the amount of RNA template used in step 2. In the second step, oocytes and HEK cells were introduced with siRNAs and their total RNA was extracted. Comparing the RNA PCR products of these samples with that of the control, a decrease of about five fold of the eRF1 mRNA was detected. The details of each are shown below. (Figure 5.4)

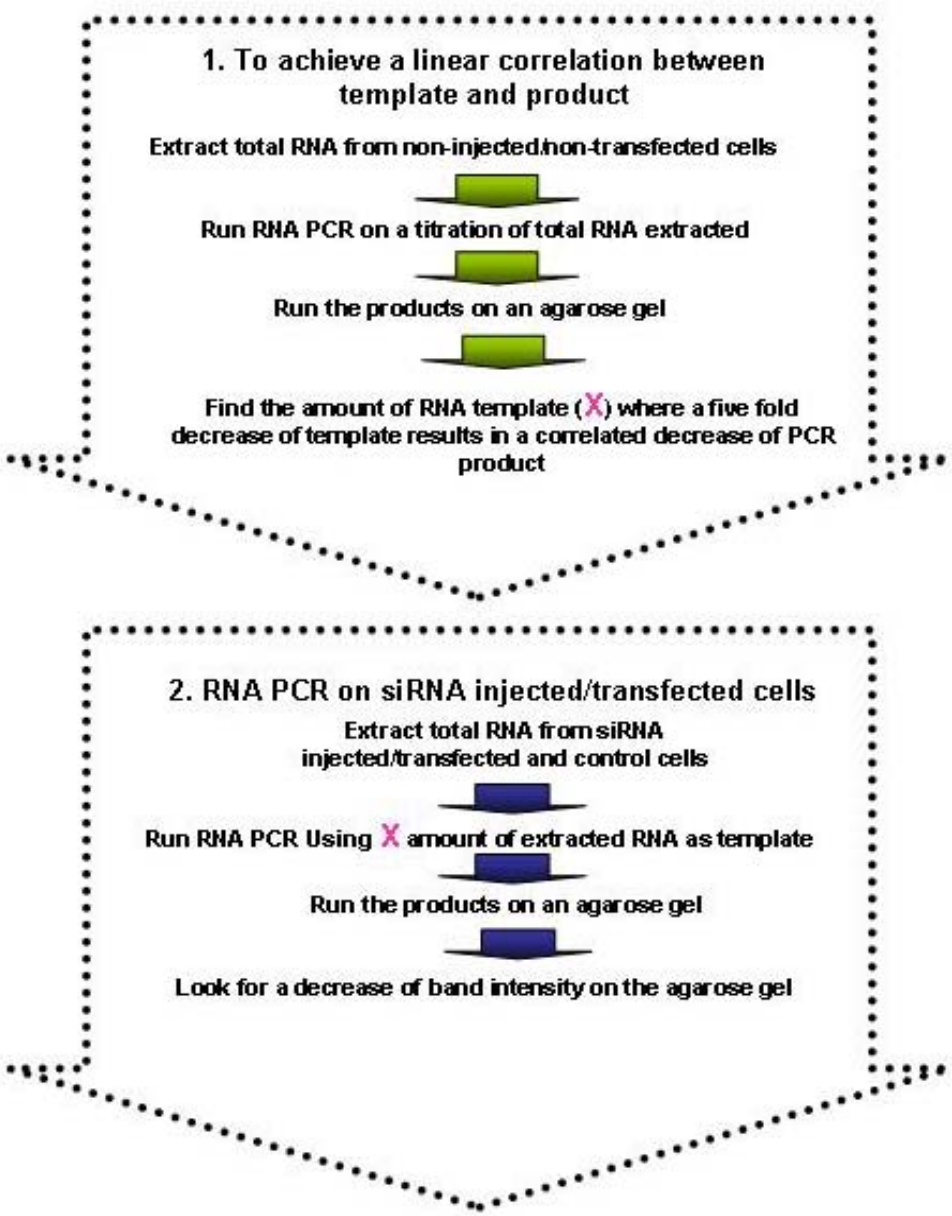

Figure 5.4 Strategy of RNA PCR experiments to detect eRF1 mRNA decrease by injecting siRNAs.

5.3.4.2 Extract total RNA from injected oocytes

Oocytes were injected with 500 pg of siRNA or siControl using classic micropipette injection. 3 hours or 24 hours after injection, 20 oocytes were lysed with 1ml of Trizol®

reagent (Invitrogen), followed by 200 μl of chloroform extraction and 500 μl of isopropanol precipitation. The RNA pellet was washed with 75% ethanol and dissolved in 30 μl of DEPC water. The remaining DNA was further cut with DNase I (RNase free) (Qiagen) and the RNA was purified using RNeasy Mini Kit (Qiagen). The concentration of RNA was measured by UV spectrometry.

5.3.4.3 Extract total RNA from transfected HEK cells

For the purpose of total RNA extraction and RNA PCR, HEK cells were transfected with siRNA using Lipofectamine (Invitrogen). 1.2 μg of each siRNA and siControl were transfected into 2.4×10^5 HEK cells on one 35 mm tissue culture plate using standard Lipofectamine transfection protocol. 3 hours or 24 hours after transfection, all the cells on the plate were lysed with 1ml of Trizol® reagent (Invitrogen), followed by the RNA extraction described before.

5.3.4.4 RNA PCR on the extracted total RNA

To detect the amount of eRF1 mRNA, GeneAmp® RNA PCR Kit (Applied Biosystems) was used following the standard protocol. Briefly, in the first step, reverse transcription was performed using a random hexamer as primer (provided) and the reaction was incubated in 42°C for 15 minutes and denatured at 99°C for 5 minutes. In the second step, PCR primers for the corresponding eRF1 and AmpTaq DNA polymerase were added and a traditional PCR reaction was performed.

5.3.5 SDS-PAGE and Western blot in *Xenopus laevis* oocytes

In order to look at the full length protein and truncated protein on Western blots, an HA tag (YPYDVPDYA) was subcloned to the N-terminus of α subunit of acetylcholine

receptor with a UAG stop codon at the position of tryptophan 149. The vitelline/plasma membranes were manually stripped from oocytes expressing nAChR. After removing the yolks of the oocytes by centrifuge, the samples containing only the vitelline/plasma membrane were analyzed by SDS-PAGE, followed by immunoblotting with the anti-hemagglutinin antibody and visualized using an ECL detection kit (Amersham). Note that the full-length proteins observed in this experiment will include not only the correctly suppressed functional protein, but also proteins produced from UAG read-through by endogenous tRNA. Observing membrane protein only instead of proteins from the whole cell excludes the full-length proteins that are not trafficked correctly to the cell surface.

5.3.6 Co-electroporation of siRNA with TAG29 GFP-TAG plasmid DNA and HSAS tRNA and microscopy in HEK cells

Because a mammalian cell is a more relevant environment for proteins of mammalian origin and would allow for studies of cell-specific signal transduction pathways, testing the effect of RNAi suppression in mammalian cells in efforts to enhance nonsense suppression is worthwhile. Before using large amounts of chemically aminoacylated tRNA necessary for electrophysiology recordings on mammalian cells, an HSAS (human serine amber suppressor) assay was applied. In this experiment, HSAS was used to suppress a TAG codon at serine 29 of EGFP DNA. HSAS is recognized by the serine synthetases (SerRS) of mammalian cells so it does not require chemical aminoacylation prior to delivery[11]. The wild type recovery of EGFP can be observed by the appearance of green cells under a fluorescent microscope. Nonsense suppression using HSAS is catalytic and therefore yields enough EGFP for observation.

Specifically 1.2 μg of siRNA molecules or siControl are co-precipitated with 10 μg Ser29TAG-EGFP plasmids and 20 μg of HSAS tRNA. This is then dissolved in 5 μl of CO_2 independent media, and electroporated into HEK cells as reported previously. Visualization of the transfected HEK cells was performed using a video imaging system in our lab equipped with an inverted microscope (Olympus IMT2). For fluorescence, a 250 W Hg/Xe lamp was used, operating at 150W. A GFP filter set (Chroma) with an excitation bandpass of 450 to 490 nm, and an emission bandpass of 500 to 550 nm was used.

5.4. Results and discussion

5.4.1 Electrophysiology of siRNA treated oocytes

Although si1187 and si36 were previously reported to be effective in suppressing eRF1 mRNA and to be able to increase UAG codon suppression effectively in HEK cells[17], they failed to show any increase of acetylcholine induced currents from nAChR produced in the nonsense suppression experiment. The size of maximal currents from each oocyte varied from 2 μA to 9 μA. The large variability of the current size required a large number of samples to give a sound statistic result. At least 6 cells were recorded in each experiment, and the ability of OpusXpress recording 8 cells each time highly facilitates the recording process. However, observed either individually or as a group, there was no consistent change of average current size in the siRNA treated oocytes, although results differed slightly from day to day. The treatment of siControl in parallel did not show any noticeable cytotoxicity. (data not shown)

The reasons that these two siRNAs did not increase the currents might include 1) the possibility that different amount of injected siRNA was needed. 500 pg of siRNA

injection was previously reported to effectively decrease the xMiRP channel expression in *Xenopus* oocytes[19]. But eRF1 is a very important protein in the cell; therefore maybe a larger amount of siRNA is needed to produce a comparable decrease. It could also be possible that a smaller amount of siRNA is needed because depletion of eRF1 may have compromised the translation accuracy.

Another reason might be that time delays were needed between the siRNA injection and mRNA/tRNA injection so that the eRF1 that had already been translated would have time to turn over before the nonsense suppression took place. Different time delays as shown in Figure 5.3 were tested.

The absence of improvement seen from different injection amounts (25 ng, 5 ng, 50 pg, 5 pg and 0.5 pg) combined with different time delays between the two injections (3 hours, 10 hours and 24 hours) left no choice but designing new siRNA molecules.

The newly designed si1151x shows an increase of average current size of about 30%. si450x, however, shows a very small effect, and siControl shows comparable signals to the control of no siRNA. The increase, of course is not as dramatic as we would hope, and the error bars shown here are large. These results are repeatable and varying the amount of siRNA by 10 folds does not have a big effect on the current sizes. (Figure 5.5)

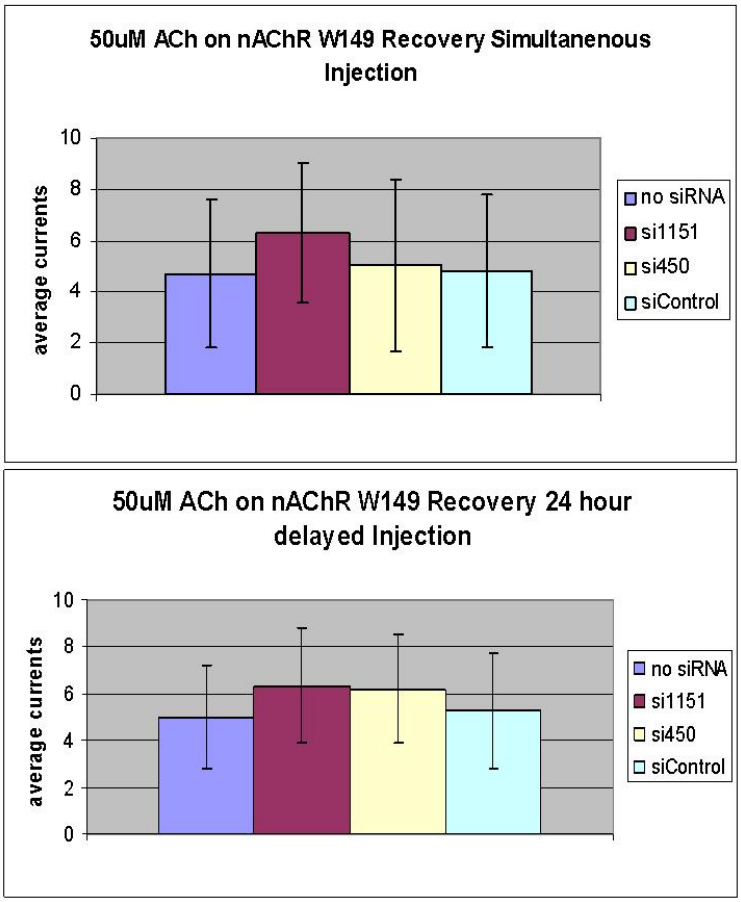

Figure 5.5 The average currents of mouse muscle nAChR α1 149 TAG mutant recovered by tryptophan charged tRNA with and without siRNA injected. There are at least 8 cells in each experiment.

It is not surprising that different siRNAs targeted toward the same gene have varying effects. For example, an enzymatically created small hairpin RNA (shRNA) library that contained 262 independent shRNAs was generated to be processed into siRNAs by Jurkat T cell machinery targeting GFP gene. In these experiments, it was found that only 30% of the constructs managed to decrease the GFP expression by a factor of larger than 2, and 56% of the constructs decreased GFP by a factor of less than 1.5[26]. Similarly, in an experiment where two sets of siRNAs were designed to target two different genes, each

set containing at least 90 independent siRNA designs, statistic analysis showed that a two-base shift in the target mRNA is sufficient to alter RNAi efficiency[27].

Unfortunately, not enough is known about the RNAi mechanism to allow such a strategy. Because of the wide usage of RNAi technology, an enormous number of experiments has been performed in search for a systematic "rational" siRNA design strategy that can "guarantee" effective target suppression. From such studies, a series of criteria was developed to aid in siRNA design, including the requirement of a low GC content, a bias towards low internal stability at the sense strand 3'-terminus, and the lack of inverted repeats. Other criteria, although proven to be valid in some specific analysis, failed to display experimental support[27].

5.4.2 RNA PCR results of uninjected oocytes and siRNA treated oocytes.

Figure 5.6 A shows a successful calibration experiment of RNA PCR on eRF1 mRNA extracted from uninjected oocytes. The number below each lane indicates the amount of total RNA used as templates. From this gel we can see that 40 ng of total RNA is a threshold where a 5 fold of decrease will cause a corresponding decrease of band intensity on the gel.

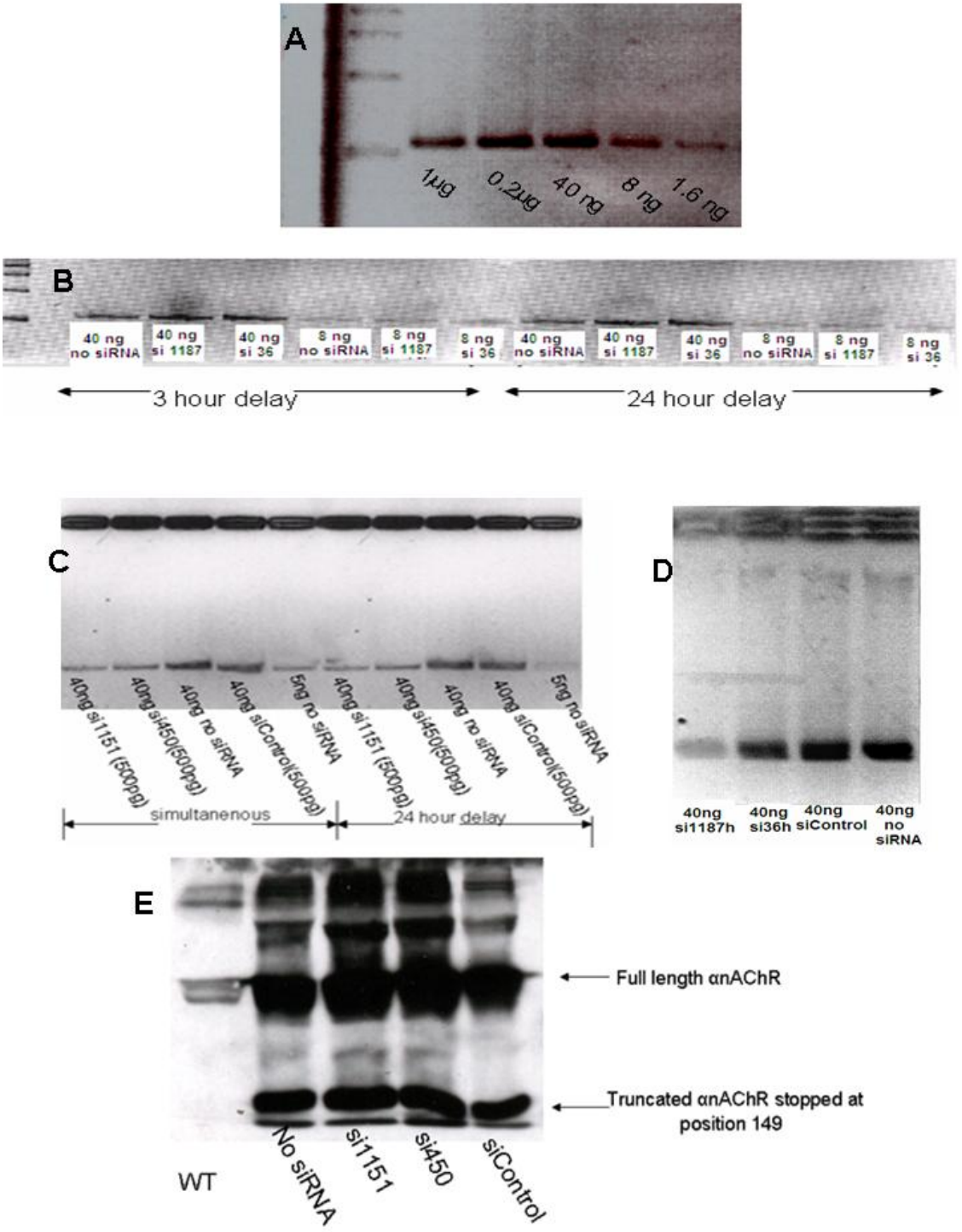

Figure 5.6 RNA PCR and Western blottting show different effects of designed siRNA molecules in *Xenopus* oocytes and in HEK cells. A: Different amount of total RNA

from uninjected oocytes used as RNA PCR templates. This experiment was performed to find the right amount of templates for RNA PCR so that a 5 fold decrease of eRF1 mRNA causes a decrease of RNA PCR product on the agarose gel. Numbers show the amount of total RNA extracted from non-injected oocytes used as templates for RNA PCR. B: RNA PCR results show that *Xenopus* eRF1 mRNA was not reduced with the injection of 500pg of si1187x or si36x. In each lane, the numbers indicate the amount of total RNA used as templates in each RNA PCR experiment. The amount of each siRNA used is 500ng. 3 hour and 24 hour time delays are used and 40ng and 8 ng of total RNA are used. C: RNA PCR results show that *Xenopus* eRF1 mRNA was reduced with the injection of 500pg of si1151x and si450x. The reduction was about 5 fold. There is no noticeable difference between simultaneous injections or 24 hour delay injections. Numbers outside the parentheses indicate the amounts of total RNA used and the ones inside the parentheses indicate the amounts of siRNA injected. D. RNA PCR result of si1187h and si36h suppressing HEK eRF1 mRNA. 40ng of total RNA was used in each lane. The HEK cells were lysed 24 hours after transfection. E. Western blot showing both full length α nAChR and truncated α nAChR the translation of which stopped at position 149. 3 oocytes were used in each lane and 500 pg of siRNAs were injected for the oocytes on the right three lanes.

The RNA PCR performed on si1187x and si36x injected oocytes explained the lack of effect on the electrophysiology level. Figure 5.6 B shows that si1187x or si36x do not decrease eRF1 mRNA in oocytes. These two siRNA molecules, although capable of inducing release factor reduction in HEK cells (the human analogs) [17], are not able to suppress release factor mRNA in oocytes.

The RNA PCR results of the newly designed siRNAs correlated with the electrophysiology readings (Figure5.6 C). However si450x, although it does not show much effect on current increase, turns out to have reduced the mRNA level of release factor, similar to si1151x.

Figure 5.6 D shows the RNA PCR result of si1187h's and si36h's effect in HEK cells. 24 hours after transfection, si1187h suppressed eRF1 in HEK cells by about 5 fold while

si36h has a much smaller effect. This result correlates with the previously reported result by the Yarus lab [17].

5.4.3 Western blots for siRNA treated oocytes

The Western blot (Figure 5.6 E) shows both the full length proteins and truncated proteins. The full length protein includes both the functional protein and the proteins with read-through by endogenous tRNA. So far, an increase in the ratio of full length protein over truncated protein has not been seen.

One explanation for the lack of difference on Western blots is that a similar calibration process to that performed with the RNA PCR experiment is needed here, and that it has to be confirmed that the proteins are not saturating the antibodies. Once a linear correlation between the amount of α nAChR protein and the darkness of the band seen on the SDS-PGE gel is established, the results will be more informative.

If it is the case that there is no ratio change of full length proteins over truncated proteins, then the increased electric signal is probably caused by increased ratio of correctly suppressed protein within this full length band. Then the decreased release factor could have increased the fidelity of the codon:anticodon recognition.

5.4.4 HSAS/TAG EGFP experiments

As is shown in Figure 5.7, si1187h has increased the number of green cells compared to no siRNA, while si36 does not seem to have an obvious effect. In this experiment, wild type EGFP and EGFP TAG mRNA transfected cells serve as a positive control (dark blue line) and a negative control (pink line) respectively. The numbers of green cells from the si1187h treated cells (light blue line), the si36h treated cells (purple line), no siRNA

treated cells (yellow line) and the random siRNA treated cells (brown line) were compared. The data here are quite preliminary and lack certain controls such as a transfection with EGFP TAG and siRNA. More importantly, an assay more accurate than counting green cells is needed for this experiment.

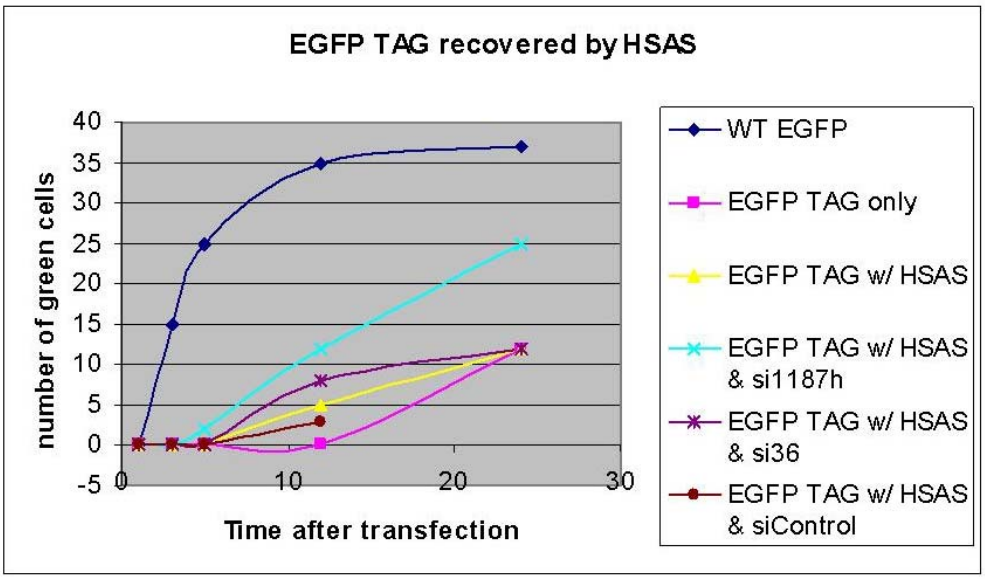

Figure 5.7 Preliminary results of Ser29TAG EGFP suppressed by HSAS.

5.5 Conclusion and future direction

From these preliminary studies performed, we found that reducing functional eukaryotic release factor 1 *in vivo* by RNAi potentially increases nonsense suppression efficiency both in *Xenopus* oocytes and in HEK cells, and the effect is more promising in HEK cells. We developed an RNA PCR experiment to look at the mRNA level of eRF1 both in *Xenopus* oocytes and in HEK cells, which can be expanded to other endogenous proteins in the future.

The experiments that will be performed in the future include:

1. In oocytes, another suppression experiment can be performed where tRNA acylated with a charged residue is incorporated into a restrictive site of the TAG mutant.

2. In oocytes, poorer-expressed ion channels (possibly a neuronal ion channel) can be studied. The wild type recovery experiment reported here has obtained high efficiency in our lab so far. Therefore, it is possible that an increase will be more obvious to see in a case where nonsense suppression efficiency is lower.

3. For EGFP/HSAS experiment in HEK cells, a more quantitative and a more accurate assay than counting the green cells under the microscope will be designed.

4. In HEK cells, nonsense suppression of one or more ion channels will be explored with the help of RNAi.

5.6 References

1. Dougherty, D.A., *Unnatural amino acids as probes of protein structure and function.* Curr Opin Chem Biol. 2000 Dec;4(6):645-52.
2. Beene, D.L., D.A. Dougherty, and H.A. Lester, *Unnatural amino acid mutagenesis in mapping ion channel function.* Curr Opin Neurobiol. 2003 Jun;13(3):264-70.
3. Beene, D.L., et al., *Cation-pi interactions in ligand recognition by serotonergic (5-HT3A) and nicotinic acetylcholine receptors: the anomalous binding properties of nicotine.* Biochemistry. 2002 Aug 13;41(32):10262-9.
4. Mu, T.W., H.A. Lester, and D.A. Dougherty, *Different binding orientations for the same agonist at homologous receptors: a lock and key or a simple wedge?* J Am Chem Soc. 2003 Jun 11;125(23):6850-1.
5. England, P.M., et al., *Backbone mutations in transmembrane domains of a ligand-gated ion channel: implications for the mechanism of gating.* Cell. 1999 Jan 8;96(1):89-98.
6. Tong, Y., et al., *Tyrosine decaging leads to substantial membrane trafficking during modulation of an inward rectifier potassium channel.* J Gen Physiol, 2001. **117**(2): p. 103-18.
7. Padgett, C.L., et al., *Unnatural amino acid mutagenesis of the GABA(A) receptor binding site residues reveals a novel cation-pi interaction between GABA and beta 2Tyr97.* J Neurosci. 2007 Jan 24;27(4):886-92.

8. Lummis, S.C., et al., *A cation-pi binding interaction with a tyrosine in the binding site of the GABAC receptor.* Chem Biol. 2005 Sep;12(9):993-7.
9. Brandt, G.S., *Site-speicific incorporation of synthetic amino acids into functioning ion channels.* Thesis (Ph. D.), 2003, California Institute of Technology.
10. Rodriguez, E.A., H.A. Lester, and D.A. Dougherty, *In vivo incorporation of multiple unnatural amino acids through nonsense and frameshift suppression.* Proc Natl Acad Sci U S A. 2006 Jun 6;103(23):8650-5. Epub 2006 May 25.
11. Monahan, S.L., H.A. Lester, and D.A. Dougherty, *Site-specific incorporation of unnatural amino acids into receptors expressed in Mammalian cells.* Chem Biol. 2003 Jun;10(6):573-80.
12. Monahan, S.L., *Site-specific incorporation of unnatural amino acids into receptors expressed in mammalian cells.* Thesis (Ph. D.), 2004, California Institute of Technology.
13. Inge-Vechtomov, S., G. Zhouravleva, and M. Philippe, *Eukaryotic release factors (eRFs) history.* Biol Cell. 2003 May-Jun;95(3-4):195-209.
14. Dykxhoorn, D.M., C.D. Novina, and P.A. Sharp, *Killing the messenger: short RNAs that silence gene expression.* Nat Rev Mol Cell Biol. 2003 Jun;4(6):457-67.
15. Song, H., et al., *The crystal structure of human eukaryotic release factor eRF1--mechanism of stop codon recognition and peptidyl-tRNA hydrolysis.* Cell. 2000 Feb 4;100(3):311-21.
16. Short, G.F., 3rd, S.Y. Golovine, and S.M. Hecht, *Effects of release factor 1 on in vitro protein translation and the elaboration of proteins containing unnatural amino acids.* Biochemistry. 1999 Jul 6;38(27):8808-19.
17. Carnes, J., et al., *Stop codon suppression via inhibition of eRF1 expression.* RNA. 2003 Jun;9(6):648-53.
18. Ilegems, E., H.M. Pick, and H. Vogel, *Downregulation of eRF1 by RNA interference increases mis-acylated tRNA suppression efficiency in human cells.* Protein Engineering, Design and Selection, 2004. **17**(12): p. 821-827.
19. Anantharam, A., et al., *RNA interference reveals that endogenous Xenopus MinK-related peptides govern mammalian K+ channel function in oocyte expression studies.* J Biol Chem. 2003 Apr 4;278(14):11739-45. Epub 2003 Jan 15.
20. Rajamanickam, J., et al., *EAAT4 phosphorylation at the SGK1 consensus site is required for transport modulation by the kinase.* J Neurochem. 2007 Aug;102(3):858-66. Epub 2007 Apr 17.
21. Dornburg, R. and R.J. Pomerantz, *HIV-1 gene therapy: promise for the future.* Adv Pharmacol. 2000;49:229-61.
22. Sharp, P.A., *RNA interference--2001.* Genes Dev. 2001 Mar 1;15(5):485-90.
23. Brummelkamp, T.R., R. Bernards, and R. Agami, *A system for stable expression of short interfering RNAs in mammalian cells.* Science. 2002 Apr 19;296(5567):550-3. Epub 2002 Mar 21.
24. Paddison, P.J., et al., *Short hairpin RNAs (shRNAs) induce sequence-specific silencing in mammalian cells.* Genes Dev. 2002 Apr 15;16(8):948-58.
25. Aigner, A., *Applications of RNA interference: current state and prospects for siRNA-based strategies in vivo.* Appl Microbiol Biotechnol. 2007 Aug;76(1):9-21. Epub 2007 Apr 25.

26. Shirane, D., et al., *Enzymatic production of RNAi libraries from cDNAs.* Nat Genet. 2004 Feb;36(2):190-6. Epub 2004 Jan 4.
27. Reynolds, A., et al., *Rational siRNA design for RNA interference.* Nat Biotechnol. 2004 Mar;22(3):326-30. Epub 2004 Feb 1.